Dr P.J.M. de Laat
Prof. Dr H.H.G. Savenije

Hydrology

Hydrology

TABLE OF CONTENTS

1   INTRODUCTION

1.1   The development of hydrology

Water has always played an important role in the life of man. Since long before the start of our calendar man has tried to control water. Some important events of ancient history are given in table 1.1 (after Biswas, 1972 and after Ponting, 1991).

The development of hydrology as a science started much later than man's attempt to control the water. The first steps towards the development of hydrology as a science were measurements of rainfall and water levels.

Some interesting developments were (Biswas, 1972, Rodda and Matalas, 1987):
* the first mention of the measurement of rainfall by Kautilya in India in the fourth century B.C.;
* the concept of Hero of Alexandria of the measurement of discharge in the first century;
* the understanding of the hydrologic cycle in China in a book of 239 B.C.;
* Plato (427-348 B.C.) describes the relation between elements of the hydrological cycle and the effect of deforestation;
* the general acceptance of the continuity principle in the seventeenth century;
* the experimental investigations by Perrault in the seventeenth century to prove that rainfall is adequate to sustain stream flow;
* the calculations of Halley in the seventeenth century to prove that water evaporates from the oceans and comes down as rainfall in ample amounts to sustain the flows of rivers;
* in the eighteenth century considerable experimental results were obtained in the field of surface water;
* the major achievement of the nineteenth century was the firm establishment of the principle of conducting experimental investigations either to establish a theory or to determine an empirical relationship.

The development of Hydrology as a science based on physical and mathematical principles, however, is of more recent date (since 1930).

The following description of hydrology is given by UNESCO (1964):

> *"Hydrology is the science which deals with terrestrial waters, their occurrence, circulation and distribution on our planet, their physical and chemical properties and their interaction with the physical and biological environment, including the effect on them of the activity of man".*

It follows that hydrology is restricted to the terrestrial occurrence of water, excluding oceanography and meteorology. Water may occur in solid, liquid or vapour phase. Hydrology studies the flow of water over land, in rivers and lakes, but also through soil, plant and atmosphere.

Hydrology does not only deal with quantitative aspects but also with qualitative aspects such as salinization and water pollution. It includes a large variety of subjects, ranging

Date[1] (B.C.)	Event
5500	First irrigation in Khuzistan (present day Iran)
3200	Reign of King Scorpion in Egypt. First evidence of irrigation in Egypt
3000	King Menes dammed the Nile and diverted its course.
3000	Nilometers were used to record the fluctuations of the Nile.
2850	Failure of the Sadd el-Kafara dam in Egypt.
2750	Origin of the Indus Valley water supply and drainage systems.
2200	Various waterworks of the Great Yü' in China.
2200	Water from spring was conveyed to the Palace of Cnossos (Crete). Dams at Makhai and Lakorian in Iran.
1950	Connection of the Nile River and the Red Sea by a navigation canal during the reign of Seostris I.
1900	Sinnor (water tunnel) constructed at Gezer.
1850	Lake Moeris and other works of Pharao Amenemhet III.
1800	Nilometers at Second Cataract in Semna.
1750	Water codes of King Hammurabi.
1700	Joseph's Well near Caïro, nearly 100 m in depth.
1500	Two springs joined by a sinnor in the city of Tell Ta'annek. Maruk Dam in the Tigris near Sammara, destroyed in 1256 A.D.
1300	Irrigation and drainage systems in Nippur. Quatinah Dam on the Orontes River in Syria constructed under the reign of either Sethi I or Ramses II.
1050	Water meters used at Oasis Gadames in North Africa.
750	Marib and other dams in river Wadi Adhanah in the Yemen Arab Republic.
714	Destruction of qanat systems (artificial underground channels) by King Saragon II. Qanat system gradually spread to Iran, Egypt and India.
690	Construction of Sennacherib's Channel.
600	Dams in the Murghab River in Iran, destroyed in 1258 A.D.

[1]In the absence of accurate information, many of these dates are approximate

Table 1.1   **A chronology of recorded hydrologic engineering prior to 600 B.C.**

from e.g. erosion and sedimentation to drinking places for wildlife. An important field of study finally concerns the environmental effects of a change in the existing hydrological regime as a result of the activity of man.

Hydrologists are traditionally concerned with the supply of water for domestic and agricultural use and the prevention of flood disasters. However, their field of interest also includes hydropower generation, navigation, water quality control, thermal pollution, recreation and the protection and conservation of nature. In fact, any intervention in the hydrological regime to fulfil the needs of the society belongs to the domain of the hydrologist. This does not include the design of structures (dams, sluices, weirs, etc.) for water management. Hydrologists contribute however, to a functional design (e.g. location and height of the dam) by developing design criteria and to water resources management by establishing the hydrological boundary conditions to planning (inflow sequences, water resources assessment). Both contributions require an analysis of the hydrological phenomena, the collection of data, the development of models and the calculation of frequencies of occurrence.

Hydrology was originally practised by many different disciplines, e.g. geology, civil engineering and agriculture. Sciences emphasizing hydrology often use the prefix <u>hydro</u> (hydrogeology, hydrobiology, hydrometeorology, etc.). Other allied sciences are for example soil science, fluid mechanics, economy, chemistry, physics and statistics.
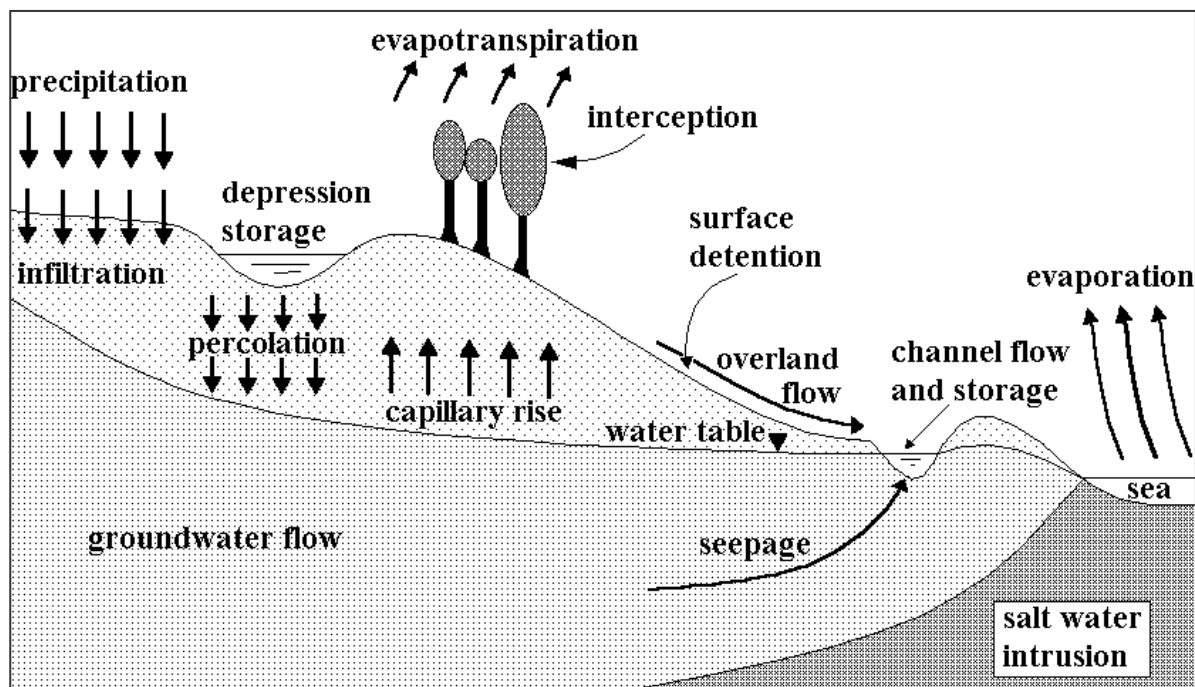

Fig. 1.1   Descriptive representation of the hydrological cycle

1.2   Hydrologic cycle

The hydrologic cycle (see figure 1.1) is the circulation of water evaporated from the sea and land surfaces, its transport through the atmosphere to the land and its return to the sea via surface, subsurface and atmospheric routes. Although called a cycle, the process is much more complex than a mere cycle. All kinds of short cut and parallel processes take place. For example, a drop of water evaporated from the sea may precipitate back into the sea without completing the entire cycle. The hydrologic cycle refers to the general circulation, which results from the fact that there is on average above the earth's land surface more precipitation than evaporation. Water precipitated over land passes through a number of storage media, which can be regarded as subsystems of the hydrological cycle. The hydrodynamics is the flow of water between and through the different storage media. A schematization of the subsystems and flow components of the terrestrial part of the hydrologic cycle is given in figure 1.2.

Surface detention and interception storage are considered as separate systems. Interception storage refers to the precipitation intercepted by vegetation before it evaporates. Detention storage is water temporarily stored in pools or depressions. This water may evaporate or infiltrate into the soil to replenish the soil moisture reservoir or to percolate to the groundwater.

The flow of soil moisture in downward direction is called percolation and in upward direction capillary rise. The annual amount of percolation is usually larger than capillary rise, resulting in a recharge of the groundwater reservoir. Groundwater flow ultimately discharges from the
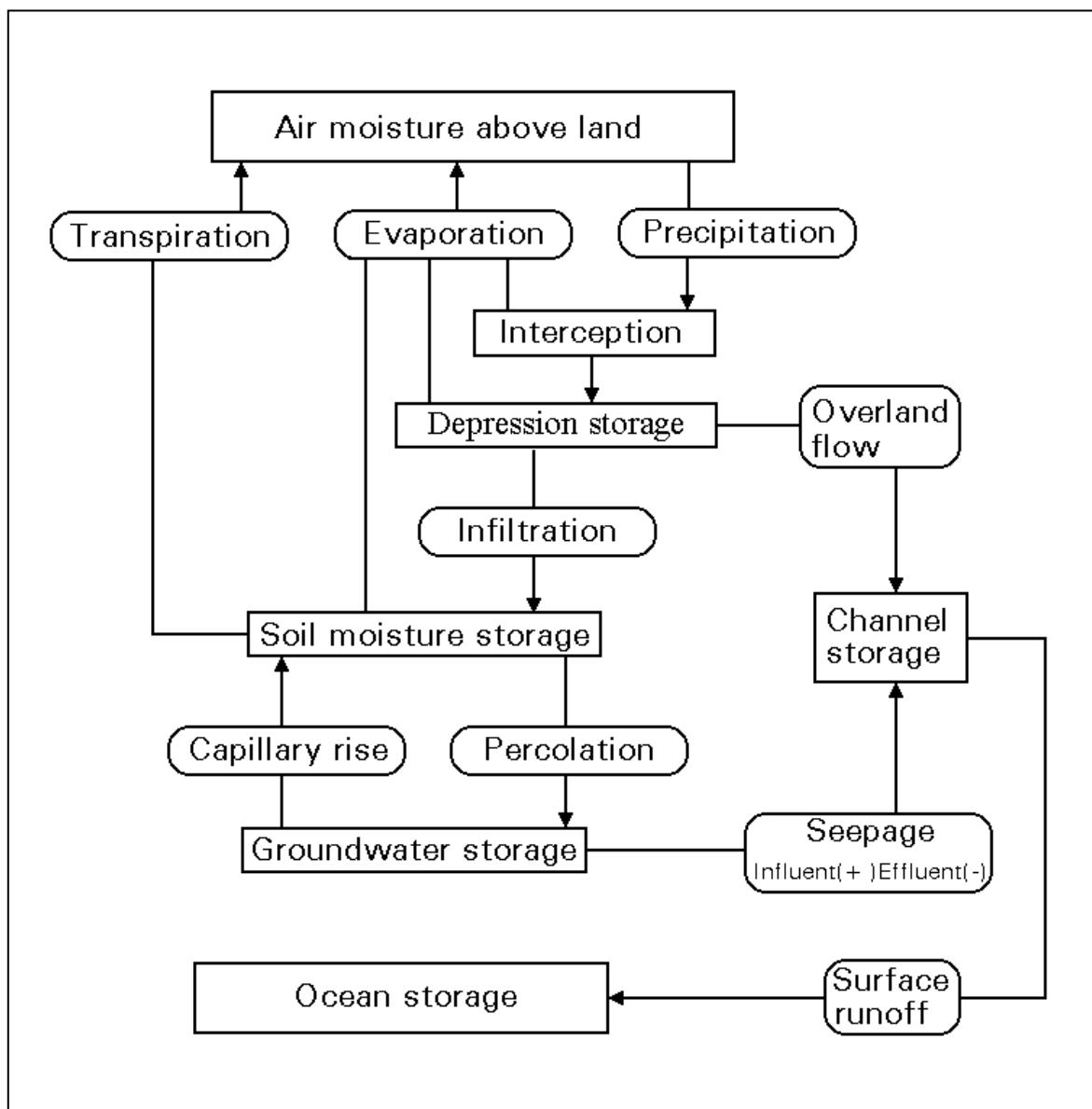
Fig. 1.2 Schematization of storages and processes of the terrestrial part of the hydrological cycle

groundwater storage into the channel system.

Vegetation transpires water taken up by roots. In practice it is impossible to differentiate between transpiration from vegetation and evaporation from the bare soil. The combined process is commonly referred to as evapotranspiration.

Attempts have been made to incorporate the interference of man in the hydrological cycle through the introduction of the water diversion cycle, which includes water withdrawal and water drainage. This diversion cycle is exerting significant influence on the terrestrial water cycle, especially in highly economically developed regions with a dense population (see figure 1.3).
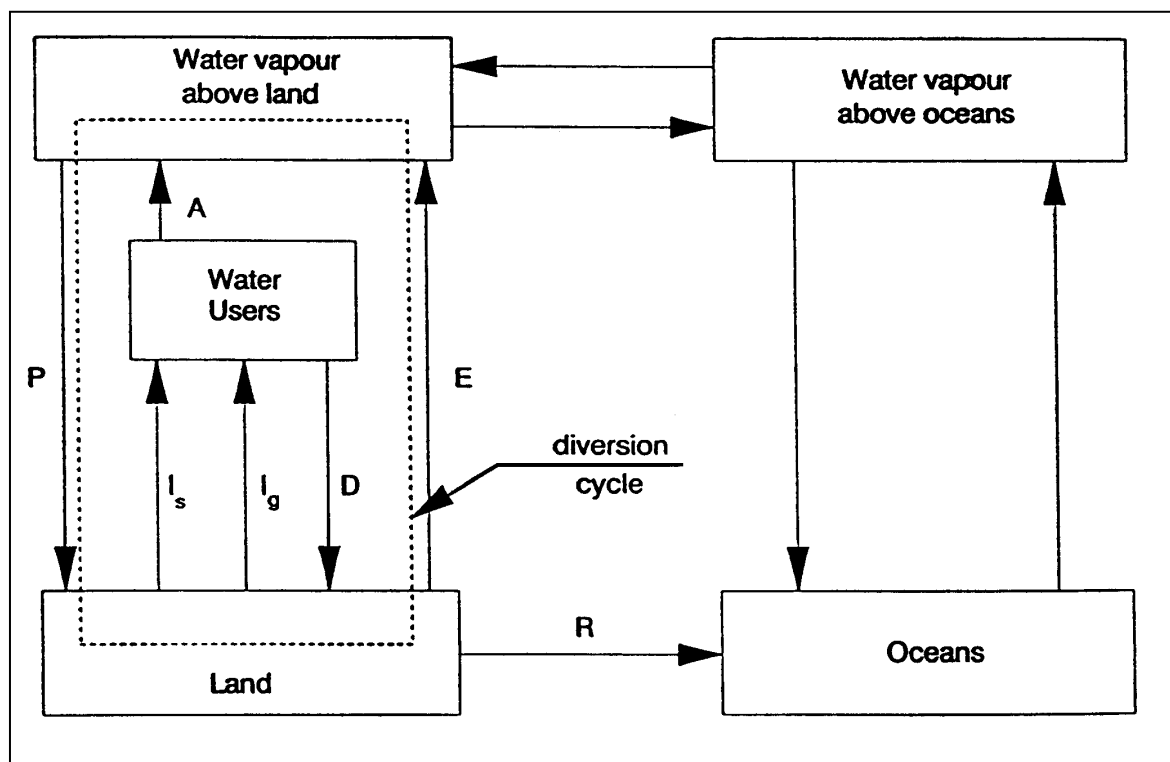
Fig. 1.3 Scheme of the hydrological cycle with the diversion cycle (after Rodda and Matalas, 1987)

1.3   Water balance

The water balance is a special case of the general control volume equation, which is the basis of the continuity, momentum, and energy equations for various hydrologic processes. This equation is called the Reynolds Transport Theorem (see Ven te Chow et al. 1988).

Reynolds Transport theorem
Reynolds theorem states that:

> *"the total rate of change of an extensive property of a fluid dB/dt is equal to the rate of change of an extensive property stored in the control volume, plus the net outflow of extensive property through the control volume".*

$$\frac{dB}{dt} \;=\; \frac{d}{dt} \iiint \beta\rho\, dV + \iint \beta\rho\, (U \bullet dA) \tag{1.1}$$

where B is the extensive property of the fluid whose values depend on the amount of mass present (e.g. mass, momentum: $B=m$, $B=mU$), β is quantity of B per unit of mass, the intensive property of the fluid, whose values do not depend on mass: $\beta = dB/dm$. B and β can be scalar or vector quantities. Furthermore, ρ is the density of the fluid; the triple integral signifies the integration over the volume V; the double integral is the integration over the cross-sectional area considered A; $U \bullet dA$ is the vector dot product of the velocity vector of the fluid U with length U, and the vector dA with length dA perpendicular to the cross-section. If θ is the angle between U and dA, *then* $U \bullet dA = U \cos \theta\, dA$. The first term of the right hand member is the

rate of change of the extensive property stored in the control volume; the second term is the net outflow of extensive property through the control surface. When using the theorem, inflows are always considered negative and outflows positive.

Integral equation of continuity

The integral equation of continuity follows from Reynolds theorem and is the basis for the water balance equation. If mass is the extensive property being considered, then *B=m*, and *β=dB/dm=1*. By the law of conservation of mass, *dB/dt=dm/dt=0* because mass cannot be created or destroyed. Substitution in Reynolds theorem yields

$$0 = \frac{d}{dt} \iiint \rho \, dV + \iint \rho \, (U \bullet dA) \tag{1.2}$$

which is the integral equation of continuity for an unsteady flow with variable density. If the flow has constant density, ρ can be divided out of both terms

$$0 = \frac{d}{dt} \iiint dV + \iint (U \bullet dA) \tag{1.3}$$

The integral $\iiint dV = S$ is the volume of fluid stored in the control volume. Hence the first term is the time rate of change of the storage *dS/dt*. The second term, the net outflow, can be split into inflow *I(t)* and outflow *O(t)*. Because for inflow the direction of the velocity vector **U** and the area vector **dA** point in different directions (the velocity vector pointing in and the area vector pointing out), their vector dot product is negative; whereas for the outflow the vector dot product is positive. Hence:

$$\frac{dS}{dt} + O(t) - I(t) = 0 \tag{1.4}$$

which is the basis for the water budget concept, widely used in the field of hydrology. Equation 1.4 may be rewritten as

$$I(t) - O(t) = \frac{\Delta S}{\Delta t} \tag{1.5}$$

where *I* is the inflow in [L^3/T], *O* is the outflow in [L^3/T], and *ΔS/Δt* is the rate of change in storage over a finite time step in [L^3/T] of the considered control volume in the system. The equation holds for a specific period of time and may be applied to any given system provided that the boundaries are well defined. Other names for the water balance equation are Storage Equation, Continuity Equation and Law of Conservation of Mass.

Several types of water balances can be distinguished, like:

- the water balance of the earth surface;
- the water balance of a drainage basin;
- the water balance of the water diversion cycle (human interference);
- the water balance of a local area like a city, a forest, or a polder.

The water balance of the earth surface

The water balance of the earth surface is composed of all the different water balances that can be distinguished. Data constituting the occurrence of water on earth are given in the table 1.2, 1.3, and 1.4. The water balance of the interaction between the earth surface and the world oceans and seas is given in table 1.5.

	Area in 10^{12} m^2	*Area in %*
Water surfaces	*361*	*71*
Continents	*149*	*29*
Total	*510*	*100*

Table 1.2. Earth surfaces (Baumgartner, 1972).

	Area in 10^{12} m^2	*Area in % of total*	*Area in % of continents*
Deserts	*52*	*10*	*35*
Forests	*44*	*9*	*30[1]*
Grasslands	*26*	*5*	*17*
Arable lands	*14*	*3*	*9*
Polar regions	*13*	*2*	*9*
Oceans	*361*	*71*	

Table 1.3. Earth land use (Baumgartner, 1972).

Water balance of a drainage basin

The water balance is often applied to a river basin. A river basin (also called watershed, catchment, or drainage basin) is the area contributing to the discharge at a particular river cross-section. The size of the catchment increases if the point selected as outlet moves downstream as shown in figure 1.4. If no water moves across the catchment boundary indicated by the broken line, the input equals the precipitation P while the output comprises the evapotranspiration ET and the river discharge Q at the outlet of the catchment. Hence, the water balance may be written as

$$P - ET - Q = \frac{\Delta S}{\Delta t} \tag{1.6}$$

where ΔS is the change of storage over the time step Δt.

All terms must be expressed in the same unit. Precipitation and evapotranspiration are usually measured in mm/d and river discharge in m^3/s. For conversion of one unit into the other the catchment area A must be known. For example, conversion of m^3/s into mm/d for a catchment area of 200 km^2 is as follows:

conversion of seconds to days: *1 m^3/s = 86400 m^3/d*
conversion of m^3 to mm :   *1 m^3/200 km^2 = 10^3/(200*10^6) mm*
resulting in: *86400 m^3/d / 2.10^8 m^2 * 10^3 mm/m = 0.432 mm/d*

---

[1]At present this number may be significantly lower

Water Occurrence	$10^{12} \ m^3$	Amount of water	
		% of water	*% of fresh water*
World Oceans	1300000	97	
Salt lakes/seas	100	0.008	
Polar ice	28500	2.14	77.6
Atmospheric water	12	0.001	0.035
Water in organisms	1	0.000	0.003
Fresh lakes	123	0.009	0.335
Water courses	1	0.000	0.003
Unsaturated zone	65	0.005	0.18
Saturated zone	8000	0.60	21.8
Total fresh water	36700	2.77	100
Total water	1337000	100	

Table 1.4   Amount of water on earth according to the survey conducted within the international geophysical year (Holy, 1982)

Region	Area	Precipitation		Evaporation		Runoff	
	$10^{12} \ m^2/a$	*m/a*	$10^{12} \ m^3/a$	*m/a*	$10^{12} \ m^3/a$	*m/a*	$10^{12} \ m^3/a$
Oceans	361	1.12	403	1.25	449	-0.13	-46
Continents	149	0.72	107	0.41	61	0.31	46

Table 1.5 The water balance of the earth according to the international geophysical year (Holy 1982).

$\Delta S /\Delta t$, the rate of change in the amount of water stored in the catchment, is difficult to measure. However, if the *account period Δt*, for which the water balance is established is taken sufficiently long, the effect of the storage variation becomes less important, because precipitation and evapotranspiration accumulate while storage varies within a certain range. When computing the storage equation for annual periods, the beginning of the balance period is preferably chosen at a time that the amount of water in store is expected not to vary much for each successive year. These annual periods, which do not necessarily coincide with the calendar years, are known as hydrologic years or as water years. The storage equation is especially useful to study the effect of a change in the hydrologic cycle.

The topographic divide between two watersheds is usually taken as the boundary of the catchment, the water divide. Figure 1.5 shows that the topographic divide applies to surface runoff, but may not necessarily coincide with the boundary for groundwater flow, the phreatic divide. Choosing in A the topographic divide as the watershed boundary, leakage of groundwater to a neighbouring catchment will

Fig. 1.4 The catchment area increases as the control point moves down stream

occur. Especially in calcareous rocks where karst regions can be expected, subterranean channels may make it very difficult or impossible to determine the exact watershed boundary.

Table 1.6 gives the water balance of some of the world's largest drainage basins. Notice the large differences in the *Runoff Coefficient* (the percentage of rainfall that comes to runoff).
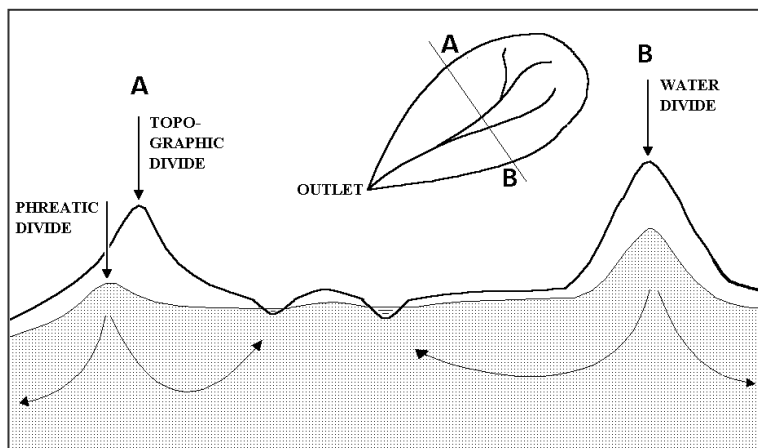

Fig. 1.5 Watershed and cross-section showing a phreatic and topographic water divide, which coincide in B and

The water balance as a result of human interference

The water diversion cycle including human interference results in the following water balance equation (Rodda and Matalas, 1987), see figure 1.3.

$$P = E + A + R \tag{1.7}$$

$$A = I_s + I_g - D \tag{1.8}$$

In which: P = precipitation on the ground surface
E = evapotranspiration from the ground surface
A = net water consumption due to water use
R = runoff from land to ocean
I_s = intake of water from surface runoff
I_g = intake of groundwater
D = drainage of waste water

River	Catchment size 10^3 km^2	Rainfall mm	Rainfall 10^9m^3	Evapo-transpiration mm	Evapo-transpiration 10^9m^3	Runoff mm	Runoff 10^9m^3	Runoff Coefficient %
Nile	2803	220	620	190	534	30	86	14
Mississippi	3924	800	3100	654	2540	142	558	18
Parana	975	1000	980	625	610	382	372	38
Orinoco	850	1330	1150	420	355	935	795	70
Mekong	646	1500	970	1000	645	382	325	34
Amur	1730	450	780	265	455	188	325	42
Lena	2430	350	850	140	335	212	514	60
Yenisei	2440	450	1100	220	540	230	561	51
Ob	2950	450	1350	325	965	131	385	29
Rhine	200	850	170	500	100	350	70	41

Table 1.6 **Indicative average annual water balances for the drainage basins of some of the great rivers**

Water balances of a local area
Examples of a water balance of a local area are presented in tables 1.7 and 1.8. Data are given for a forested area, a deforested area and for a housing area. The data for the forested and deforested areas were derived by Baumgartner based on a number of catchment studies. The data are given as relative numbers (Baumgartner, 1972). The data for the housing area are only valid for the study area concerned.

	P	*L*	*R*	*Expressed in % of L*		
				E	*I*	*T*
Forests	*100*	*52*	*48*	*29*	*26*	*45*
Open land	*100*	*42*	*58*	*62*	*15*	*23*

Table 1.7   **Average annual water balances in forested and deforested areas
                        in % (Baumgartner, 1972).
                        P = Precipitation; L = E + I + T; R = Runoff; E = Evaporation,
                        I = Interception; T = Transpiration**

	Rainfall	*Sewer discharge*	*Subsurface drain discharge*	*Evapo-transpiration*
In mm	*687*	*159*	*212*	*316*
In %	*100*	*23*	*31*	*46*

Table 1.8   Average annual water balance for a housing area in the new town Lelystad, The Netherlands

1.4   Influence of man on the hydrological cycle

The activities of man with the intention to bring about changes in the hydrological regime are generally referred to as water management. These activities are related to the protection against flooding (e.g. dams, retention basins, dikes, storm surge barriers), the provision of adequate water supply for irrigation, domestic and industrial use, navigation, etc. The direct influence of man on the hydrological cycle is then mainly restricted to the world's land surface, and usually to a relatively small region. About one-third of the terrestrial part of this planet can be farmed. Nearly all the precipitation falling on the land is derived directly from the oceans and only about ten percent of it, even on the largest landmasses, arises from the land surface. There is, therefore, very little that man can do, on a global scale, to influence rainfall or snow.

That does not mean that the hydrological cycle has not bee changed by man, but these changes were caused unintentionally. A well-known example is the sea level rise. The sea level is approximately 10 to 20 cm higher than a century ago as a result of the warmer climate. Higher temperatures cause an expansion of the water in the oceans and the melting of ice. Part of the sea level rise is, however, a direct result of human activities, such as the mining of fossil water from deep aquifers. Sahagian et al. (1994) have estimated that the anthropogenic contribution to sea level rise in the twentieth century is almost 12 mm (see table 1.9).

On a local scale the effect of man-induced environmental change (e.g. desertification or urbanisation) on the hydrological regime (e.g. the amount of local rainfall) can be considerable (see table 1.10).

Water Reservoir	Total removable volume (10^{12} m^3)	Sea level equivalent (cm)	Present net extraction rate $(10^{10} \text{ m}^3/\text{a})$	Estimated sea level rise to date (mm)
High Plains (USA)	4.0	1.10	1.20	1.10
South West USA	3.0	0.83	1.00	0.92
California	10.0	2.70	1.30	1.20
Sahara	600.0	167.00	1.00	0.56
Arabian peninsula	500.0	140.00	1.60	0.89
Aral Lake (1960)	1.1	0.30	2.70	2.20
Aral (ground water)	2.2	0.60	3.70	3.10
Caspian sea (lake)	56.0	15.40	0.77	1.30
Caspian sea (groundwater)	220.0	61.20	0.47	0.78
Sahel (soil water)	0.1	0.03	0.34	0.28
Deforestation	3.3	0.90	4.90	3.40
Wetland reduction	8.6	2.40	0.20	1.30
Dams	-1.9	-0.52	-	-5.20
Total	**1406.7**	**392.10**	**19.20**	**11.80**

Table 1.9   **Anthropogenic contributions to sea level rise**

In general, however, rainfall is a hydrological parameter undisturbed by the influence of man. When rain or snow reaches the ground, water comes into the range of man's direct influence. Then, whether this water becomes a productive source or a destructive hazard depends very largely on man's management of vegetation and soils.

The control of water by man is through hydraulic constructions and protection works. By doing so, man influences, affects or even destroys ecosystems. Especially the latter is an important factor to be taken into account by hydraulic engineers.

The use of water can be distinguished in consumptive use and non-consumptive use. Consumptive use entails:

- irrigation
- drainage
- water supply
- cooling by evaporation
- pollution

Non-consumptive use entails:

- hydropower
- transport
- recreation
- fishery

Element	Comparison with rural area	
Sunshine duration	*5 – 15*	*% less*
Annual rainfall	*5 – 15*	*% more*
Thunderstorms	*10 – 15*	*% more*
Mean annual temperature	*0.5 – 3*	*% more*
Mean annual relative humidity	*6*	*% less*
Mean annual wind speed	*20 – 30*	*% less*

Table 1.10   **Effect of urbanisation on climate (After Landsberg, 1981)**

Water is polluted by man in several ways such as solid, or liquid wastes from industries, domestic wastewater, discharge of cooling water. Since water after pollution - in most cases - is no longer of use to other users (without treatment and subsequent losses), pollution is a type of water use.

The interference of man with the natural system is as old as man himself. Ponting (1991) in "A Green History of the World" sketches a striking picture of the way in which man, even before the start of our calendar, has destroyed the environment in which he was living by progressive deforestation, shifting cultivation, dry framing, irrigation and hunting. Impressive civilizations grew and prospered on the exploitation of natural resources, which led to a serious deterioration of the environment and to the eventual collapse of the civilization. The first example of a civilization, which prospered and perished is the Sumerian empire (5000-2500). Leonard Wooley who wrote a book about the Sumerian civilization and who was puzzled by the desolate, largely treeless landscape wrote:

> *"Only to those who have seen the Mesopotamian desert will the evocation of the ancient world seem well-nigh incredible, so complete is the contrast between past and present. It is yet more difficult to realise, that the blank waste ever blossomed, bore fruit for the sustenance of a busy world. Why, if Ur was an empire's capital, if Sumer was once a vast granary, has the population dwindled to nothing, the very soil lost its virtue?"*

The answer to this question, which Ponting gives, is that the Sumerians themselves destroyed the world they created so painstakingly out of the difficult environment of southern Mesopotamia. Similarly the Greek civilization deteriorated, although already Herodotus, Xenophon and Aristotle were aware of the problem. Plato, in his "Critias", gave proof of his excellent hydrological insight by describing the environmental deterioration:

> *"What now remains compared with what then existed is like the skeleton of a sick man, all fat and soft earth having wasted away, and only the bare framework of the land being left. There are some mountains that now have nothing but food for bees, but they had trees not very long ago. There were many lofty trees of cultivated species and boundless pasturage for flocks. Moreover, it was enriched by the yearly rains from Zeus, which were not lost to it, as now, by flowing from the bare land into the sea; but the soil it had was deep, and therein it received the water, storing it up in the retentive loamy soil, and provided all the various districts with abundant supplies of springwaters and streams, whereof the shrines still remain even now, at the spots where the fountains formerly existed."*

In Lebanon, the land of the famous Cedar trees, and Syria much the same thing happened. The process of long-term man-induced environmental decline can be traced around the Mediterranean and the Near East in every area. Overall it is now estimated (Ponting, 1991) that no more than 10% of the original forest that once stretched from Morocco to Afghanistan, even as late as 2000 BC, still exist.

In America much the same happened to the Maya empire (450-800 AD). There is a strong suspicion that the collapse of the great city of Teotihuacan in the valley of Mexico and some of the early city states in the coastal areas of Peru in the first centuries AD were linked to problems arising from the overuse of irrigation and the consequent failure of the agricultural base leading to an inability to maintain the superstructure of the state (Ponting, 1991).

The activities of man also affect the climate. Overgrazing for example, may be an important reason for the climatic change and the consequent desertification of the Sahel region (see section 3.10). Urbanisation affects the climate as is clearly shown in table 1.10.

In summary, man has significantly influenced the environment and the hydrological cycle since the introduction of fixed settlements and agriculture which started about 8000 BC in

Mesopotamia. It will continue to do so as population pressure forces man to intensify the use of natural resources. The hydrologist can not but incorporate these effects in his analysis of the natural system. It is the task of the water resources engineer to look for ways to minimize negative impacts, to restore what has been destroyed and to safeguard what is left for future generations (see lectures on Water Resources Management).

1.5   Hydrological data

In order to make hydrological computations, to establish design criteria and to make forecasts the hydrologist needs data. Data have to be collected, processed and stored in such a way that they can be used easily to solve problems.

Hydrological data can be obtained from several sources. Typical sources are:

- National and regional archives or libraries of agencies responsible for the data acquisition and publication of hydrological, hydrometeorological and related factors, as well as their publications, which usually take the form of annual or monthly compilations and summaries, original records are sometimes available at these sources or in field offices. These records include aerial photographs and information received via satellites;
- Private organizations such as power authorities or companies having an interest in hydrological measurements, e.g. agricultural product marketing companies and oil drilling companies;
- Research papers and project reports;
- Survey reports of research and development agencies;
- Archives of established newspapers;
- Field observations;
- Interviews of people living in the area;
- Maps on related topics.

Hydrological data are usually time series. A time series is a set of data on a certain phenomenon (e.g. water levels) which is ordered in time. A distinction is made between time series of constant time step (equidistant data) and data with varying time step. Data on water levels, flows and rainfall are normally time series at equal time step. A typical characteristic of time series is that serial auto-correlation may be present; i.e. that an observation of a phenomenon at a certain time is related to earlier observations.

Hydrological information systems
A hydrological information system consists of:

- an observation network
- hydrological data base
- hydrological models

The observation network should allow the observation of all relevant components and processes of the hydrological cycle at a sufficiently accurate density, both in time and in space.

The hydrological database is used to store, screen, process and retrieve data at relevant time intervals. Often adequate use can be made of spreadsheets. In this lecture and in the Workshop

Hydrology the basic principles of data screening and processing will be dealt with.

Models are used to describe the processes involved in the hydrological cycle and the links between the different components of the hydrological cycle (e.g. rainfall-runoff models, flood routing models, etc.).

Processing of data
To be able to make a good use of data, the data have to be stored in such a way that all possible errors are removed and that the data are accessible. Several steps are required to get a good storage of data:
- data screening;
- data correction and completion;
- data aggregation;
- data storage;
- publication;

A number of hydrological database systems are on the market for storage and retrieval of hydrological data and time series analysis. They can be used to perform the above steps. Software packages worth mentioning are:

- HYMOS, Hydrological Modelling Systems of Delft Hydraulics
- HYDATA, Hydrological Database System of Wallingford Institute of Hydrology
- REGIS, groundwater database system of TNO-NITG
- Spreadsheets such as EXCEL

The database facilities of EXCEL are quite powerful for pre-processing, screening, analysis and for storage of limited amounts of data. Spreadsheet software is transparent, easy to use and widely available. Of the hydrological databases, HYMOS has the largest amount of routines for time series analysis.

Data screening
Collected data can contain errors due to failures of the measuring device, or the recorder, or to mistakes by the observer. So before storing the data, they have to be checked and errors have to be removed. Sometimes this work is done by the researcher. In larger services there is often a special registration division.

Two types of errors can be distinguished:
- systematic errors;
- accidental errors.

Systematic errors can be caused for example by errors in the installation or insufficient calibration of an instrument, systematic misreading or rounding off errors, etc. Accidental errors can occur, for example, due to occasional misreading of the observer, or malfunctioning of the recorder at some time interval.

Hydrological data are generally time series. For statistical analysis and frequency analysis, time series are required to be stationary, meaning that the statistical properties (mean, standard deviation etc.) of the time series are independent on the choice of the origin of the series. Non-

stationarity occurs in the form of jumps, trends (instability of the mean) and instabilities of the variance. Trends can be either inconsistencies or non-homogeneities. Inconsistencies (external effects) result from changes in the recording of the data, such as those arising from changes in instrumentation or observational practices. Non-homogeneities (internal effects) result from changes in the phenomenon itself, either natural or man-induced, such as changes in land use, water use, climatic changes.

Tests for stability are:
- Spearman's rank test for the absence of trend
- Split record test for stability of the mean (t-test) and variance (F-test)
- Pettitt test to identify change points
- Double mass analysis to identify relative instabilities

After instabilities have been identified, the cause of the instability has to be determined and, where and if possible, be corrected.

Data aggregation
Especially with automatic recorders a tremendous amount of data can be recorded. A great deal of these observations may be unnecessary, as variations in the process are often slow. Therefore, two types of registration can be distinguished:
- fixed time step;
- fixed differences.

By fixed differences only those data are stored where a significant change takes place. The disadvantage of observations at fixed differences is that they are less easy to process automatically. Although observations at fixed time steps are more easy to process, they are generally bulky. Observations at time steps of minutes and hours should be condensed to daily, monthly and annual data.

Data aggregation is the condensation of data with short time steps to data with larger time steps. For instance the aggregation of hourly rainfall to daily, monthly or annual rainfall, or the aggregation of instantaneous discharges to daily, monthly or annual runoff. Two types of aggregation are distinguished:
- through accumulation
- through averaging

Examples of aggregation through accumulation are rainfall and runoff, where short time step data are added up to form large time step data. Whereas examples of aggregation through averaging are temperature, wind speed, water levels and discharge.

Data storage
Data can be stored in paper files, computer files and databases. It is advantageous to store data on computer files or in databases. However two aspects should be kept in mind. In the first place the original paper files must be well guarded. They are the files that are nearest to the original observation and which have not yet accumulated the errors of processing. Secondly, one should analyze carefully what information to store in a database and at which time step. For example, there is not much use in storing large amounts of hourly observations on rainfall and water levels in a data base; they can be kept in a backup file somewhere off-line. Data

which are mostly frequently used, like daily, monthly or annual data, should be kept available on-line.

Publications

When the data are collected over a long period, which is often the case with hydrological data, it is advisable to publish them after screening and pre-processing, preferably in yearbooks.

2   PRECIPITATION

2.1   The atmosphere

The lower layer of the atmosphere, up to a height of approximately10 km, known as the troposphere, is the most interesting part from a hydrologic point of view as it contains almost all of the atmospheric moisture. The percentage of water in moist air is usually less than 4 %. The composition of dry air is given in table 2.1.

	Mass %	**Volume %**
Nitrogen N$_2$	75.5	78.1
Oxygen O$_2$	23.1	20.9
Argon A	1.3	0.9
Others	0.1	0.1

Table 2.1. Composition of dry air.

The atmosphere depends for its heat content on the radiant energy from the sun. About one-sixth of the available solar energy is directly absorbed by the atmosphere, more than one third is reflected into space and less than one half is absorbed by the earth's surface. Heat from the earth's surface is released to the atmosphere by conduction (action of molecules of greater energy on those of less), convection (vertical interchange of masses of air) and radiation (long wave radiation). The process of conduction does not play a significant role. Radiation is an important link in the energy balance of the atmosphere. The "greenhouse effect", the increase of the atmospheric temperature as a result of a decrease in the long wave radiation, has grown into a world-wide concern. It is believed that man-produced gasses such as CO_2, CH_4 and N_2O obstruct the outgoing radiation, gradually leading to an accumulation of energy and hence a higher atmospheric temperature. The effect of long wave radiation is further discussed in Chapter 3.

Convection involves the vertical interchange of masses of air. The process is usually described assuming a parcel of air with approximate uniform properties, moving vertically without mixing with the surroundings. When a parcel of air moves upward it expands due to a decrease of the external pressure. The energy required for the expansion causes the temperature to fall. If the heat content of the air parcel remains constant, which is not uncommon (the parcel is transparent and absorbs little radiant heat), the conditions are called *adiabatic*. The rate of change of air temperature with height is known as the *lapse rate*. The average lapse rate is 0.65 ^{o}C per 100 m rise and varies from 1.0 under *dry-adiabatic* conditions to 0.56 under *saturated-adiabatic* conditions. The lower value for the lapse rate of saturated air results from the release of latent heat due to condensation of water vapour. Its value depends on the air temperature.

The pressure of the air is often specified in mbar and generally taken equal to 1013 mbar or 1.013 bar at mean sea level. In this note the SI unit for pressure Pa (Pascal) will be used, where 1000 mbar = 1 bar = 100,000 Pa = 100 kPa. Hence the pressure at mean sea level is taken as 101.3 kPa. The atmospheric pressure decreases with the height above the surface. For the lower atmosphere this rate is approximately 10 kPa per kilometre.
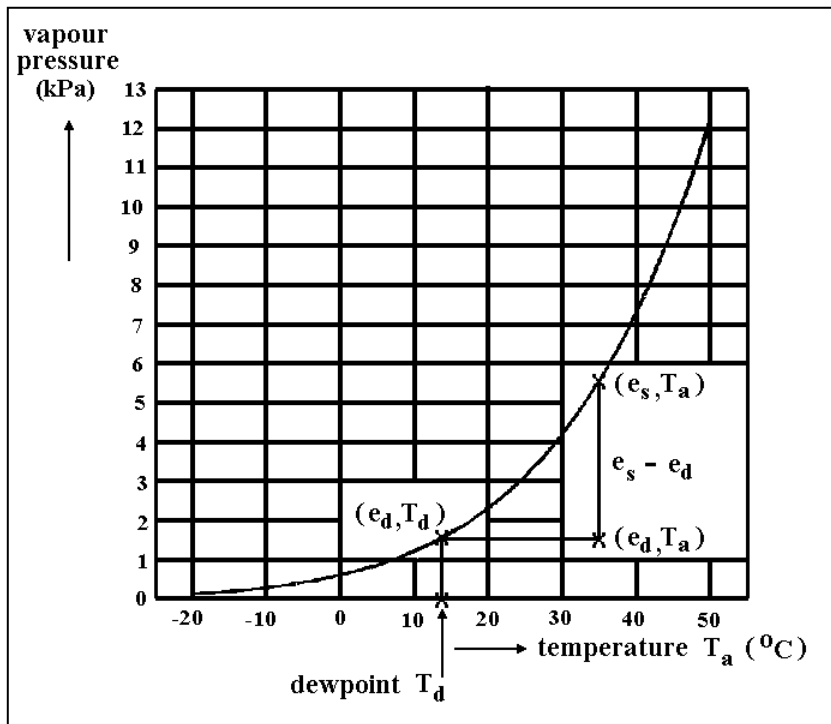
Fig. 2.1 Relation between saturation vapour pressure of the air e_s and air temperature T_a

The water vapour content of the air, or humidity, is usually measured as a water vapour pressure (kPa). The water vapour pressure at which the air is saturated with water vapour, the *saturation vapour pressure* of the air, e_s is related to the temperature of the air as shown in figure 2.1. If a certain mass of air is cooled while the vapour pressure remains constant, the air mass becomes saturated at a temperature known as *dewpoint temperature*, T_d. The corresponding *actual or dewpoint vapour pressure* of the air mass is indicated by e_d. The *vapour pressure deficit* is defined as the difference between the actual vapour pressure and the saturation vapour pressure that applies for the prevailing air temperature T_a, thus *(e_s - e_d)*. The *relative humidity* of the air is the ratio of actual and saturation vapour pressure, or when expressed as a percentage

$$RH = \frac{e_d}{e_s} \, 100 \tag{2.1}$$

2.2   Formation of precipitation

The conditions for precipitation to take place may be summarized stepwise as follows:

1. supply of moisture
2. cooling to below point of condensation
3. condensation
4. growth of particles

The supply of moisture is obtained through evaporation from wet surfaces, transpiration from vegetation or transport from elsewhere. The cooling of moist air may be through contact with a cold earth surface causing dew, white frost, mist or fog, and loss of heat through long wave radiation (fog patches). However, much more important is the lifting of air masses under adiabatic conditions (dynamic cooling) causing a fall of temperature to near its dew point.

Five lifting mechanisms can be distinguished:

1. *Convection*, due to vertical instability of the air. The air is said to be unstable if the temperature gradient is larger than the adiabatic lapse rate. Consequently a parcel moving up obtains a temperature higher than its immediate surroundings. Since the pressure on both is the same the density of the parcel becomes less than the environment and buoyancy causes the parcel to ascend rapidly. Instability of the atmosphere usually results from the heating of the lower air layers by a hot earth surface and the cooling of the upper layers by outgoing radiation. Convective rainfall is common in tropical regions and it usually appears as a thunderstorm in temperate climates during the summer period. Rainfall intensities of convective storms can be very high locally; the duration, however, is generally short.

2. *Orographic lifting*. When air passes over a mountain it is forced to rise which may cause rainfall on the windward slope. As a result of orographic lifting rainfall amounts are usually highest in the mountainous part of the river basin.

3. *Frontal lifting*. The existence of an area with low pressure causes surrounding air to move into the depression, displacing low pressure air upwards, which may then be cooled to dew point. If cold air is replaced by warm air (warm front) the frontal zone is usually large and the rainfall of low intensity and long duration. A cold front shows a much steeper slope of the interface of warm and cold air usually resulting in rainfall of shorter duration and higher intensity (see figure 2.2). Some depressions are died-out cyclones.

4. *Cyclones, tropical depressions or hurricanes*. These are active depressions, which gain energy while moving over warm ocean water, and which dissipate energy while moving over land or cold water. They may cause torrential rains and heavy storms. Typical characteristics of these tropical depressions are high intensity rainfall of long duration (several days). Notorious tropical depressions occur in the Caribbean (hurricanes), the Bay of Bengal (monsoon depressions), the Far East (typhoons), Southern Africa (cyclones), and on the islands of the Pacific (cyclones, willy-willies). This group of depressions is quite different in character from other lifting mechanisms; data on extreme rainfall originating from cyclones should be treated separately from other rainfall data, as they belong to a different statistical population. One way of dealing with cyclones is through mixed distributions (see Section 2.8).

5. *Convergence*. The Inter-Tropical Convergence Zone is the tropical region where the air masses originating from the Tropics of Cancer and Capricorn converge and lift. In the tropics, the position of the ITCZ governs the occurrence of wet and dry seasons. This convergence zone moves with the seasons. In July, the ITCZ lies to the North of the equator and in January it lies to the South (see figure 2.3). In the tropics the position of the ITCZ determines the main rain-bringing mechanism which is also called monsoon. Hence, the ITCZ is also called the Monsoon Trough, particularly in Asia. In certain places near to the equator, such as on the coast of Nigeria, the ITCZ passes two times per year, causing two wet seasons; near the Tropics of Capricorn and Cancer (e.g. in the Sahel), however, there is generally only one dry and one wet season.
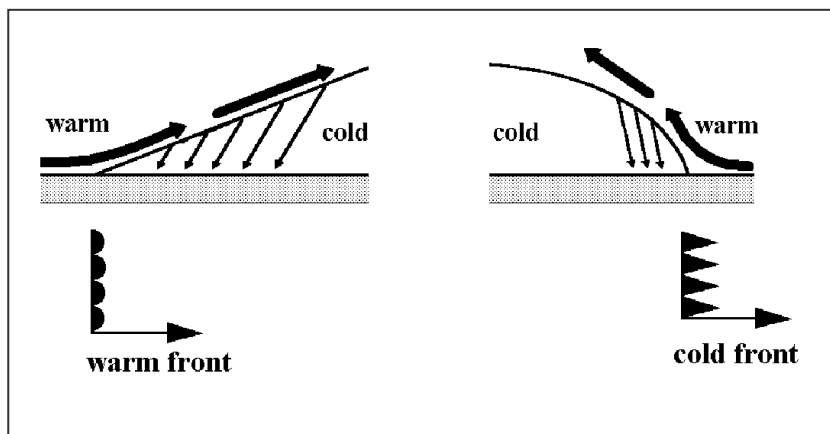
Fig. 2.2 Frontal lifting

Condensation of water vapour into small droplets does not occur immediately when the air becomes saturated. It requires small airborne particles called aerosols, which act as nuclei for water vapour to condense. Nuclei are salt crystals from the oceans, combustion products, dust, ash, etc. In the absence of sufficient nuclei the air becomes supersaturated.

When the temperature drops below zero, freezing nuclei with a structure similar to ice are needed for condensation of water vapour into ice crystals. These nuclei are often not available and the droplets become super-cooled to a temperature of -40 °C.

Cloud droplets with a diameter of 0.01 mm need an updraught of only 1 cm.s^{-1} to prevent the droplet from falling. A growth of particles is necessary to produce precipitation. This growth may be achieved through coalescence, resulting from collisions of cloud droplets. Small droplets moving upwards through the clouds collide and unite with larger droplets which have a different velocity or move downwards. Another method of growth known as the Bergeron process is common in mixed clouds, which consist of super-cooled water droplets and ice crystals. Water vapour condenses on the ice crystals, the deficit being replenished by the evaporation of numerous droplets. In the temperature range from -12 °C to -30 °C the ice crystals grow rapidly and fall through the clouds. Aggregates of many ice crystals may form snowflakes. Depending on the temperature near the surface they may reach the ground as rain, snow, hail or glazed frost.
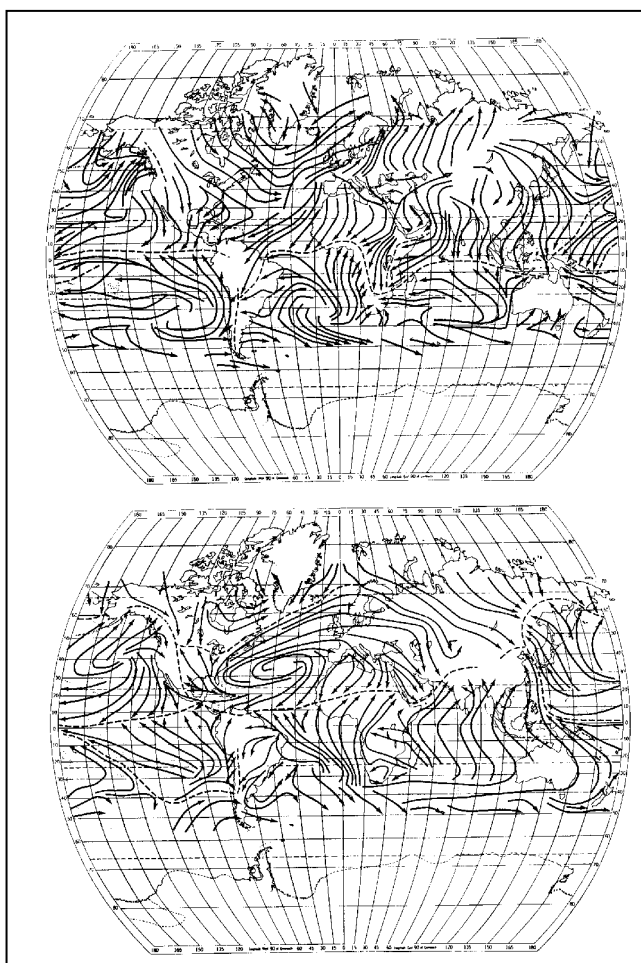

Fig. 2.3 Position of the Inter-Tropical Convergence Zone in January (top) and July (below)

2.3.   Rainfall measurement

The standard raingauge as depicted in figure 2.4 is used for daily readings. The size of the aperture and the height varies between countries but is usually standardized within each country (The Netherlands: aperture 200 cm^2, height 40 cm).

The requirements for gauge construction are:

1.   The rim of the collector should have a sharp edge.
2.   The area of the aperture should be known with an accuracy of 0.5 %.
3.   Design is such that rain is prevented from splashing in or out.
4.   The reservoir should be constructed so as to avoid evaporation.
5.   In some climates the collector should be deep enough to store one day's snowfall.

Wind turbulence affects the catch of rainfall. Experiments in the Netherlands using a 400 cm^2 raingauge have shown that at a height of 40 cm the catch is 3-7 % less than at ground level and as much as 4-16 % at a height of 150 cm. Tests have shown that raingauges installed on the roof of a building may catch substantially less rainfall as a result of turbulence (10-20%).
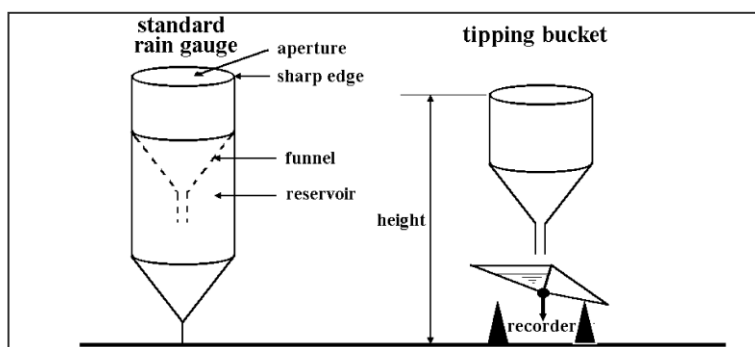

Fig. 2.4 Raingauges

Wind is probably the most important factor in rain-gauge accuracy. Updrafts resulting from air moving up and round the instrument reduce the rainfall catch. Figure 2.5 shows the effect of wind speed on the catch according to Larson & Peck (1974). To reduce the effects of wind, raingauges can be provided with windshields. Moreover, obstacles should be kept far from the rainguage (distance at least twice the height of such an object) and the height of the gauge should be minimised (e.g. ground-level raingauge with screen to prevent splashing).

Recording gauges are of three different types: the weighing type, the tilting bucket type and the float type. The weighing type observes precipitation directly when it falls (including snow) by recording the weight of the reservoir e.g. with a pen on a chart. With the float type the rain is collected in a float chamber. The vertical movement of the float is recorded by pen on a chart. Both types have to be emptied manually or by automatic means. The tilting or tipping bucket type (figure 2.4) is a very simple recording raingauge, but less accurate (only registration when bucket is full, losses during tipping and losses due to evaporation).
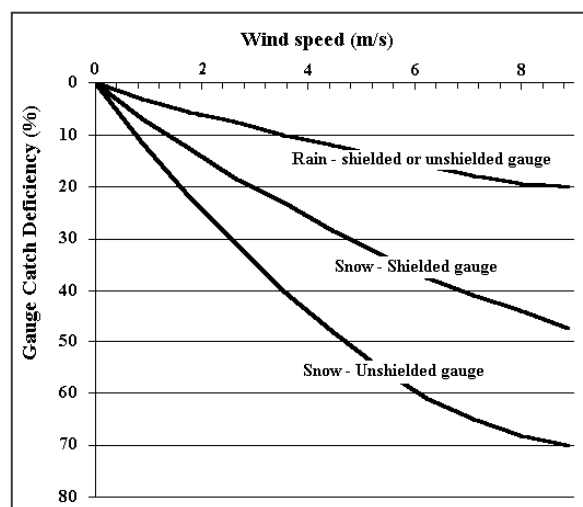

Fig. 2.5 Effect of wind speed on rain catch
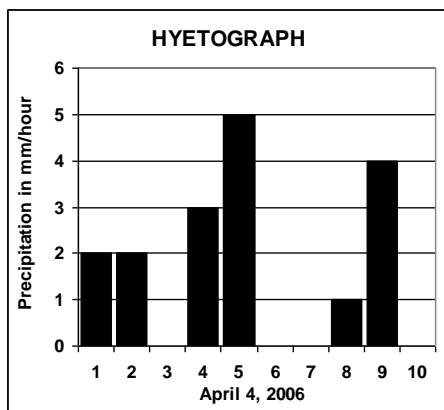
HYETOGRAPH

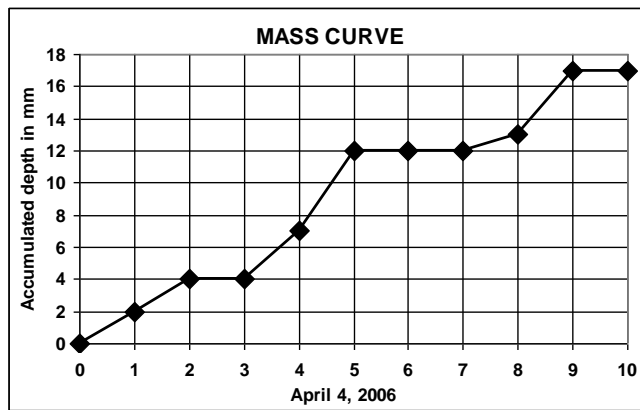**MASS CURVE**

Fig. 2.6a Hyetograph

Fig. 2.6b Corresponding mass curve

Storage gauges for daily rainfall measurement are observed at a fixed time each morning. Recording gauges may be equipped with charts that have to be replaced every day, week or month, depending on the clockwork. The rainfall is usually recorded cumulatively (mass curve) from which the hyetograph (a plot of the rainfall with time) is easily derived (see figure 2.6). The tipping bucket uses an electronic counter or magnetic tape to register the counts (each count corresponds to 0.2 mm), for instance, per 15 minutes time interval.

Rainfall measurement by radar and satellite
Particularly in remote areas or in areas where increased spatial or time resolution is required radar and satellite measurement of rainfall can be used to measure rainfall. Radar works on the basis of the reflection of an energy pulse transmitted by the radar which can be elaborated into maps that give the location (plan position indicator, PPI) and the height (range height indicator, RHI) of the storms (see figure 2.7, after Bras, 1990).

A technology, which has a large future, is rainfall monitoring through remote sensing by satellite. Geostationary satellites that orbit at the same velocity as the earth's rotation are able to produce a film of weather development with a time interval between observations of several minutes. The resolution of the images is in the order of 1 km. This allows to monitor closely the development of convective storms, depressions, fronts, orographic effects and tropical cyclones.
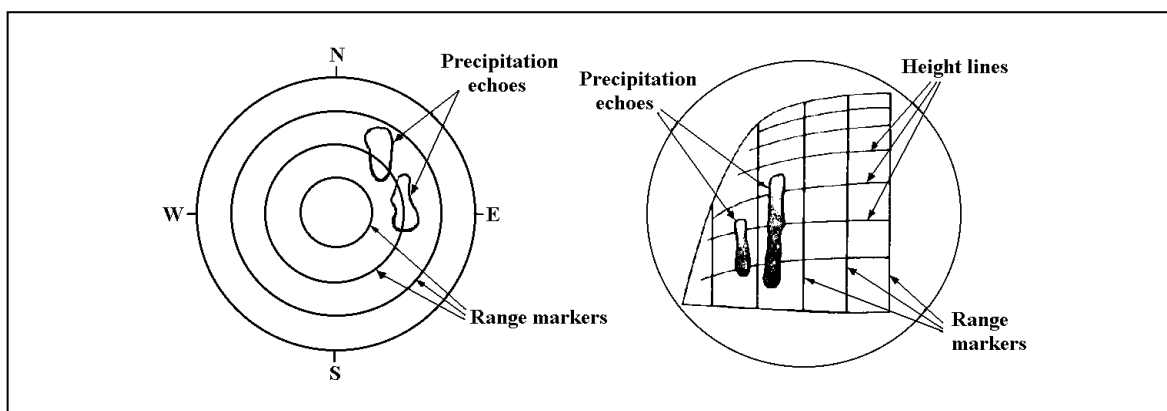
Fig. 2.7 Forms of radar display: PPI (left) and RHI (right)

Successful efforts have been made to correlate rainfall with Cold Cloud Coverage (CCC) and Cold Cloud Duration (CCD) through simple mathematical regression. Particularly in remote areas the benefits of such methods are obvious.

Parameters defining rainfall
When discussing rainfall data the following elements are of importance:
1. Intensity or rate of precipitation: the depth of water per unit of time in m/s, mm/min, or inches/hour (see Section 2.4).
2. Duration of precipitation in seconds, minutes or hours (see Section 2.4).
3. Depth of precipitation expressed as the thickness of a water layer on the surface in mm or inches (see Section 2.4).
4. Area, that is the geographic extent of the rainfall in km^2 (see Section 2.5).
5. Frequency of occurrence, usually expressed by the 'return period' e.g. once in 10 years (see Section 2.7).

2.4. Intensity, duration and rainfall depth

We have seen that rainfall storms can be distinguished by their meteorological characteristics (convective, orographic, frontal, cyclonic). Another way to characterize storms is from a statistical point of view. Distinction is made between "interior" and "exterior" statistics:

* exterior statistics refer to total depth of the storm, duration of the storm, average intensity of the storm and time between storms;
* interior statistics refer to the time and spatial distribution of rainfall rate within storms.

The exterior statistics can generally be described by probabilistic distributions, which can be seasonally and spatially dependent. They are generally not statistically independent. Depth is related to duration: a long duration is associated with a large depth; average high intensity is related to short duration. Moreover there is spatial correlation between points.

With regard to storm interior, Eagleson (1970) observed that for given locations and climatic conditions some type of storms gave similar histories of rainfall accumulation. The percentage-mass curve of figure 2.8 shows how typical curves are obtained for thunderstorms (convective storms) and cyclonic storms. The derivative (slope) of these curves is a graph for the rainfall intensity over time. Such a graph is referred to as the hyetograph and is usually presented in histogram form (see figure 2.6). It
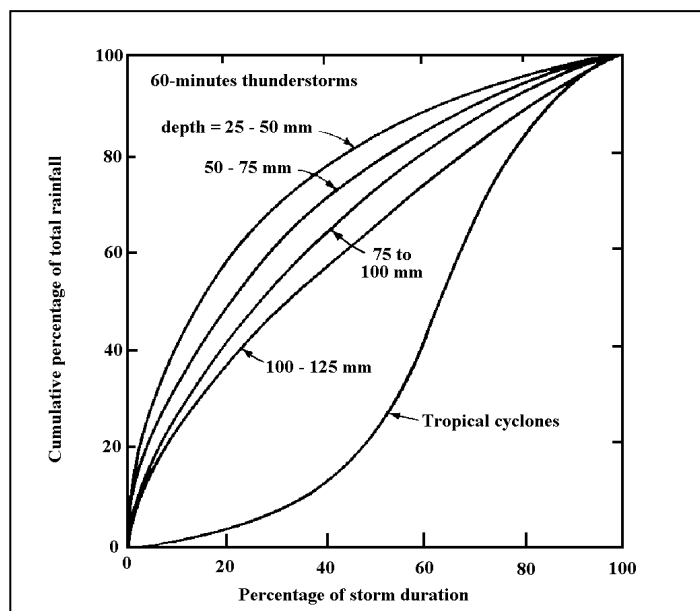

Fig. 2.8 Typical percentage mass curves of rainfall for thunderstorms and cyclones

can be seen from figure 2.8 that convective storms have more or less triangular (moundlike) hyetographs with the highest intensity at the beginning of the storm (a steep start), whereas tropical cyclones have a bell-shaped hyetograph with the largest intensity in the middle of the storm. It should be observed that tropical cyclones have a much longer storm duration and a much larger rainfall depth than thunderstorms.

Another interior characteristic of a storm is the spatial distribution. The spatial distribution of a storm generally concentrates around one or two centres of maximum depth. The total depth of point rainfall distributed over a given area is a decreasing function of the distance from the storm centre. One can draw lines of equal rainfall depth around the centres of maximum depth (isohyets).

When two rainfall stations are closely together, data from these stations may show a good correlation. The further the stations lay apart, the smaller the chances of coincidence become. In general, correlation is better when the period of observation is larger. For a given period of observation, the correlation between two stations is defined by the correlation coefficient ρ (*-1 < ρ < 1)*. If there is no correlation, ρ is near to zero, if the correlation is perfect, $\rho = 1$. It is defined by:

$$\rho = \frac{\mathbf{cov\,(x,y)}}{\sigma(\mathbf{x})\,\sigma(\mathbf{y})} \tag{2.2}$$

For a number of stations in a certain area the correlation coefficient can be determined pairwise. In general, the larger the distance, the smaller the correlation will be. If r is defined as the distance between stations, then the correlation between stations at a distance r apart is often described by Kagan's formula:

$$\rho(\mathbf{r}) = \rho_0\; e^{-\frac{r}{r_0}} \tag{2.3}$$
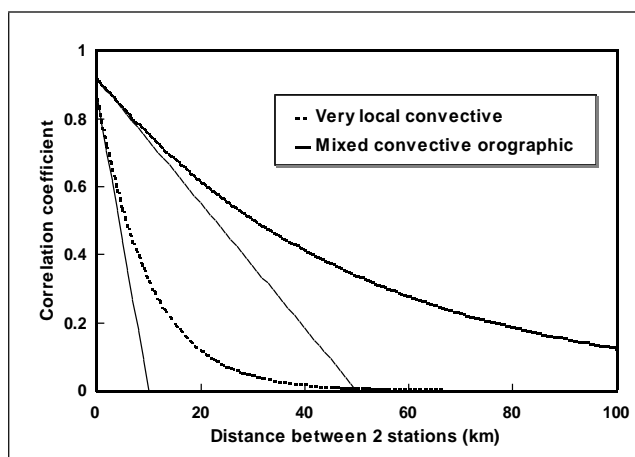
Fig. 2.9 Spatial correlation of daily rainfalls

This is an exponential function which equals ρ_o at $r = 0$ and which decreases gradually as r goes to infinity. The distance r_o is defined as the distance where the tangent at $x = 0$ intersects the *x*-axis (see figure 2.9). For convective storms, the steepness is very large and the value of r_o is small; for frontal or orographic rains, the value is larger. Also the period considered is reflected in the steepness; for a short period of observation r_o is small. Table 2.2 gives indicative values of r_o and ρ_o.

Rain type	Period 1 hour		Period 1 day		Period 1 month	
	r_o (km)	ρ_o	r_o (km)	ρ_o	r_o (km)	ρ_o
Very local convective	5	0.80	10	0.88	50	0.95
Mixed convective orographic	20	0.85	50	0.92	1500	0.98
Frontal rains from depressions	100	0.95	1000	0.98	5000	0.99

Table 2.2   **Typical spatial correlation structure for different storms**

2.5   Areal rainfall

In general, for engineering purposes, knowledge is required of the average rainfall depth over a certain area: the areal rainfall. Some cases where the areal rainfall is required are: design of a culvert or bridge draining a certain catchment area, design of a pumping station to drain anFigure 1 urbanized area; design of a structure to drain a polder, etc.

Fig. 2.10 Thiessen polygons

There are various methods to estimate the average rainfall over an area (areal rainfall) from point-measurements.
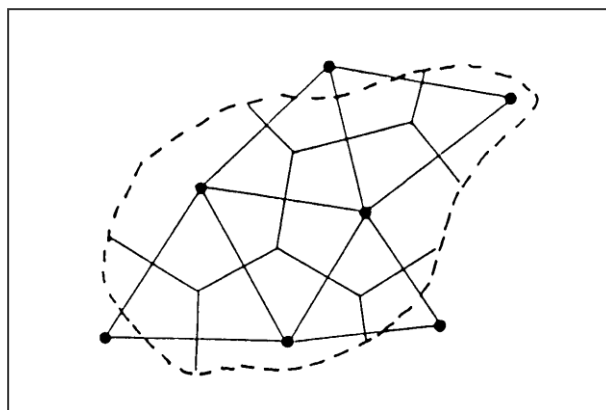
1. *Average depth method*. The arithmetic mean of the rainfall amounts measured in the area provides a satisfactory estimate for a relatively uniform rain. However, one of the following methods is more appropriate for mountainous areas or if the raingauges are not evenly distributed.

2. *Thiessen method*. Lines are drawn to connect reliable rainfall stations, including those just outside the area. The connecting lines are bisected perpendicularly to form a polygon around each station (see figure 2.10). To determine the mean, the rainfall amount of each station is multiplied by the area of its polygon and the sum of the products is divided by the total area.

3. *Kriging*. D.G. Krige, a mining expert, developed a method for interpolation and averaging of spatially varying information, which takes account of the spatial variability and which - unlike other methods - can also indicate the level of accuracy of the estimates made. The Kriging weights obtained are tailored to the variability of the phenomenon studied. Figure 2.11 shows the comparison between weights obtained through Thiessen's method (a) and Kriging (b).

4. *Isohyetal method*. Rainfall observations for the considered period are plotted on the map and contours of equal precipitation depth (isohyets) are drawn (figure 2.12). The areal rainfall is determined by measuring the area between isohyets, multiplying this by the average precipitation between isohyets, and then by dividing the sum of these products by the total area.
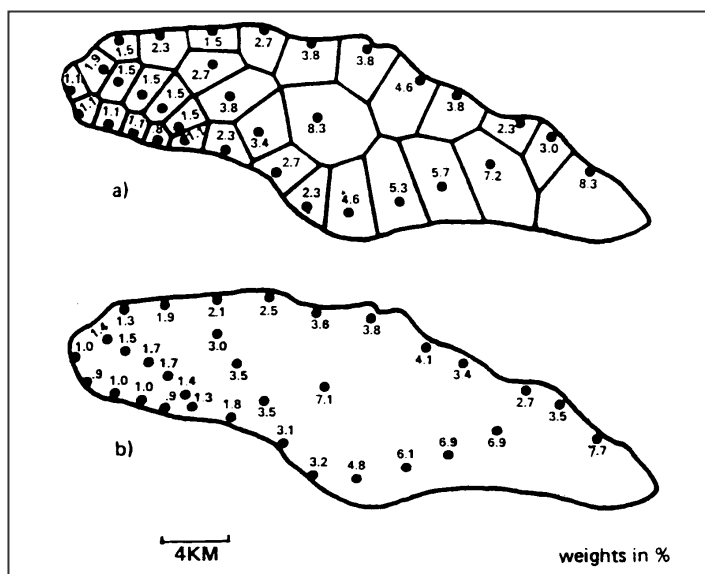
Fig. 2.11 Comparison of Thiessen (a) and Kriging (b) methods
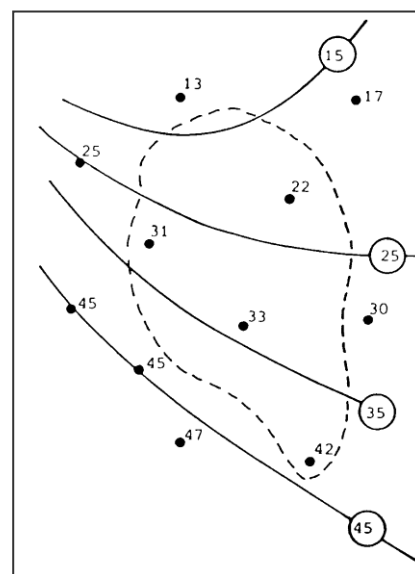
Fig. 2.12 Isohyetal method

As a result of the averaging process, and depending on the size of the catchment area, the areal rainfall is less than the point rainfall. The physical reason for this lies in the fact that a rainstorm has a limited extent. The areal rainfall is usually expressed as a percentage of the storm-centre value: the *areal reduction factor* (ARF). The ARF is used to transfer point rainfall P_p extremes to areal rainfall P_a :

$$\mathbf{ARF} = \mathbf{P_a} \, / \, \mathbf{P_p} \tag{2.4}$$

Basically the ARF is a function of:
- rainfall depth
- storm duration
- storm type
- catchment size
- return period (see Section 2.7).

The ARF increases (comes nearer to unity) with increasing total rainfall depth, which implies higher uniformity of heavy storms. It also increases with increasing duration, again implying that long storms are more uniform. It decreases with the area under consideration, as a result of the storm-centred approach.

Storm type varies with location, season and climatic region. Published ARF's are, therefore, certainly not generally applicable. From the characteristics of storm types, however, certain conclusions can be drawn.

A convective storm has a short duration and a small areal extent; hence, the ARF decreases steeply with distance. A frontal storm has a long duration and a much larger area of influence; the ARF, hence, is expected to decrease more slowly with distance. The same applies to orographic lifting. Cyclones also have long durations and a large areal extent, which also leads to a more gradual reduction of the ARF than in the case of thunderstorms. In general, one can
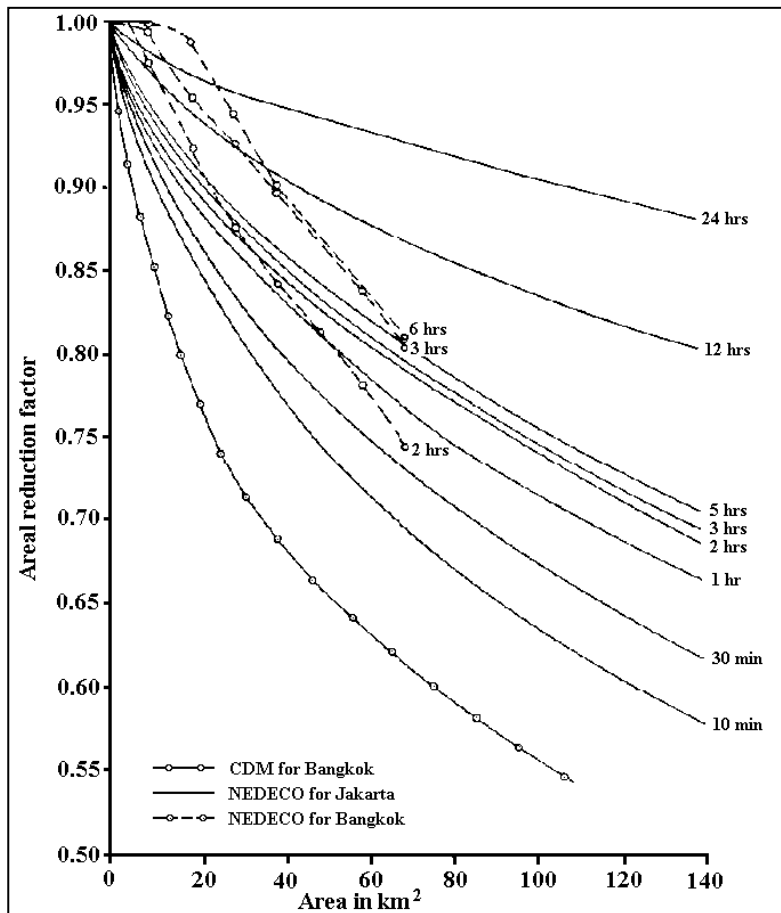
Fig. 2.13   The areal reduction factor as a function of drainage area and duration (after NEDECO et al., 1983)

say that the ARF-curve is steepest for a convective storm, that a cyclonic storm has a more moderate slope and that orographic storms have an even more moderate slope.

The functional relationship between the ARF and return period is less clear. Bell (1976) showed for the United Kingdom that ARF decreased more steeply for rainstorms with a high return period. Similar findings are reported by Begemann (1931) for Indonesia. This is, however, not necessarily so in all cases. If widespread cyclonic disturbances, instead of more local convective storms, constitute the high return period rainfall, the opposite may be true.

Again, it should be observed that cyclones belong to a different statistical population from other storm types, and that they should be treated separately. If cyclones influence the design criteria of an engineering work, then one should consider a high value of the ARF.

Figure 2.13, as an example, shows ARF's as a function of catchment size and rainfall duration for Bangkok by Nedeco (1983), and Camp, Dresser and McKee (1968), and for Jakarta by Nedeco (1973).

2.6   Rainfall data screening

Of all hydrological data, rainfall is most readily available. Though quantitatively abundant its quality should not, a priori, be taken for granted, despite the fact that precipitation data are easily obtained. Several ways of specific rainfall data screening are available besides the ones described in Section 1.5.

daily rainfall

- tabular comparison, maximum values check
- time series plotting and comparison
- spatial homogeneity test

monthly rainfall

- tabular comparison, maximum, minimum, P_{80}, P_{20} check
- time series plotting
- spatial homogeneity test
- double mass analysis

tabular comparison

In a table a number of checks can be carried out to screen rainfall data. One way is through internal operations and another through comparison with other tables. Internal operations are the computation of the maximum, minimum, mean and standard deviation for columns or ranges in the table. Spreadsheet programs are excellent tools for this purpose. A table of daily rainfall organised in monthly columns can be used to compute the monthly sums, the annual total, and the annual maximum. Comparison of these values with those of a nearby station could lead to flagging certain information as doubtful. A table showing monthly totals for different years can be used for statistical analysis. In many cases the normal or lognormal distribution fits well to monthly rainfall. In such a case the computation of the mean and standard deviation per month (per column) can be used to compute the rainfall with a probability of non-exceedence of 20% (a dry year value) or 80% (a wet year value) through the following simple formula:

$$P_{20} = Mean - 0.84 * Std$$
$$P_{80} = Mean + 0.84 * Std$$

If the lognormal distribution performs better (as one would expect since rainfall has a lower boundary of 0), than the values of mean and standard deviations should be based on the logarithms of the recorded rainfall: *Lmean*, and *Lstd*. The values of P_{20} and P_{80} then read:

$$P_{20} = Exp (Lmean - 0.84 * Lstd)$$
$$P_{80} = Exp (Lmean + 0.84 * Lstd)$$

If individual monthly values exceed these limits too much, they should be flagged as suspect, which does not, a priori, mean that the data are wrong; it is just a sign that one should investigate the data in more detail.

double mass

The catch of rainfall for stations in the same climatic region is, for long-time periods, closely related. An example showing the mass curves of cumulative annual precipitation of two nearby stations *A* and *B* is given in figure 2.14a. The double mass curve of both stations plots approximately as a straight line (see figure 2.14b). A deviation from the original line indicates a change in observations in either station *A* or *B* (e.g. new observer, different type of raingauge, new site, etc.). This is called a spurious (= false) trend, not to be mistaken for a real trend, which is a gradual change of climate. If the cumulative annual rainfall data of station *X* are plotted against the mean of neighbouring stations the existence of a spurious trend indicates that the data of station *X* are inconsistent (figure 2.15). When the cause of the discrepancy is clear, the monthly rainfall of station *X* can be corrected by a factor equal to the proportion of the angular coefficients.

time series plotting
Although these tabular operations can help to identify possible sources of errors, there is nothing as powerful to pinpoint suspect data as a graphical plot. In a spreadsheet a graphical plot is easy to perform. One can use a bar-graph for a simple

Fig. 2.14 **Mass curves of individual stations A and B (left) and double mass curve of stations A and B (right)**

time plot, a stacked bar-graph to view two combined sets, or an X -Y relation to compare one station with another nearby station. The latter is a powerful tool to locate strange values.

spatial homogeneity
In the spatial homogeneity test a base station is related to a number of surrounded stations. A maximum distance r_{max} is defined on the basis of (2.3) beyond which no significant correlation is found (e.g. $\rho < 0.75$ or 0.5). To investigate the reliability of

Fig. 2.15 **Double mass curve showing apparent trend for station X**

point rainfall, the observed rainfall is compared with an estimated rainfall depth on the basis of spatial correlation with others (computed from a weighted average through multiple regression).

A formula often used for the weighted average is by attributing weights that are inversely proportional to the square of the distance from the station in question:

$$P_{est} = \frac{\Sigma\left(\dfrac{P}{r^b}\right)_i}{\Sigma\left(\dfrac{1}{r^b}\right)_i} \tag{2.5}$$

where *b* is the power for the distance, which is often taken as 2, but which should be determined from experience. If the observed and the estimated rainfall differ more than an acceptable error criterion, both in absolute and relative terms, then the value should be further scrutinized, or may have to be corrected (see Workshop on Hydrology).
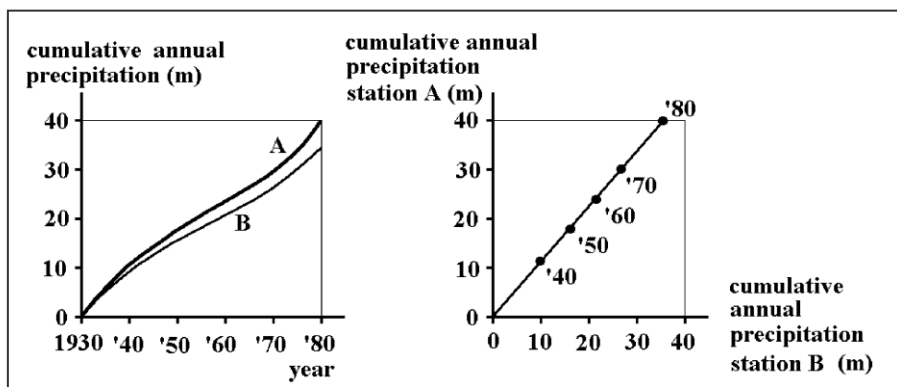
Fig. 2.16a **Frequency distribution daily rainfall data for Wageningen**
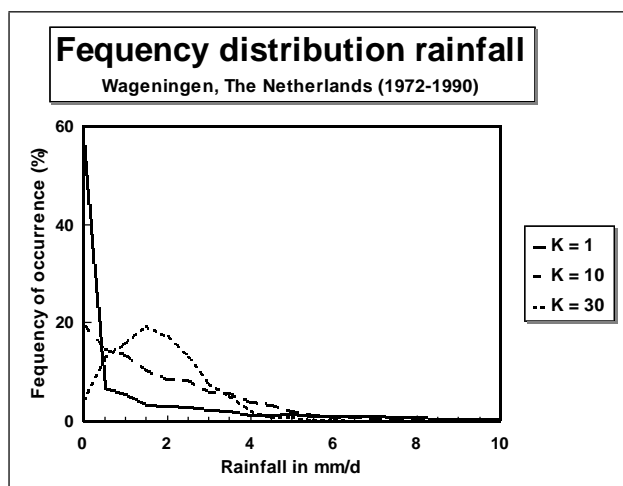
Fig. 2.16b **Frequency distribution of average rainfall data with a K-day duration, Wageninegn**

2.7   Frequency analysis

Consider daily rainfall data over a period of many years and compute the percentage of days with rainfall between 0 - 0.5 mm, 0.5 - 1.0 mm, 1.0 - 1.5 mm, etc. The frequency of occurrence of daily rainfall data may then be plotted. An example for a station in the Netherlands is given in figure 2.16A. It shows that the frequency distribution is extremely skew, as days without rain or very little rain occur most frequently and high rainfall amounts are scarce. The distribution becomes less skew if the considered duration (k) is taken longer. Table 2.3 gives an example of the derivation of rainfall data for longer durations ($k = 2$, 5 and 10 days) from daily values for a record length of 15 days. An example of frequency distributions of average rainfall data for $k = 1$, 10 and 30 days for a rainfall station in the Netherlands is given in figure 2.16B.

no.	1	2	3	4	5	6	7	8	9	10	11	12	13	14	15
k															
1	0	0	2	8	0	0	0	0	0	12	3	8	24	2	0
2		0	2	10	8	0	0	0	0	12	15	11	32	26	2
5				10	10	10	8	0	12	15	23	47	49	37	
10										22	25	33	55	49	49

Table 2.3   Derivation of rainfall data for duration (k) of 2, 5 and 10 days from 15 daily values

For the design of drainage systems, reservoirs, hydraulic works in river valleys, irrigation schemes, etc. knowledge of the frequency of occurrence of rainfall data is often essential.

The type of data required depend on the purpose; for the design of an urban drainage system rainfall intensities in the order of magnitude of mm/min are used, while for agricultural areas the frequency of occurrence of rainfall depths over a period of several days is more appropriate.

When dealing with extremes it is usually convenient to refer to probability as the *return period* that is, the average interval in years between events which equal or exceed the considered magnitude of event. If *p* is the probability that the event will be equalled or exceeded in a particular year, the return period *T* may be expressed as

$$\mathbf{T} = \frac{1}{\mathbf{p}} \tag{2.6}$$

One should keep in mind that a return period of a certain event e.g. 10 years does not imply that the event occurs at 10 year intervals. It means that the probability that a certain value (e.g. a rainfall depth) is exceeded in a certain year is 10%. Consequently the probability that the event does not occur (the value is not exceeded) has a probability of 90%. The probability that the event does not occur in ten consecutive years is $(0.9)^{10}$ and thus the probability that it occurs once or more often in the ten years period is $1 - (0.9)^{10} = 0.65$; i.e. more than 50%. Similarly, the probability that an event with a return period of 100 years is exceeded in 10 years is $1 - (0.99)^{10} = 10\%$. This probability of 10% is the actual risk that the engineer takes if he designs a structure with a lifetime of 10 years using a design criterion of $T = 100$. In general, the probability *P* that an event with a return period *T* actually occurs (once or more often) during an *N* years period is:

$$\mathbf{P} = \mathbf{1} - \left(\mathbf{1} - \frac{\mathbf{1}}{\mathbf{T}}\right)^{\mathbf{N}} \tag{2.7}$$

A frequency analysis to derive intensity-duration-frequency curves requires a length of record of at least 20 - 30 years to yield reliable results. The analysis will be explained with a numerical example, using hypothetical data. Consider a record of 50 years of daily precipitation data, thus $365.25 * 50 = 18262$ values (provided there are no missing or unreliable data). Compute the number of days with rainfall events greater than or equal to 0, 10, 20, 30, etc. mm. For this example large class intervals of 10 mm are used to restrict the number of values. In practice a class interval of 0.5 mm (as in fig. 2.16a) or even smaller is more appropriate.

Table 2.4 shows that all 18262 data are greater than or equal to zero (of course), and that there is only one day on which the amount of rainfall equalled or exceeded 40 mm. Similar to the procedure explained in table 2.3, rainfall data are derived for $k = 2$, 5 and 10 days. For $k = 2$ this results in 18261 values which are processed as for the daily rainfall data, resulting in two values with 60 mm or more. The results for $k = 2$, 5 and 10 are also presented in table 2.4 The data are used to construct duration curves as shown in figure 2.18.

The procedure is the following. Consider the data for $k = 1$ which show that on one day in 50 years only the amount of rainfall equals or exceeds 40 mm, hence the probability of occurrence in any year is $P = 1/50 = 0.02$ or 2 % and the return period $T = 1/P = 50$ years. This value is plotted in figure 2.17. Similarly for rainfall events greater than or equal to 30 mm, $P = 5/50 =- 0.1$ or $T = 10$ years and for 20 mm, $P = 48/50 = 0.96$ or $T \approx 1$ year. Figure 2.17 shows the resulting curves for a rainfall duration of one day as well as for $k = 2$, 5 and 10 days.

Cumulative frequency or duration curves often approximate a straight line when plotted as in figure 2.17 on semi-logarithmic graph paper, which facilitates extrapolation. Care should be taken with regard to extrapolation of frequency estimates, in particular if the return period is larger than twice the record length.

Figure 2.17 shows that for durations of 1, 2, 5 and 10 days the rainfall events equal or exceed respectively 20, 30, 60 and 100 mm with a return period of one year. These values are plotted in figure 2.18 to yield the depth-duration curve with a frequency
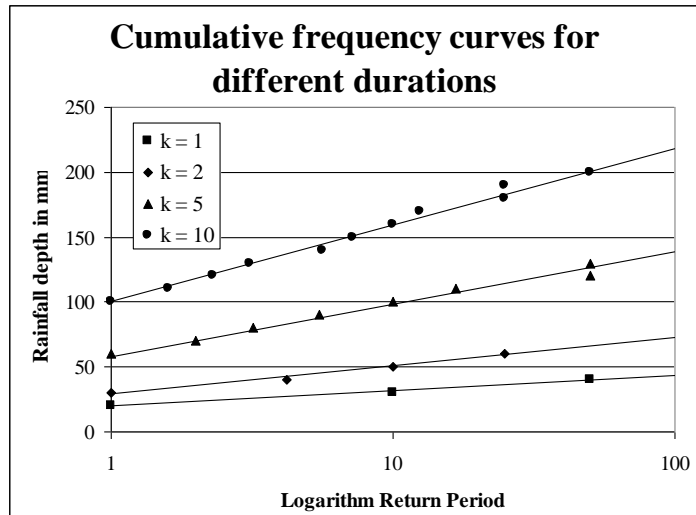

Fig. 2.17 Cumulative frequency curves for different durations (k = 1, 2, 5 and 10 days).
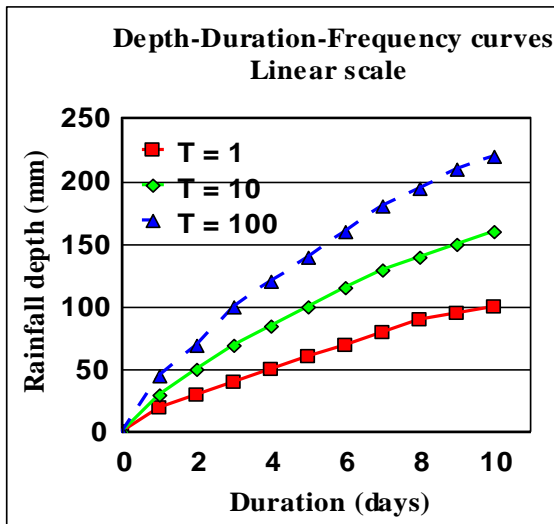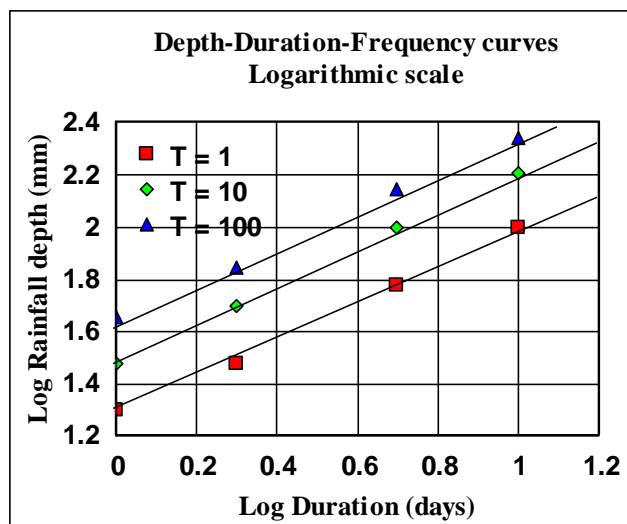

Fig. 2.18a Depth-Duration-Frequency curves

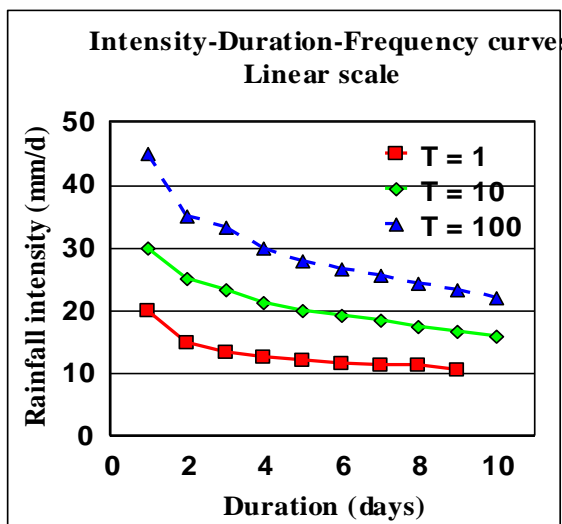**Fig. 2.18b Double logarithmic plot of DDF curves**

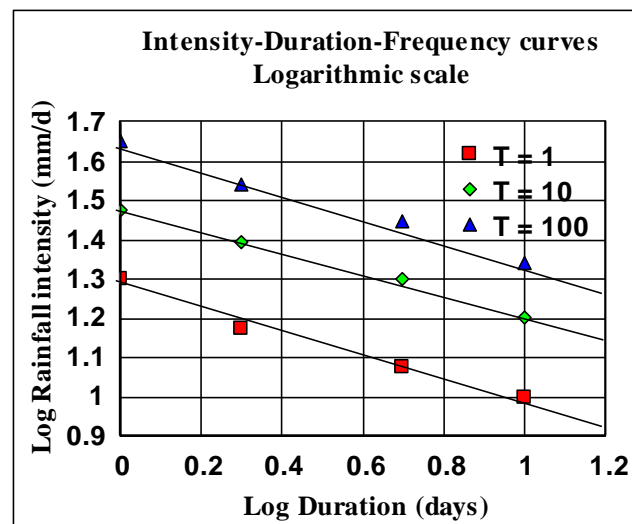**Fig. 2.19a Intensity-Duration-Frequency curves**

Fig. 2.19b Double logarithmic plot of IDF curves

of $T = 1$ year. Similarly the curves for $T = 10$ and the extrapolated curve for $T = 100$ years are constructed. On double logarithmic graph paper these curves often approximate a straight line. Dividing the rainfall depth by the duration yields the average intensity. This procedure is used to convert the *depth-duration-frequency curves* into *intensity-duration-frequency curves* (figure 2.19).

For the above analysis *all* available data have been used, i.e. the *full series*. As the interest is limited to relatively rare events, the analysis could have been carried out for a *partial duration series*, i.e. those values that exceed some arbitrary level. For the analysis of extreme precipitation amounts a series, which is made up of annual extremes, the *annual series*, is favoured as it provides a good theoretical basis for extrapolating the series beyond the period of observation. The partial duration series overcomes an objection to the annual series since it is made up of all the large events above a given base, thus not just the annual extreme.

Class interval (mm)	1	2	5	10
0	18262	18261	18258	18253
10	384	432	730	2001
20	48	127	421	1539
30	5	52	243	713
40	1	12	158	493
50		5	83	286
60		2	49	221
70			25	170
80			16	96
90			9	76
100			5	49
110			3	31
120			1	22
130			1	16
140				9
150				7
160				5
170				4
180				2
190				2
200				1

Table 2.4 **Totals of *k*-day periods with rainfall greater than the bottom of the class interval for k = 1, 2, 5 and 10 days**

Langbein (see Chow, 1964) developed a theory for partial duration series which considers all rainfall exceeding a certain threshold. The threshold is selected in such a way that the number of events exceeding the threshold equals the number of years under consideration. Then, according to Langbein, the relationship between the return period of the annual extremes T and return period of the partial series T_p is approximately:

$$p = \frac{1}{T} = 1 - e^{-\frac{1}{T_p}}$$
(2.8)

Figure 2.20 shows the comparison between the frequency distribution of the extreme hourly rainfall in Bangkok computed with partial duration series (= annual exceedences) and with annual extremes. A comparison of the two series shows that they lead to the same results for larger return periods, say $T > 10$ years. Hershfield (1961) proposes to multiply the rainfall depth obtained by the annual extremes method by 1.13, 1.04, and 1.01 for return periods of 2, 5 and 10 years respectively.

The analysis of annual extreme precipitation is illustrated with the following numerical example. For a period of 10 years the maximum daily precipitation in each year is listed in table 2.5. For convenience a (too) short period of 10 years is considered. Rank the data in descending order (see table 2.6). Compute for each year the probability of exceedence using the formula

$$p = \frac{m - \alpha}{N + 1 - 2\alpha}$$
(2.9)
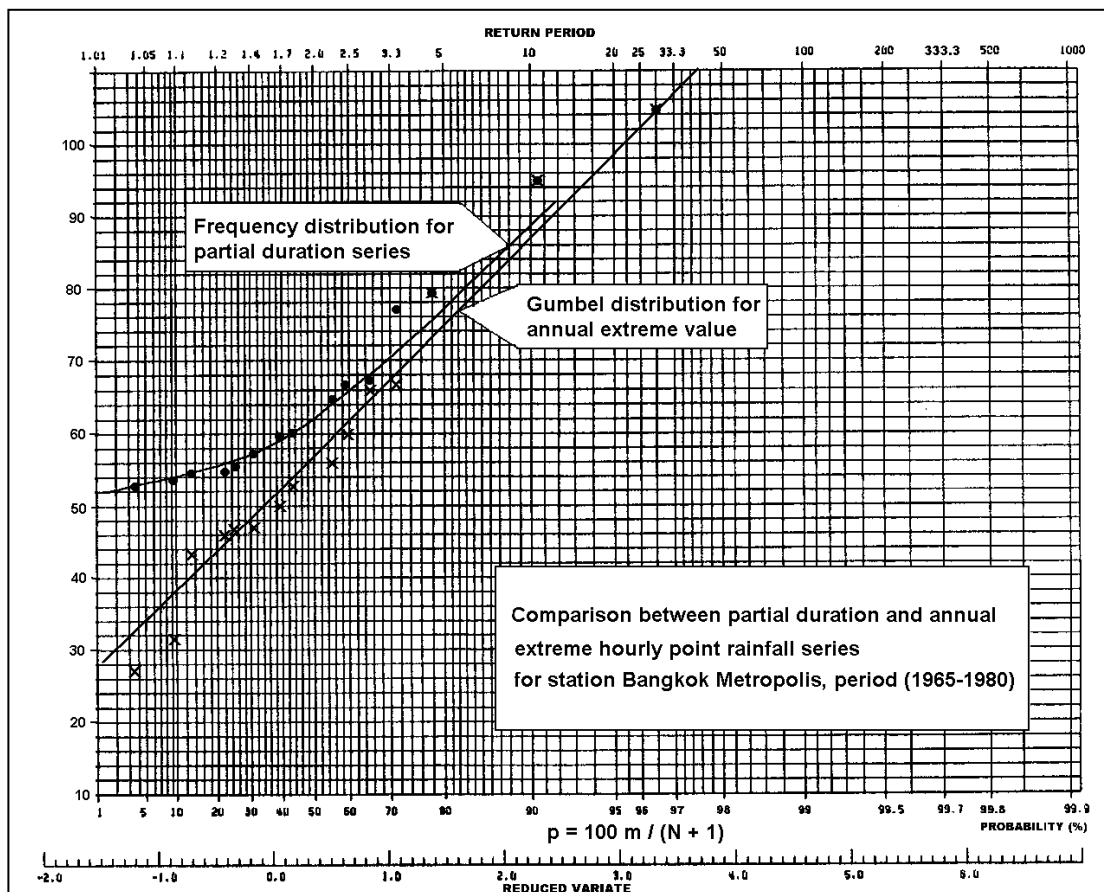
Fig. 2.20 Comparison between the method of annual exceedences and annual extremes for extreme hourly rainfall in Bangkok

where N is the number of years of record and m is the rank number of the event and α a parameter less than one. Equation (2.9) is also known as the plotting position. In the example above α is taken equal to zero (Weibull formula). For the Gumbel distribution the Gringerton formula with $\alpha = 0.44$ is often used (see Cunnane, 1977). The return period T is computed as $T = 1/p$ and is also presented in table 2.6. A plot of the annual extreme precipitation versus the return period on linear paper does not yield a straight line as shown in figure 2.21. Using semilogarithmic graph paper may improve this significantly as can be seen in figure 2.22.

Annual rainfall extremes tend to plot as a straight line on extreme-value-probability (Gumbel) paper (see figure 2.23). The extreme value theory of Gumbel is only applicable to annual extremes. The method uses, in contrast to the previous example, the probability of non-exceedence $q = 1 - p$ (the probability that the annual maximum daily rainfall is less than a certain magnitude). The values are listed in table 2.6.

Gumbel makes use of a reduced variate y as a function of q, which allows the plotting of the distribution as a linear function between y and X (the rainfall depth in this case).

$$\mathbf{y \ = \ a \, (\, X - b \,)} \tag{2.10}$$

Year	1971	72	73	74	75	76	77	78	79	80
	56	52	60	70	34	30	44	48	40	38

Table 2.5. Annual maximum daily rainfall amounts.

Rank	Rainfall amount (mm)	p Probability of exceedence	T Return period	Log T	q Probability of non-exc.	y Reduced variate
1	70	0.09	11.0	1.041	0.91	2.351
2	60	0.18	5.5	0.740	0.82	1.606
3	56	0.27	3.7	0.564	0.73	1.144
4	52	0.36	2.8	0.439	0.64	0.794
5	48	0.45	2.2	0.342	0.55	0.501
6	44	0.54	1.8	0.263	0.46	0.238
7	40	0.64	1.6	0.196	0.36	-0.012
8	38	0.73	1.4	0.138	0.27	-0.262
9	34	0.82	1.2	0.087	0.18	-0.533
10	30	0.91	1.1	0.041	0.09	-0.875

Table 2.6   Rank, probability of exceedence, return period and reduced variate for the data in table 2.5

The equation for the reduced variate reads:

$$y = -\ln(-\ln(q)) = -\ln(-\ln(1-p)) \tag{2.11}$$

meaning that the probability of non-exceedence equals:

$$P(X \le X_0) = q = \exp(-\exp(-y)) \tag{2.12}$$
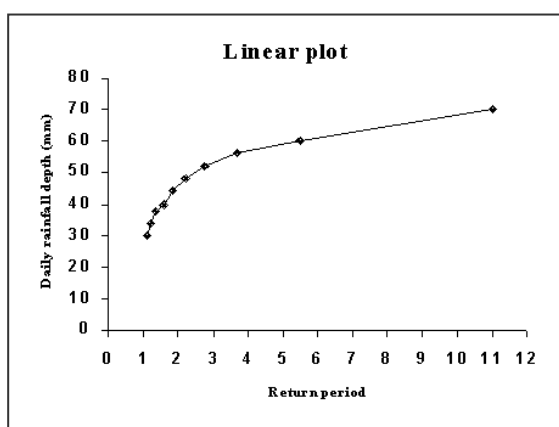
Fig. 2.21 Annual maximum daily rainfall (linear plot).
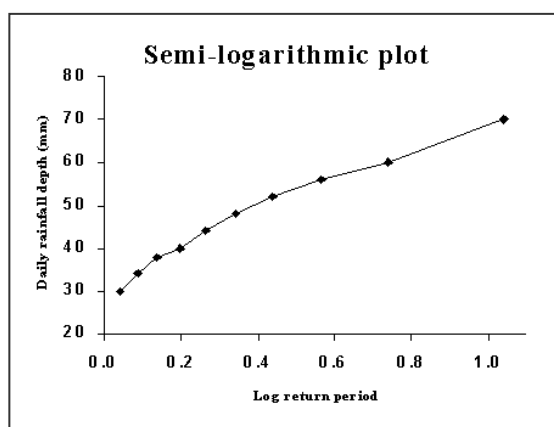
Fig. 2.22 Annual maximum daily rainfall (semi-log plot).
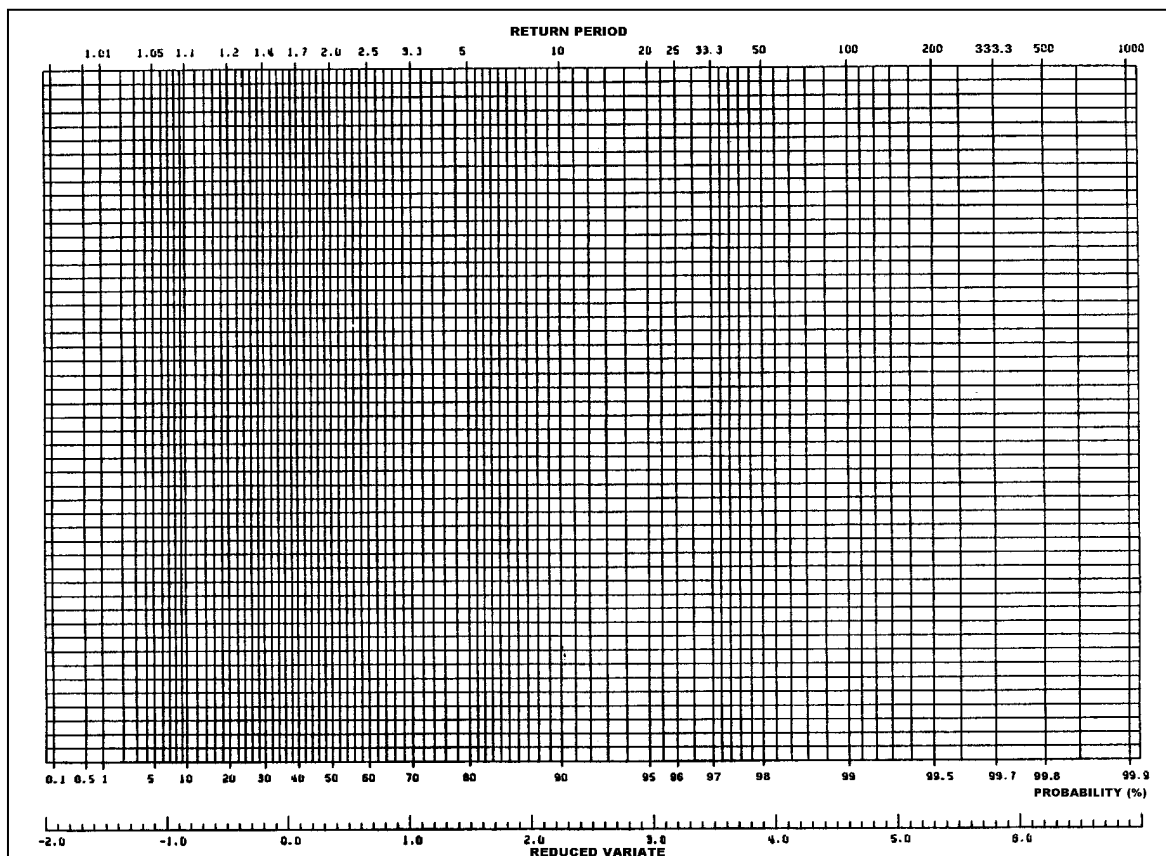
Fig. 2.23 Gumbel paper

The computed values of *y* for the data in table 2.5 are presented in table 2.6. A linear plot of these data on extreme-value-probability paper (see figure 2.24) is an indication that the frequency distribution fits the extreme value theory of Gumbel. This procedure may also be applied to river flow data.

In addition to the analysis of maximum extreme events, there also is a need to analyze minimum extreme events; e.g. the occurrence of droughts. The probability distribution of Gumbel, similarly to the Gaussian probability distribution, does not have a lower limit; meaning that negative values of events may occur. As rainfall or river flow do have a lower limit of zero, neither the Gumbel or Gaussian distribution is an appropriate tools to analyze minimum values. Because the logarithmic function has a lower limit of zero, it is often useful to first transform the series to its logarithmic value before applying the theory. Appropriate tools for analyzing minimum flows or rainfall amounts are the Log-Normal, Log-Gumbel, or Log-Pearson distributions.
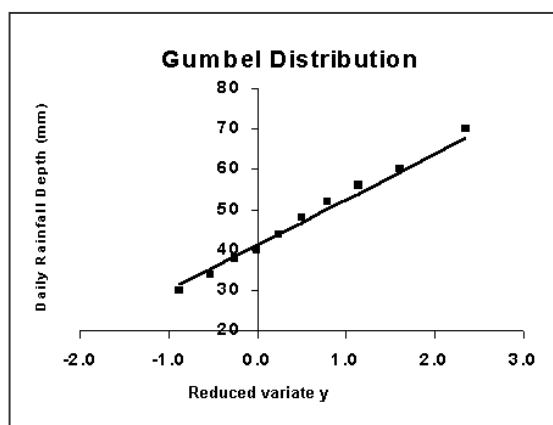
Fig. 2.24 Annual daily rainfall (Gumbel distribution).

A final remark of caution should be made with regard to frequency analysis. None of the above mentioned frequency distributions has a real physical background. The only information having physical meaning are the measurements themselves. Extrapolation beyond the period of observation is dangerous. It requires a good engineer to judge the value of extrapolated events of high return periods. A good impression of the relativity of frequency analysis can be acquired through the comparison of results obtained from different statistical methods. Generally they differ considerably. And finally, in those tropical areas where cyclonic disturbances occur, one should not be misled by a set of data in which the extreme event has not yet occurred at full force. The possibility always exists that the cyclone passes right over the centre of the study area. If that should occur, things may happen that go far beyond the hitherto registered events.

| Year	Max. Daily Rainfall	Thunderstorm (T) or Cyclone (C)
1952/53	155.3	T
1953/54	87.1	T
1954/55	103.8	T
1955/56	150.6	T
1956/57	55.3	T
1957/58	46.9	T
1958/59	70.3	T
1959/60	54.2	T
1960/61	71.2	T
1961/62	75.0	T
1962/63	108.2	T
1963/64	61.2	T
1964/65	50.5	T
1965/66	228.6	C (Claud)
1966/67	90.0	T
1967/68	64.6	T
1968/69	83.3	T
1969/70	71.5	T
1970/71	51.3	T
1971/72	104.4	T
1972/73	105.4	T
1973/74	103.5	T
1974/75	92.0	T
1975/76	189.3	C (Danae)
1976/77	130.0	C (Emilie)
1977/78	71.8	T
1978/79	84.6	T
1979/80	77.7	T
1980/81	97.1	T
1981/82	53.5	T
1982/83	56.9	T
1983/84	107.0	C (Demoina)
1984/85	89.2	T

Table 2.7 Maximum annual precipitation as a result of cyclonic storms and thunderstorms

2.8 Mixed distributions

We have seen in Section 2.2 that there are four types of lifting mechanisms that cause quite distinct rainfall types with regard to depth, duration and intensity. Of these, the tropical cyclones, or a combination of tropical depressions with orographic effects are the ones which, by far, exceed other lifting mechanisms with regard to rainfall depth and intensity. As a result, such occurrences, which are generally rare, should not be analyzed as if they were part of the total population of rainfall events; they belong to a different statistical population. However, our rainfall records contain events of both populations. Hence, we need a type of statistics that describes the occurrence of extreme rainfall on the basis of a mixed distribution of two populations: say the population of cyclones and the population of non-cyclones, or in the absence of cyclones, the population of orographic lifting and the population of other storms. Such a type of statistics is presented in this section. Assume that the rainfall occurrences can be grouped in two sub-sets: the set of tropical cyclone events which led to an annual maximum daily rainfall *C* and the set of non-cyclone related storms that led to an annual extreme daily rainfall *T*. Given a list of annual maximum rainfall events, much in the same way as one would prepare for a Gumbel analysis, one indicates whether the event belonged to subset *C* or *T* (see table 2.7). The probability *P(C)* is defined as the number of times in *n* years of records that a cyclone occurred. In this case $P(C) = 4/33$. The probability *P(T)*, similarly, equals 29/33. The combined occurrence $P(X > X_0)$, that the stochast representing annual rainfall *X* is larger than a certain value X_0 is computed from:

$$P(X > X_0) = P(X > X_0 \mid C) \bullet P(C) + P(X > X_0 \mid T) \bullet P(T) \tag{2.13}$$

where:

$P(X > X_0 \mid C)$ is the conditional probability that the rainfall is more than X_0 given that the rainfall event was a cyclone;

$P(X > X_0 \mid T)$ is the conditional probability that the rainfall is more than X_0 given that the rainfall event was a thunder storm.

In figure 2.25, representing the log-normal distribution, three lines are distinguished. One straight line representing the log-normal distribution of thunderstorms, one straight line the log-normal distribution of the cyclones, and one curve which goes asymptotically from the thunderstorm distribution to the cyclone distribution representing the mixed distribution. The data plots can be seen to fit well to the mixed distribution curve.
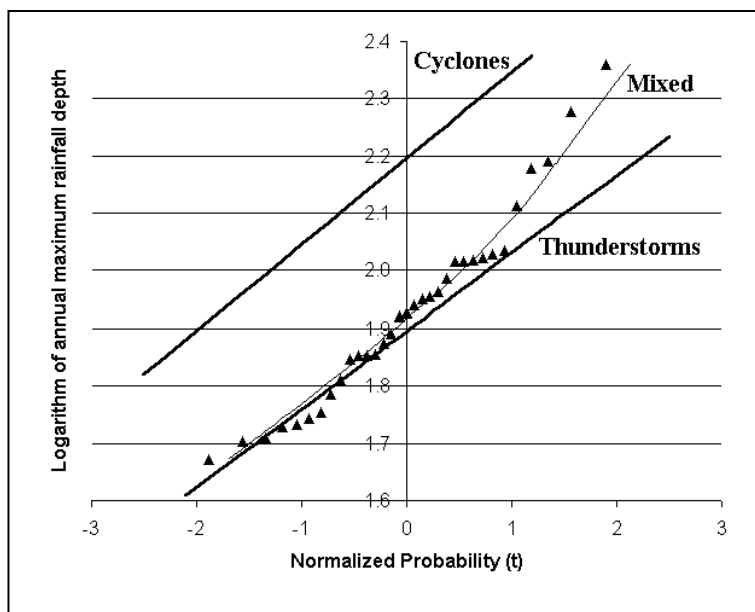
Fig. 2.25 Mixed distribution of combined cyclonic storms and thunderstorms

2.9 Probable maximum precipitation

In view of the uncertainty involved in frequency analysis, and its requirement for long series of observations which are often not available, hydrologists have looked for other methods to arrive at extreme values for precipitation. One of the most commonly used methods is the method of the *Probable Maximum Precipitation* (PMP).

The idea behind the PMP method is that there must be a physical upper limit to the amount of precipitation that can fall on a given area in a given time. An accurate estimate is both desirable from an academic point of view and virtually essential for a range of engineering design purposes, yet it has proven very difficult to estimate such a value accurately. Hence the word probable in PMP; the word probable is intended to emphasize that, due to inadequate understanding of the physics of atmospheric processes, it is impossible to define with certainty an absolute maximum precipitation. It is not intended to indicate a particular level of statistical probability or return period.

The PMP technique involves the estimation of the maximum limit on the humidity concentration in the air that flows into the space above a basin, the maximum limit to the rate at which wind may carry the humid air into the basin and the maximum limit on the fraction of

the inflowing water vapour that can be precipitated. PMP estimates in areas of limited orographic control are normally prepared by the maximization and transposition of real, observed storms while in areas in which there are strong orographic controls on the amount and distribution of precipitation, storm models have been used for the maximization procedure for long-duration storms over large basins.

The maximization-transposition technique requires a large amount of data, particularly volumetric rainfall data. In the absence of suitable data it may be necessary to transpose storms over very large distances despite the considerable uncertainties involved. In this case reference to published worldwide maximum observed point rainfalls will normally be helpful. The world envelope curves for data recorded prior to 1948 and 1967 are shown in
figure 2.26, together with maximum recorded falls in the United Kingdom (from: Ward & Robinson, 1990). By comparison to the world maxima, the British falls are rather small, as it is to be expected that a temperate climate area would experience less intense falls than tropical zones subject to hurricanes or the monsoons of southern Asia. The values of Cherrapunji in India are from the foothills of the Himalayas mountains, where warm moist air under the influence of monsoon depressions are forced upward resulting in extremely heavy rainfall. Much the same happens in La Reunion where moist air is forced over a 3000 m high mountain range. Obviously, for areas of less rugged topography and cooler climate, lower values of PMP are to be expected.
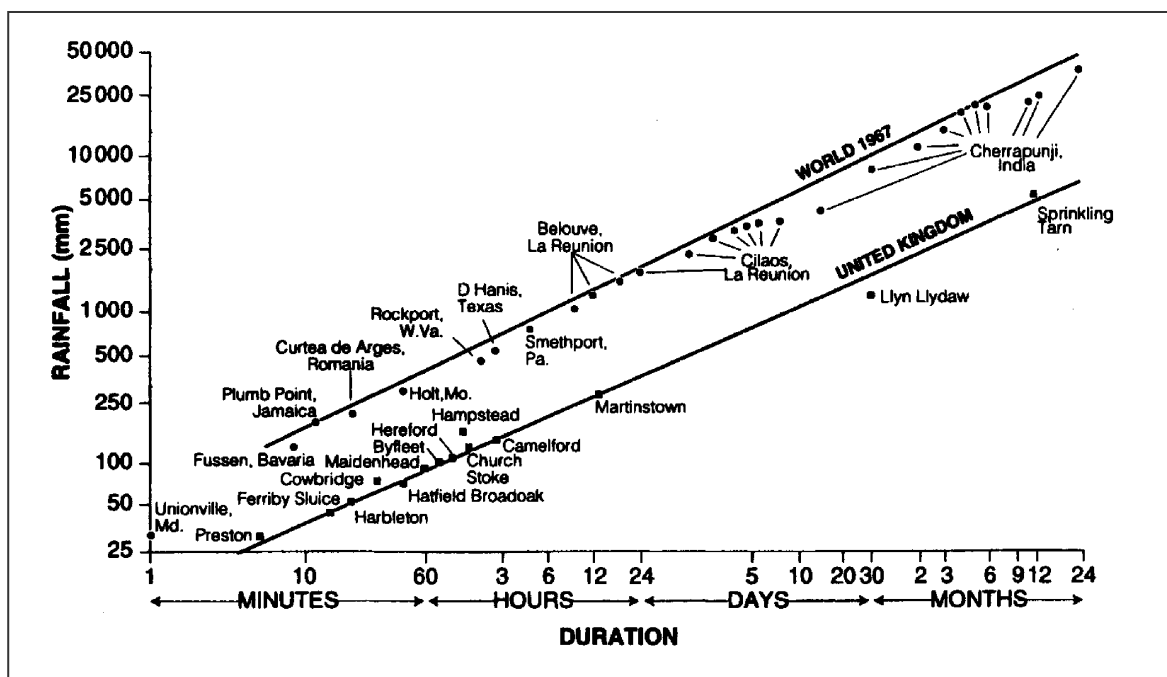

Fig. 2.26 Magnitude-duration relationship for the world and the UK extreme rainfalls (source: Ward & Robinson, 1990).

2.10 Analysis of dry spells

The previous sections dealt with extremely high, more or less instantaneous, rainfall. The opposite, extremely low rainfall, is not so interesting, since the minimum rainfall is no rainfall. Although some statistics can be applied to minimum annual or monthly rainfall, in which case often adequate use can be made of the log-normal distribution, for short periods of observation statistical analysis is nonsense. What one can analyse, however, and what has particular relevance for rainfed agriculture, is the occurrence of dry spells. In the following analysis, use is made of a case in the north of Bangladesh where wet season agriculture takes place on sandy

spell dura- tion	number of spells	accum- ulated spells	days per season	number of days			
t days	i	I	n	N	p	q	P
3	46	165	151	2718	0.0607	0.9393	0.9999
4	20	119	150	2700	0.0441	0.9559	0.9988
5	29	99	149	2682	0.0369	0.9631	0.9963
6	15	70	148	2664	0.0263	0.9737	0.9806
7	11	55	147	2646	0.0208	0.9792	0.9544
8	8	44	146	2628	0.0167	0.9833	0.9150
9	2	36	145	2610	0.0138	0.9862	0.8665
10	5	34	144	2592	0.0131	0.9869	0.8506
11	3	29	143	2574	0.0113	0.9887	0.8022
12	1	26	142	2556	0.0102	0.9898	0.7659
13	2	25	141	2538	0.0099	0.9901	0.7524
14	1	23	140	2520	0.0091	0.9909	0.7230
15	0	22	139	2502	0.0088	0.9912	0.7070
16	1	22	138	2484	0.0089	0.9911	0.7070
17	1	21	137	2466	0.0085	0.9915	0.6901
18	2	20	136	2448	0.0082	0.9918	0.6723
19	2	18	135	2430	0.0074	0.9926	0.6335
20	1	16	134	2412	0.0066	0.9934	0.5901
21	1	15	133	2394	0.0063	0.9937	0.5665
22	0	14	132	2376	0.0059	0.9941	0.5416
23	0	14	131	2358	0.0059	0.9941	0.5416
24	0	14	130	2340	0.0060	0.9940	0.5416
25	0	14	129	2322	0.0060	0.9940	0.5417
26	0	14	128	2304	0.0061	0.9939	0.5417
27	2	14	127	2286	0.0061	0.9939	0.5417
28	0	12	126	2268	0.0053	0.9947	0.4875
29	2	12	125	2250	0.0053	0.9947	0.4875
30	0	10	124	2232	0.0045	0.9955	0.4270
31	1	10	123	2214	0.0045	0.9955	0.4270
33	1	9	121	2178	0.0041	0.9959	0.3941
34	1	8	120	2160	0.0037	0.9963	0.3593
35	1	7	119	2142	0.0033	0.9967	0.3226
42	1	6	112	2016	0.0030	0.9970	0.2838
43	1	5	111	1998	0.0025	0.9975	0.2428
49	1	4	105	1890	0.0021	0.9979	0.1995
50	1	3	104	1872	0.0016	0.9984	0.1536
52	1	2	102	1836	0.0011	0.9989	0.1052
61	1	1	93	1674	0.0006	0.9994	0.0541

Table 2.8   **Probability of occurrence of dry spells in the Buri Teesta catchment**

soils. It is known that rainfed agriculture seldom succeeds without supplementary irrigation. In view of the small water retaining capacity of the soil, a dry spell of more than five days already causes serious damage to the crop.

The occurrence of dry spells in the wet season is analyzed through frequency analysis of daily rainfall records in Dimla in northern Bangladesh during a period of 18 years. The wet season consists of 153 days. In table 2.8 the procedure followed is presented, which is discussed briefly below.

In the 18 years of records, the number of times i that a dry spell of a duration t occurs has been counted. Then the number of times I that a dry spell occurs of a duration longer than or equal to t is computed through accumulation. The number of days within a season on which a dry spell of duration t can start is represented by $n = 153+1 - t$. The total possible number of starting days is $N = n * 18$. Subsequently the probability p that a dry spell starts on a certain day within the season is defined by:

$$p = \frac{I}{N} \tag{2.14}$$

The probability q that a dry spell of a duration longer than t does not occur at a certain day in the season, hence, is defined by:

$$q = 1 - \frac{I}{N} \tag{2.15}$$

The probability Q that a dry spell of a duration longer than t does not occur during an entire season, hence, is defined by:

$$Q = \left(1 - \frac{I}{N}\right)^n \tag{2.16}$$

Finally the probability that a dry spell of a duration longer than t does occur at least once in a growing season is defined by:

$$P = 1 - \left(1 - \frac{I}{N}\right)^n \tag{2.17}$$

In figure 2.27, the duration of the dry spell t is plotted against this probability P. It can be seen that the probability of a dry spell longer than five days, which already causes problems in the sandy soils, has a probability of occurrence of 99.6%, meaning that these dry spells occur virtually every year. Hence, figure 2.27 illustrates the fact that rainfed agriculture is impossible in the area during the wet season.
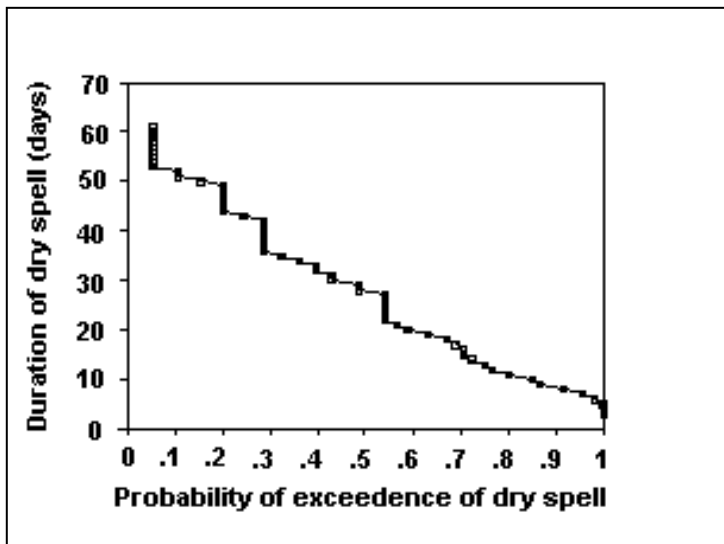
Fig. 2.27.   **Probability of occurrence of dry spells in the Buri Teesta catchment**

3 EVAPORATION

3.1 Land surface - atmosphere exchange processes

Until recently the interest of hydrologists in the atmosphere was restricted to processes related to rainfall and evaporation. The atmosphere was considered the domain of the meteorologist, who developed General Circulation Models (GCM) to forecast the weather. In these models the atmosphere is represented by cells with horizontal dimensions in the order of 100 to 500 km and a few kilometres in the vertical direction. GCMs simulate parameters such as temperature, wind speed, humidity and pressure of each cell on a time basis of say 10 minutes. As a result of the growing awareness of the 'greenhouse effect' on a possible climatic change, GCMs were gradually used as climatic models to predict long term changes of the weather. It was then found that the models did not adequately describe the exchange of momentum, heat and water vapour between the atmosphere and the land surface. The first models considered the earth surface to be homogeneous for each cell, with one type of vegetation and one type of soil, while the hydrological processes were schematised into a simple single reservoir with limited storage and a linear relation between soil moisture availability and evaporation. The integration of much better models for the simulation of the soil water balance such as SWATRE (Feddes et al., 1978) and MUST (De Laat, 1995) into the GCMs is hampered by the problem that the atmospherical and terrestrial hydrological components of the earth system operate on different time and space scales. Changes in atmospheric parameters are manifest over distances of hundreds of kilometres, while the heterogeneity in the properties of soil and vegetation may already be exhibited over distances of hundreds of metres. And with regard to the time scale it is found that the atmosphere reacts much faster to changes than the soil-vegetation system. Hence, GCMs require for their atmospheric processes a large space and a small time scale, while for the exchange processes with the land surface a much more detailed spatial resolution and a larger time step is needed. A simple averaging over the various time and space scales is, however, not possible due to the nonlinearity of the transport processes.

At present, research is directed towards methods to upscale Soil-Vegetation-Atmosphere Transfer (SVAT) processes at the patch level to the meso and macro scale, on which level the atmospheric circulation models operate. SVAT processes at the patch level are considered to occur in an area with (nearly) homogeneous land surface characteristics and a uniform hydrological regime. Patches allow parameters, state variables and fluxes to be averaged over the homogeneous small area. SVAT models are being developed to simulate the vertical processes of energy, water and carbon transfer between soil, vegetation and atmosphere. SVATs form the basis of coupled hydrological/atmosphere models on mesoscale level, and they are also used to analyze the influence of a future climatic change on the response of components of the ecosystem such as leaf area, soil water depletion, soil temperature, nutrient cycle, timing of snow melt etc. The atmosphere interaction models at mesoscale level will have to take into account the heterogeneity of the area and the resulting horizontal transfer of energy, water, carbon and nutrients (advective processes). Next, the most significant physical, biological and ecological processes have to be determined and parameterized in order to be incorporated into the models of global change.

Much effort is put into the research on land surface - atmosphere exchange processes and in particular in the resolution of the scaling incongruities. It is clear that evaporation plays an important role in the development of the soil-vegetation-atmosphere transfer models.

However, traditionally hydrologists are interested in evaporation because it is an important component in many water balance studies and often considered as a loss (see section 3.9). In irrigation water development projects an accurate assessment of the crop water use is a prerequisite for a proper design. Methods to estimate evaporation rates are discussed below.

3.2   Types of evaporation

Evaporation is the transfer of water into vapour. The following types are distinguished:

a) **Evaporation** into the atmosphere from:
   1. free water surface, E_o (open water evaporation)
   2. bare soil, E_s
   3. wet crop (after rain or dew), E_{wet} also referred to as evaporation of intercepted water, E_i.
b) **Transpiration**, E_t the transfer of water vapour into the atmosphere through the stomata of living plants.
c) **Evapotranspiration**, E a combination of evaporation and transpiration. For a vegetated surface evapotranspiration is most commonly used as it is very difficult to distinguish between the various types of evaporation.

The evapotranspiration of a partly wet crop, not completely shading the ground may be estimated from

$$\mathbf{E = S_c\ (E_t + E_i)\ +\ (1 - S_c)\ E_s} \tag{3.1}$$

where S_c is the fraction of soil covered by the crop. In irrigation engineering the crop water use if often estimated for a dry crop ($E_i = 0$), completely covering the ground ($S_c = 1$).
The evapotranspiration of a crop, actively growing, completely covering the surface and not short of water is known as the potential evapotranspiration, E_{pot}. The potential rate (mm/d) is largely determined by the atmospheric conditions and also referred to as the atmospheric demand. The actual evapotranspiration E_{act} may be less than the maximum possible rate (E_{pot}) due to shortness of water. It follows that $E_{act} \le E_{pot}$. Furthermore, it may be seen from the long term water balance of a catchment (neglecting $\Delta S / \Delta t$ in equation 1.6) that $E_{act} < P$, where P is the amount of precipitation in the considered period. Typical values for catchments in three different climates are given in table 3.1.

3.3   Factors affecting evaporation

The transfer of water in the liquid state into water vapour requires energy, which is known as the *latent heat of vaporization*. The energy is, directly or indirectly, supplied by the solar radiation. The amount of radiation that is available for evapotranspiration depends on the latitude, atmospheric conditions (e.g. cloudiness), reflection from the earth surface, absorption by the atmosphere and the storage in the ground (or water body). It is necessary for the process of evaporation to continue that the water vapour is removed from the evaporating surface. This is a process of diffusion and turbulent transport, which is affected by the temperature, and humidity of the air, the roughness of the surface and the wind speed. Moreover, for the process of transpiration the resistance to flow of water in the plant and the percentage of the soil covered by the crop play an important role.

Annual amounts		Tropical humid Singapore	Arid Iraq	Temperate humid Netherlands
Precipitation	P	2500	150	750
Open water evaporation	E_o	1500	2250	650
Potential evapotranspiration	E_{pot}	1400	1800	525
Actual evapotranspiration	E_{act}	1200	100	450

Table 3.1   **Global values (mm) of annual rainfall and evaporation data for three different climates**

Summarizing, evaporation or potential evapotranspiration is affected by factors, which are determined by (A) the evaporating surface and (B) the atmospheric conditions.

A   For an evaporating surface consisting of bare soil or open water the factors include:
1. reflection coefficient
2. roughness of the surface
3. heat storage capacity

For a cropped surface two additional factors play a role:
4. soil cover
5. crop resistance

B   The atmospheric conditions affecting evapotranspiration comprise:
1. temperature
2. wind velocity
3. relative humidity
4. solar radiation

A short description of each of the factors that affect evapotranspiration is given below.

Reflection coefficient or albedo
Typical values for the reflection of solar radiation reaching the earth's surface are given in table 3.2.

Roughness
The transfer of water vapour from the evaporating surface into the atmosphere may be regarded as turbulent transport, except for a very thin layer at the surface known as the laminar sub-layer, where the transfer is caused by molecular diffusion. The thickness of the laminar sub-layer, the roughness length, depends on the roughness of the surface (e.g. crop height). The resistance to the transport of water vapour from the evaporating surface into the atmosphere is called the aerodynamic resistance and may for a specific surface (roughness length) be written as a function of the wind speed.

Free water surface	**0.06**
Grass	**0.22 – 0.25**
Bare soil	**0.10 – 0.30**
Fresh snow	**0.90**

Table 3.2   **Albedo, or reflection coefficients, r (fraction)**

Heat storage capacity

In climates with a distinct summer and winter period, part of the energy that becomes available in spring is used to warm up the surface which energy is released during the next autumn and winter. A deep lake or a wet soil has a large heat storage capacity. Hence, the evaporating surface will remain relatively cold in spring, which affects the evaporation. The subsequent release of heat during the autumn and winter causes a phase shift in the evaporation cycle of deep lakes as compared to shallow lakes.

Soil cover

The fraction of soil that is covered by the crop directly affects the transpiration of the considered area.

Crop resistance

Transpiration of a cropped surface is usually less than the evaporation of an open water surface due to the additional resistance to the flow of water in the plant and the transfer of water vapour through the stomata. For tall crops, however, the increased turbulence lowers the aerodynamic resistance, which may result in higher values for the transpiration as compared to open water evaporation.

Temperature

The saturation vapour pressure of the air depends on the temperature (figure 2.1). Moreover, the long wave radiation is temperature dependent. Both factors affect evapotranspiration. For a proper observation of the temperature, the thermometer must measure the air temperature only, hence the energy should be supplied by convection (air currents) and not by radiation, condensation or conduction. The thermometer should, therefore, be naturally ventilated and sheltered from rain and sun. Observations are often taken from a thermometer situated inside a white, louvred, structure (Stevenson's hut) at a height of 2.0 m.

Wind velocity

The aerodynamic resistance to water vapour transport, r_a is a function of the wind speed, as discussed above. Wind speed is measured with anemometers. The observation may be based on various principles: rotation, pressure, swinging plate, sound, cooling rate, etc. For estimating evaporation the direction of the wind is not important. The Robinson cup-anemometer with a vertical axis is most commonly used. Wind speed is a function of the height. Values, which apply for a height of 2 m, are generally used to estimate evaporation. For observations over short grass the windspeed U_2 at a height of 2 m may then as follows be estimated from U_h, the velocity obtained at a height h (m)

$$U_2 = \frac{2.11 \ U_h}{\log (\ 66.7 \ h \ - \ 5.3 \ )} \tag{3.2}$$

At many stations the wind speed is measured over short grass at a height of 10 m. Equation (3.2) shows that these values are easily converted to a height of 2 m with $U_2 \approx 0.75 U_{10}$.

Relative humidity

Evaporation is very sensitive to the humidity of the air and it ceases completely when the air becomes saturated with water vapour ($RH = e_d/e_s = 1$), provided the temperature remains the same. The relative humidity is most easily measured with a hair-hygrometer, which is based on the property that the length of the hair varies with the relative humidity. More accurate

measurements are obtained with a psychrometer. This instrument consists of two thermometers, one with its bulb wrapped in wet muslin and one dry. A fan is used to force a flow of air past the bulbs. This results in a temperature of the wet bulb, T_{wet} below the temperature of the dry bulb, T_{dry} due to the extraction of latent heat for the evaporation of water from the wet cloth. The actual vapour pressure is computed with the formula

$$\mathbf{e_d} = \mathbf{e_s} - \gamma \left(\mathbf{T_{dry}} - \mathbf{T_{wet}} \right) \tag{3.3}$$

where the saturation vapour pressure, e_s is obtained from figure 2.1 for $T_a = T_{wet}$ and γ is the psychrometric constant, which value depends on the type of instrument and the altitude. For the widely used *Assmann* psychrometer with an aspiration of 5 m.s^{-1}, $\gamma = 0.067$ kPa.$^{\circ}$C^{-1} at sea level.

Solar radiation

The latent heat of vaporization, L required for the transfer of water into vapour is, directly or indirectly, provided by energy from the sun $(L = 2.45 * 10^6 \ J/kg)$. Solar radiation is, therefore, the most dominant factor determining the evaporation rate. The incoming short-wave radiation from the sun and the sky (the global radiation) is measured with a solarimeter. More important for estimating evaporation is the radiometer which measures the net radiation, i.e. the difference between on the one hand the incoming short wave
radiation, and on the other hand the fraction that is reflected, including the outgoing long wave radiation from the earth's surface.

Net radiation estimates may also be obtained from observed hours of sunshine using empirical formulae. A simple instrument to measure the number of hours of sunshine is the *Campbell-Stokes* type of sunshine recorder.

The factors mentioned above affect the *potential* evapo(transpi)ration rate. The *actual* evapo(transpi)ration becomes less than its potential value when water is not readily available, which does, of course, not apply for a free water surface. The evaporation from a wet bare soil may, after a short while, reduce drastically when desiccation of a thin top layer prevents a sufficient supply of water from below. The deviation of the actual evapotranspiration rate from its potential value for a cropped surface occurs more gradually due to the larger depths over which the roots can take up the soil moisture (figure 3.1).
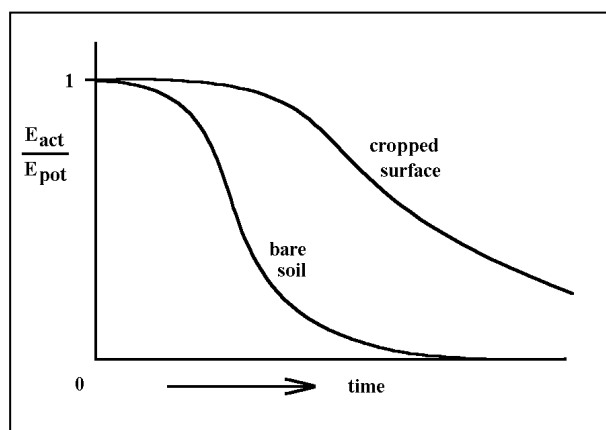

Fig. 3.1 Relative evapo(transpi)ration from an initially wet (bare and cropped) surface during a rainless period.

3.4   The energy balance

The energy balance of e.g. a lake may be set up analogue to the water balance. The most important term is the net radiation or heat budget R_N that comprises the net contribution of both short and long wave radiation (figure 3.2).

R_N may be measured with a radiometer. It should be noted that R_N values obtained above a grass cover are different from those measured over an open water surface due to differences in albedo and long wave radiation. In the absence of radiation measurements R_N is to be estimated from standard meteorological data using empirical formulae. The procedure is the following.

The short wave radiation energy (wavelengths 0.3 - 3 µm) that is received at the outer limits of the atmosphere, R_A may be read from tables for a given latitude and

Fig. 3.2 Radiation balance (simplified)

time of the year. Table 3.3 gives values of R_A in W.m^{-2}. R_S is the short wave radiation that is received at the earth surface. Its value depends on the local atmospheric conditions (consider e.g. polluted industrial area versus mountain village) and the cloudiness *n/N* defined as:

$$\frac{n}{N} = \frac{\text{actual hours of sunshine}}{\text{possible hours of sunshine}}$$

The actual hours of sunshine are easily measured with a *Campbell-Stokes sunshine recorder* and the possible hours of sunshine (day length) are read from table 3.4 for the given latitude and time of the year. Examples of empirical relations for R_S are given in table 3.5. The fraction of the short wave radiation reaching the earth's surface that is reflected depends on the albedo (table 3.2). The net short wave radiation thus equals $R_S - rR_S = (1 - r) R_S$.

Every object with a temperature above absolute zero emits long wave radiation (wave lengths 3 - 50 µm). Long wave radiation is emitted by the earth's surface, but also by water vapour and droplets (clouds!) in the air. The *net* outgoing long wave radiation R_{nL} (W.m^{-2}) may be estimated from the following empirical formula

	Lat	Jan	Feb	Mar	Apr	May	Jun	Jul	Aug	Sept	Oct	Nov	Dec
	NORTHERN HEMISPHERE												
	60	40	103	200	317	417	469	446	360	243	134	57	26
	52	91	157	252	357	440	475	457	389	292	192	111	74
	50	106	172	263	363	443	475	460	392	297	203	126	89
	40	177	240	317	395	455	477	466	420	346	266	194	160
	30	232	300	366	420	460	472	463	435	386	320	260	226
	20	309	354	400	435	449	452	452	440	412	369	323	297
	10	366	397	423	435	429	423	426	429	423	406	375	357
Equator	0	415	429	435	420	397	383	389	409	426	429	417	409
	10	455	449	432	397	357	334	343	375	412	440	449	452
	20	489	457	415	357	306	277	289	332	389	437	469	483
	30	492	452	386	312	246	214	226	277	352	423	477	500
	40	495	432	349	254	183	149	160	217	306	395	472	509
	50	483	403	297	192	117	83	97	154	249	357	457	503
	60	472	360	237	123	51	26	37	89	186	309	432	500
	SOUTHERN HEMISPHERE												

Table 3.3   Short wave radiation R$_A$ received at the outer limits of the atmosphere expressed in W.m^{-2}.

North Lats. South Lats.	Jan July	Feb Aug	Mar Sept	Apr Oct	May Nov	June Dec	July Jan	Aug Feb	Sept Mar	Oct Apr	Nov May	Dec June
60	6.7	9.0	11.7	14.5	17.1	18.6	17.9	15.5	12.9	10.1	7.5	5.9
58	7.2	9.3	11.7	14.3	16.6	17.9	17.3	15.3	12.8	10.3	7.9	6.5
56	7.6	9.5	11.7	14.1	16.2	17.4	16.9	15.0	12.7	10.4	8.3	7.0
54	7.9	9.7	11.7	13.9	15.9	16.9	16.5	14.8	12.7	10.5	8.5	7.4
52	8.3	9.9	11.8	13.8	15.6	16.5	16.1	14.6	12.7	10.6	8.8	7.8
50	8.5	10.0	11.8	13.7	15.3	16.3	15.9	14.4	12.6	10.7	9.0	8.1
48	8.8	10.2	11.8	13.6	15.2	16.0	15.6	14.3	12.6	10.9	9.3	8.3
46	9.1	10.4	11.9	13.5	14.9	15.7	15.4	14.2	12.6	10.9	9.5	8.7
44	9.3	10.5	11.9	13.4	14.7	15.4	15.2	14.0	12.6	11.0	9.7	8.9
42	9.4	10.6	11.9	13.4	14.6	15.2	14.9	13.9	12.6	11.1	9.8	9.1
40	9.6	10.7	11.9	13.3	14.4	15.0	14.7	13.7	12.4	11.2	10.0	9.3
35	10.1	11.0	11.9	13.1	14.0	14.5	14.3	13.5	12.4	11.9	10.3	9.8
30	10.4	11.1	12.0	12.9	13.6	14.0	13.9	13.2	12.4	12.0	10.6	10.8
25	10.7	11.3	12.0	12.7	13.3	13.7	13.5	13.0	12.3	12.0	10.9	10.6
20	11.0	11.5	12.0	12.6	13.1	13.3	13.2	12.8	12.3	12.0	11.2	10.9
15	11.3	11.6	12.0	12.5	12.8	13.0	12.9	12.6	12.2	12.0	11.4	11.2
10	11.6	11.8	12.0	12.3	12.6	12.7	12.6	12.4	12.1	12.0	11.6	11.5
5	11.8	11.9	12.0	12.2	12.3	12.4	12.3	12.3	12.1	12.0	11.9	11.8
Equator 0	12.0	12.0	12.0	12.0	12.0	12.0	12.0	12.0	12.0	12.0	12.0	12.0

Table 3.4. Mean daily duration of maximum possible sunshine hours (N)

$$\mathbf{R_{nL} = \sigma \ \frac{(273 + T_{min})^4 + (273 + T_{max})^4}{2} \ (0.34 - 0.139 \sqrt{e_d}) \ (0.1 + 0.9 \, n/N)} \qquad (3.4)$$

where σ is the Stefan-Boltzmann constant ($\sigma = 5.6745 * 10^{-8}$ W.m^{-2}.K^{-4}), e_d is the actual vapour pressure of the air, and T_{min} and T_{max} are the minimum and maximum temperatures of the air in ^{o}C, respectively.

Using the above empirical relations the net radiation, R_N (W.m^{-2}) may be estimated from

$$\mathbf{R_N = (1 - r) R_s - R_{nL}} \qquad (3.5)$$

This energy is used for evaporation, heating the atmosphere and the earth surface. Only one half percent is used for photosynthesis, which amount is so small that is usually neglected. The energy balance for the earth's surface may be written as:

$$\mathbf{R_N = LE^* + H + A + \Delta S / \Delta t} \qquad (3.6)$$

where LE^* is the energy required for evaporation, H is the loss of sensible heat to the atmosphere (i.e. convective heat transport from the surface to the air), A is the exchange of heat with the environment (advection) and ΔS is the increase in the storage of heat below the surface. The term ΔS may be neglected if R_N is rather constant over the considered period. Moreover, ΔS will be relatively small when considering the energy balance of a

The Netherlands	$R_S = (0.20 + 0.60 \, n/N)R_A$
New Delhi	$R_S = (0.31 + 0.60 \, n/N)R_A$
Singapore	$R_S = (0.21 + 0.48 \, n/N)R_A$
General	$R_S = (0.25 + 0.50 \, n/N)R_A$

Table 3.5 Examples of empirical relations for R_S

shallow lake or a land surface due to the small heat storage capacity. Advection may in general be disregarded except for situations such as a small irrigated area situated in a desert. Equation 3.6 then reduces to

$$\mathbf{R_N = LE^* + H} \tag{3.7}$$

where the evaporation, E^* in mm.s^{-1}, is approximately equal to kg.s^{-1}.m^{-2}. The latent heat of vaporization, L is in the unit J.kg^{-1}, so that evaporation written in terms of energy, LE^* is consistently expressed in the units J.s^{-1}.m^{-2} = W.m^{-2}.

3.5   Penman Open Water Evaporation

There are three major approaches to calculate the evaporation from open water, E_o. The mass transfer method, the energy balance approach and a combination of the two.

1. *Mass transfer method.* The following empirical aerodynamic equation was proposed by Dalton in the beginning of the last century to estimate the evaporation of open water

$$\mathbf{E_o = f(U)\left(e_s - e_d\right)} \tag{3.8}$$

where *f(U)* is a function of the wind speed, e_s is the saturation vapour pressure corresponding to the temperature, T_s of the laminar sub-layer at the surface and e_d is the actual vapour pressure of the air at a standard height (usually 2 m). In practice it is impossible to measure T_s. Therefore, the saturation vapour pressure, e_w for the temperature of the water, T_w is often used instead.

Some examples of the aerodynamic approach to compute E_o in mm.d^{-1} are given below:

IJssel lake (The Netherlands):

$$\mathbf{E_o = 2.5\left(1 + 0.25U_6\right)\left(e_w - e_d\right)} \tag{3.9a}$$

Lake Hefner (USA):

$$\mathbf{E_o = 1.22\,U_4\left(e_w - e_d\right)} \tag{3.9b}$$

General equation (Harbeck, 1962):

$$\mathbf{E_o = 2.91\,A^{-0.05}\,U_2\left(e_w - e_d\right)} \tag{3.9c}$$

where A is the size of the lake in m^2.

Other mass transfer methods which are not (yet) suitable for routine application are based on measurements of wind speed and vapour pressure over a small height difference (turbulent transfer of water vapour), or on measurements of vertical wind velocity and vapour content of the air at a single point above the evaporating surface (eddy-transfer method).

2. *Energy balance approach.* Equation 3.6 may be used to compute the evaporation of a lake. The net radiation is obtained with a radiometer, but other terms require for their computation a detailed observation network to measure temperatures of water and air. The

method is very laborious and expensive, but applied over a limited period of time it may be used to derive the coefficients of the aerodynamic equation (3.9).

3. *Combined approach, the Equation of Penman*. Penman (1948) derived a formula which is based on the empirical Dalton equation and the energy balance approach. This formula, which may be used for estimating the evaporation of an open water surface, is written as

$$E_o = \frac{C}{L} \frac{sR_N + c_p\rho_a(e_s - e_d)/r_a}{s + \gamma} \tag{3.10}$$

where

E_o	open water evaporation in $mm.d^{-1}$
C	constant to convert units from $kg.m^{-2}.s^{-1}$ to $mm.d^{-1}$ (C = 86400)
R_N	net radiation at the earth's surface in $W.m^{-2}$
L	latent heat of vaporization (L = $2.45 * 10^6$ $J.kg^{-1}$)
s	slope of the temperature-saturation vapour pressure curve ($kPa.K^{-1}$)
c_p	specific heat of air at constant pressure (c_p = 1004.6 $J.kg^{-1}.K^{-1}$)
ρ_a	density of air (ρ_a = 1.2047 $kg.m^{-3}$ at sea level)
e_d	actual vapour pressure of the air at 2 m height in kPa
e_s	saturation vapour pressure for the air temperature at 2 m height in kPa
γ	psychrometric constant (γ = 0.067 $kPa.K^{-1}$ at sea level)
r_a	aerodynamic resistance in $s.m^{-1}$

Values for e_s and s may be obtained from figure 2.1, tables or formulae such as

$$e_s = 0.6108 \; e^{\frac{17.27\,T_a}{237.3 + T_a}} \tag{3.11}$$

$$s = \frac{4098\,e_s}{(237.3 + T_a)^2} \tag{3.12}$$

where T_a is the 24 hour mean temperature of the air in °C.

The aerodynamic resistance, r_a ($s.m^{-1}$) is a function of the wind speed, U_2 measured at a height of 2 m. Penman proposed the following expression for an open water surface

$$r_a = \frac{245}{0.54\,U_2 + 0.5} \tag{3.13}$$

The formula of Penman has found world-wide application because it has a strong physical basis. It requires the following standard meteorological data:

T_{min}, T_{max}	minimum and maximum temperature of the air (°C), or if not available, the mean temperature, T_a
RH	relative humidity
U_2	wind speed (m/s)
R_N	net radiation ($W.m^{-2}$) or the relative sunshine duration, n/N

The data refer to 24 hour mean values and apply to a height of 2 m above soil surface.

3.6   Penman-Monteith Evapotranspiration

In 1965 the equation of Penman has been adapted so that it can be used to estimate the actual transpiration, ET (mm.d^{-1}) of a (dry) crop (Rijtema, 1965; Monteith, 1965):

$$ET = \frac{C}{L} \frac{sR_N + c_p \rho_a (e_s - e_d)/r_a}{s + \gamma (1 + r_c / r_a)} \tag{3.14}$$

where r_c (s.m^{-1}) is the crop resistance. The crop resistance depends on the pressure head in the root zone, h or the 'dryness of the soil'. If the crop is amply supplied with water the crop resistance, r_c reaches a minimum value, known as the *basic canopy resistance*. The transpiration of the crop is then maximum and referred to as potential transpiration, ET_{pot}. The relation between r_c and h is crop dependent. Minimum values of r_c range from 30 (s.m^{-1}) for arable crops to 150 (s.m^{-1}) for forest. For grass a value of 70 (s.m^{-1}) is often used. It should be noted that r_c cannot be measured directly, but has to be derived from the Penman-Monteith formula where ET is obtained from e.g. the water balance of a lysimeter. The approach requires that the aerodynamic resistance, r_a is known. The value of r_a is difficult to estimate, because the vegetation layer is often poorly described. For short grass the following formula may be derived (see e.g. Feddes & Lenselink, 1994)

$$r_a = \frac{208}{U_2} \tag{3.15}$$

The equation of Penman-Monteith is widely used to estimate potential evaporation rates of various crops for which the crop resistance is known. Application of the equation to estimate actual evapotranspiration requires information on the pressure head in the root zone. Simulation models for the transport of soil moisture and the water uptake by the roots often use Penman-Monteith to estimate the actual evapotranspiration. The equation, however, only yields the loss of water from the living plants. Additional procedures are required to estimate the loss of water from the soil directly and due to interception. Large interception rates, up to 50% of the annual precipitation, may be found in coniferous forests in temperate regions. It is obvious that the soil evaporation depends on the percentage of the soil covered by the crop, often expressed in terms of the *Leaf Area Index* (LAI, square metres leaf per square metre soil, m^2.m^{-2}).

3.7   Methods to estimate potential evapotranspiration

Potential evapotranspiration is preferably calculated directly with the Penman-Monteith equation. This is known as the *one-step method*. The approach requires data on the crop resistance, which are not always available. It is to be expected that the one-step method will expand in use in the next decade.

The *two-step method* is at present most popular. It computes the potential evapotranspiration of the crop from

$$ET_{pot} = k_c \, ET_{ref} \tag{3.16}$$

where k_c is a crop factor and ET_{ref} is the reference evaporation. The rate of evapotranspiration

is determined by the evaporating surface (type of land use) and the atmospheric conditions. In (3.16) the empirical crop factor represents the conditions at the surface and the reference evaporation the weather conditions. In various handbooks crop factors are tabulated in relation to a particular ET_{ref}. The reference evaporation is often taken as the evaporation of an open water surface, E_o neglecting the storage of heat (3.10). In The Netherlands potential evapotranspiration of grass may then be estimated from

$$\mathbf{ET_{pot} = 0.8\,E_o} \quad \textbf{for the summer period}$$

$$\mathbf{ET_{pot} = 0.7\,E_o} \quad \textbf{for the winter period}$$

This shows that the crop coefficient, k_c is time-variant. FAO defines ET_{ref} as the potential evapotranspiration of short grass. It should be realised that a different definition of ET_{ref} results in a different set of crop factors.

In this section various methods for the computation of reference evaporation are discussed.

FAO Modified Penman
The FAO Modified Penman method is most widely used. The procedure is described by Doorenbos & Pruitt in *FAO's Irrigation and Drainage Paper 24 (FAO-ID24, 1977)*. The reference evaporation is defined as

> *The rate of evapotranspiration from an extensive surface of an 8 to 15 cm tall green grass cover of uniform height, completely shading the ground and not short of water.*

The modified formula is essentially the Penman equation for open water, where the albedo for the computation of the net short wave radiation, *(1 - r) R_S* has been set to *r* = 0.25, the wind function has been adapted to short grass and a correction factor has been added to adapt the formula to conditions deviating from the standard. The FAO Modified Penman equation may be written as

$$\mathbf{ET_{ref} = c\left[\dfrac{s}{s+\gamma}\,R_N^* + \dfrac{\gamma}{s+\gamma}\,2.7\,f(U)\left(e_s - e_d\right)\right]} \tag{3.17}$$

where
  ET_{ref} FAO Modified Penman reference evaporation rate (mm.d^{-1})
  c   adjustment factor
  R_N^* net radiation in equivalent evaporation in mm.d^{-1}. ($R_N^* \approx CR_N/L$)
  f (U)   wind function; $f(U) = 1 + 0.864U_2$
  All other symbols have been defined earlier.

For moderate winds, a maximum humidity (at night) of about 70% and a day-night wind ratio of 1.5 to 2, the adjustment factor, *c* equals 1. In the FAO-ID24 values for the adjustment factor are tabulated for conditions that differ from this average situation.

FAO Penman-Monteith
In 1990 FAO organized a meeting of experts on the revision of the FAO methodologies for crop water requirements (Smith, 1991). It was then recognized that the Penman-Monteith

equation should become the new standard for estimating potential evapotranspiration. The method is suitable to directly estimate potential evapotranspiration if the crop resistance is known (the one-step method), but it may also be used for estimating the reference crop evaporation in the two-step method. For this purpose the expert meeting came with the following definition of the reference crop.

> *The reference evapotranspiration, ET_{ref} is defined as the rate of evapotranspiration from a hypothetical crop with an assumed crop height (12 cm) and a fixed canopy resistance ($r_c = 70$ s.m^{-1}) and albedo ($r = 0.23$) which would closely resemble evapotranspiration from an extensive surface of green grass cover of uniform height, actively growing, completely shading the ground and not short of water.*

The major difference between the Modified Penman equation and the Penman-Monteith approach is that the first method does not use a crop resistance and has a different wind function (3.15).

Comparison of both methods shows that the reference evaporation as computed with the Modified Penman method is systematically higher than with the equation of Penman-Monteith. Consequently, the Penman-Monteith method requires for its use new crop factors. Since these new crop factors are not yet available, Penman-Monteith cannot be used as a two-step method.

Radiation method

The evapotranspiration flux of a grass crop, amply supplied with water, is largely governed by the available radiation energy. *Makkink* (1957) found that the saturation deficit of the air and the wind speed were relatively unimportant factors in the equation of Penman. He proposed a simplified expression of Penman's equation. The equation of Makkink is based on global radiation and temperature data only. Neglecting the storage of heat below the surface, a slightly adapted version of the reference evaporation according to Makkink may be written as

$$ET_{Makkink} = C\, C_M\, \frac{s}{s+\gamma}\, \frac{R_s}{L} \tag{3.18}$$

where C_M is a constant. All other parameters in (3.18) have been specified earlier. With the constant $C_M = 0.8$ equation 3.18 yields the evaporation of open water. The equation of Makkink, with $C_M = 0.65$ is presently used as the standard method to estimate reference crop evaporation (the potential evapotranspiration of grass) by the Royal Meteorological Institute of The Netherlands. A comparison of the equations of Penman-Monteith and Makkink for meteorological data given in table 3.6, which apply for Lelystad, The Netherlands is given in figure 3.3.

In the FAO-ID24 on Crop water requirements the radiation method is recommended in the absence of detailed data on humidity and wind speed. The parameter C_M is related to estimates of *annual mean* values of the relative humidity and daytime wind. It was later recognized (Smith, 1991) that radiation methods are particularly suitable under humid conditions.

Using data from Verhoef & Feddes (1991), the FAO methods (Penman-Monteith, Modified Penman and Makkink) have been applied to data from Mansoura in Egypt and Hyderabad in

	U_2 m/s	n/N %	RH %	T_a °C
Jan	4.4	28.3	89.3	1.7
Feb	3.8	26.2	90.0	5.6
Mar	3.3	32.5	85.7	7.6
Apr	2.6	30.6	80.7	11.1
May	3.3	38.3	74.0	12.2
Jun	2.4	45.5	73.3	16.7
Jul	2.7	27.3	77.0	16.6
Aug	2.4	30.8	86.0	17.1
Oct	2.9	35.3	87.0	12.1
Nov	3.3	20.1	89.7	4.8
Dec	3.4	27.8	88.7	1.2

Table 3.6 Meteorological data for 1961, Lelystad, The Netherlands
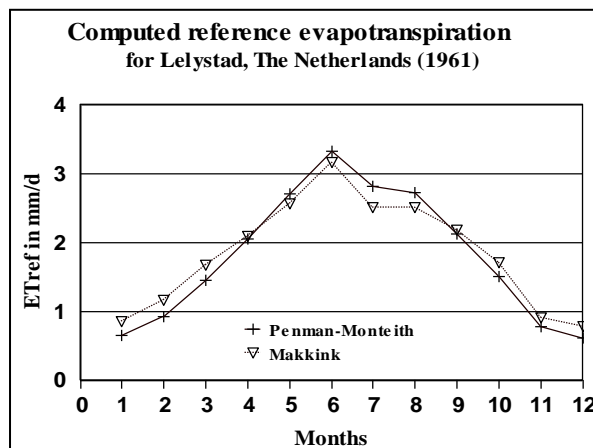

Fig. 3.3 Comparison of ET_{ref} computed with Penman-Monteith and Makkink

Pakistan. The results, plotted in figures 3.4 and 3.5, clearly show the 'collapse' of the radiation method for Hyderabad during months with high wind velocities.

The Penman-Monteith method was proven to be superior in lysimeter experiments (Jensen et al., 1990) as the potential evapotranspiration rates computed with this equation for grass compared very well with measured data. The computations for Mansoura and Hyderabad show that the widely used FAO Modified Penman method overestimates the potential evapotranspiration of grass by more than 25%.

Temperature methods
The methods of Blaney-Criddle and Thornthwaite as discussed below are applicable if monthly mean air temperature is the only data available. The methods were developed in the USA for estimating monthly crop water use. Although the formulae make use of the day length, thus indirectly of the extraterrestrial radiation, the methods are very approximate.

Blaney & Criddle (1950) recommend the following formula, written here in SI units, to estimate the seasonal consumptive use
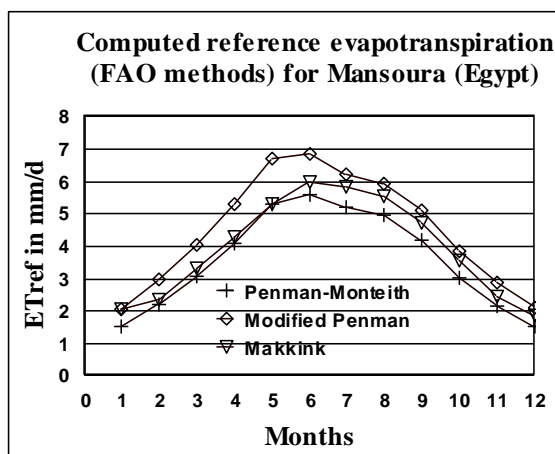

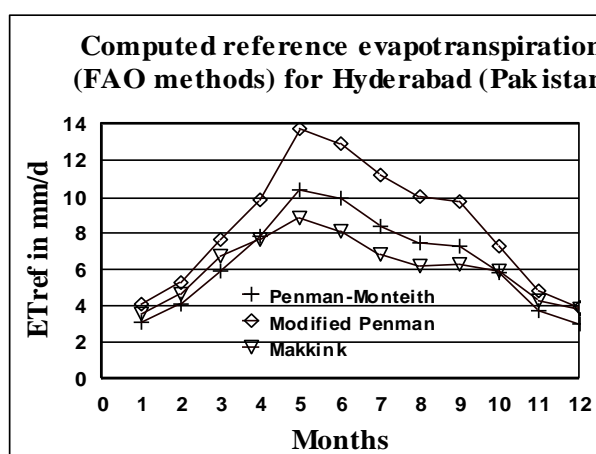**Fig. 3.4 Comparison of ET_{ref} for Mansoura**

Fig. 3.5 Comparison of ET_{ref} for Hyderabad

$$ET_{B\&C} = K\, p\,(0.457\,T_a + 8.13) \tag{3.19}$$

where
$ET_{B\&C}$	potential evapotranspiration in mm/month
K	crop coefficient
p	monthly percentage of day light hours in the year
T_a	mean monthly air temperature (24 hour means) in $^{\circ}$C

Values for *K* have been determined for the western, arid, part of the USA (e.g. K = 0.75 for grass, *K = 0.80 - 0.85* for alfalfa and *K = 1.0 - 1.2* for rice). The formula is popular in the USA, since the method only requires the air temperature as input data. Application elsewhere is recommended if temperature is the only data available. Care should be taken in equatorial regions with fairly constant temperature, small islands and coastal regions, high altitudes and in climates with a wide variability in sunshine duration. Under these circumstances the radiation method is preferred, even if the radiation data have to be obtained from global maps.

In the FAO-ID24 the Blaney-Criddle method has been adapted to include the effect of different climates on the computation of the evaporation. Information on general monthly or seasonal humidity, sunshine and wind velocity data are taken into account, which makes the method applicable to climatic regions outside the USA. However, since these data are often not available in remote areas, the procedure is no longer recommended in the report on the revision of FAO methods (Smith, 1991).

Another method applicable to the arid west of the USA was presented by *Thornthwaite* in 1948. Monthly potential evapotranspiration of a short crop (e.g. grass) is estimated from monthly average daily temperatures, T_n. Use is made of a monthly heat index *j*, defined as

$$j = \left(\frac{T_n}{5}\right)^{1.514} \tag{3.20}$$

where T_n is the average temperature ($^{\circ}$C) in month *n*, based on 24 hour means. The yearly heat index *J* is then computed from

$$J = \sum_{n=1}^{12} j_n \tag{3.21}$$

The potential evapotranspiration *EP* (mm/month) in a standard month of 30 days and a day length of 12 hours follows from

$$EP = 16\left(\frac{10\,T}{J}\right)^a \tag{3.22}$$

where *T* is the mean monthly temperature in any month. The coefficient *a* is estimated from

$$a = \left(675 * 10^{-9}\right)J^3 - \left(771 * 10^{-7}\right)J^2 + \left(179 * 10^{-4}\right)J + 0.492 \tag{3.23}$$

The potential evapotranspiration according to Thornthwaite for a month with D_n number of

days and an average day length N_n then follows from

$$ET_{THORN} = EP \frac{D_n \; N_n}{360}$$

(3.24)

In table 3.6 an example computation is given for Mansoura in Egypt.

Evaporation pans

At many meteorological stations the evaporation from a small water body, an evaporation pan, is monitored. Various types of pans are in use, such as the sunken pan, floating pan and surface pan. Although the sunken and floating types of pans have distinct advantages (reducing certain boundary effects such as exchange of heat through the sidewalls), the use of the surface pan is most widespread because it causes less difficulties to operate. The most

Mansoura, Egypt							
	Tn	j	EP	D_n	N_n	ET	ET
	°C	(-)	mm/month	d	hr	mm/month	mm/d
Jan	13.3	4.4	26.4	31.0	10.4	23.7	0.8
Feb	14.0	4.8	30.1	28.0	11.1	26.0	0.9
Mar	16.3	6.0	42.7	31.0	12.0	44.2	1.4
Apr	19.6	7.9	66.0	30.0	12.9	71.0	2.4
May	24.4	11.0	111.2	31.0	13.6	130.2	4.2
Jun	26.1	12.2	130.2	30.0	14.0	151.9	5.1
Jul	26.6	12.5	135.6	31.0	13.9	162.3	5.2
Aug	27.0	12.8	141.1	31.0	13.2	160.3	5.2
Sep	25.8	12.0	126.2	30.0	12.4	130.4	4.3
Oct	22.9	10.0	95.8	31.0	12.0	98.9	3.2
Nov	19.9	8.1	68.8	30.0	10.6	60.8	2.0
Dec	15.2	5.4	36.5	31.0	10.8	34.0	1.1
J = 107.0, a = 2.4						Average = 3.0	

Table 3.6 Example computation of ET$_{THORN}$

common surface pan is the *U.S. Weather Bureau Class A pan* (see figure 3.6). The diameter of the pan is 1.21 m and the depth is 255 mm with a water level that is maintained at 50 - 75 mm below the rim. The pan is placed on a wooden structure so that the bottom is 150 mm above the ground. Evaporation is recorded from water level changes, corrected by rainfall depths. *Annual* evaporation from a nearby lake is approximately 0.7 times the observation from a pan.

This factor 0.7 is known as the pan coefficient. Its value varies over the different climatic regions between 0.67 and 0.81. The larger evaporation rates from the pan are due to the extra energy that is received from the sides of the pan, which are exposed to the sun. Moreover, the vapour pressure deficit as well as the temperature of the air over the pan is generally higher than above the lake. Another factor of importance is the larger roughness of the surface at the meteo-site as compared to the lake surface. Furthermore, differences between the heat capacities of pan and lake may produce large
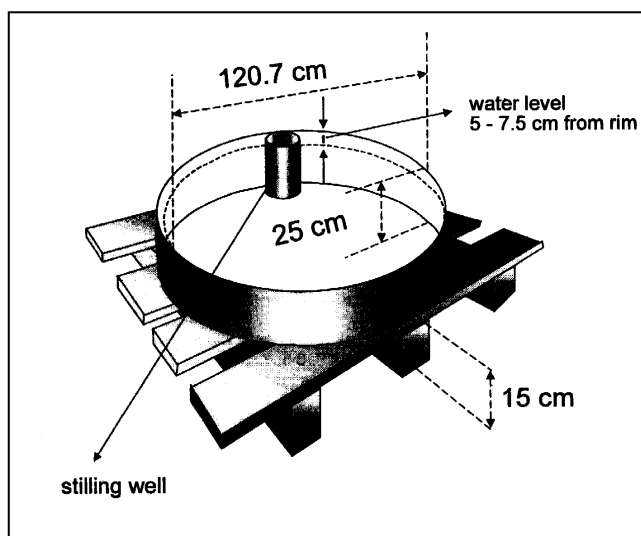

Fig. 3.6 Class A pan

variations in pan coefficients when considering short time periods. E.g. monthly pan coefficients for lake Hefner (USA) range from 0.34 in May to 1.31 in November. For these reasons the pan evaporation method is not considered accurate. Moreover, the data are often affected by inadequate maintenance of the pan, birds using the device for drinking, algae growth, etc.

The FAO-ID24 uses pan evaporation data E_{pan} to estimate reference evaporation ET_{ref} as follows

$$\mathbf{ET_{ref} = k_{pan} \ E_{pan}} \tag{3.25}$$

where the pan coefficient, k_{pan} is to be found in relation to the type of pan, the siting, and general information on wind speed and relative humidity. It is expected that the relation between the pan evaporation and the evapotranspiration of grass is even less well established. FAO pan coefficients for the Class A pan vary from 0.35 to 0.85.

3.8 Example calculations

For the example calculations meteorological data collected in Marib (Yemen) will be used. The data are (where appropriate 24 hour) averages for the month of June.

Latitude	: 15 °North
Altitude	: 1000 m
Sunshine duration	: 10.4 hr
Relative humidity	: 38.4 %
Minimum air temperature	: 23.4 °C
Maximum air temperature	: 38.6 °C
Wind speed at 2 m height	: 2.1 m/s

Penman Open Water Evaporation
Values given in the text above for the pressure and density of the atmosphere, and the psychrometric constant apply at sea level. The formulae below may be used to estimate values at higher altitudes.
For a temperature at mean sea level of 20 °C, the atmospheric pressure, p_a (kPa) as a function of the height, z in metres above mean sea level may be approximated with

$$\mathbf{p_a \ = \ 101.3 \left(\frac{293 \ - \ 0.0065 \ z}{293} \right)^{5.26}} \tag{3.26}$$

The atmospheric density ρ_a (kg.m^{-3}) depends on the temperature T_a (°C) and the pressure of the air p_a (kPa). Its value may be approximated with the following formula

$$\mathbf{\rho_a = \frac{p_a}{0.287 \left(T_a + 275 \right)}} \tag{3.27}$$

The psychrometric constant may be estimated from

$$\mathbf{\gamma \approx 0.00066 \ p_a} \tag{3.28}$$

The computations for Penman open water evaporation are tabulated in (3.7).

Parameter	Symbol	Equation	Computation	Result
Atmospheric pressure	p_a	3.26	101.3x{(293-6.5)/293}^5.26	90.0 kPa
Psychrometric constant	γ	3.28	0.00066x90.0	0.059 kPa/^{o}C
Mean air temperature	T_a		(23.4 + 38.6)/2	31.0 ^{o}C
Atmospheric density	r_a	3.27	90.0/{0.287(31+275)}	1.025 kg.m^{-3}
Saturation vapour pressure of air	e_s	3.11	0.6108 exp{17.27x31/(31+237.3)}	4.49 kPa
Slope sat. vapour pressure-temp. curve	s	3.12	4098x4.49/(31+237.3)^2	0.256
Actual or dew point vapour pressure	e_d	2.1	4.49x38.4/100	1.72 kPa
Extraterrestrial radiation	R_A	table 3.3	(423+452)/2	437.5 W.m^{-2}
Day length	N	table 3.4		13.0 hr
Relative sunshine duration	n/N		10.4/13	0.8
Sort wave radiation	R_S	table 3.5	(0.25+0.5x0.8)437.5	284.4 W.m^{-2}
Long wave radiation	R_{nL}	3.4	5.6745x10^(-8)x{(273+23.4)^4 +(273+38.6)^4}/2x(0.34-0.139 /1.72) (0.1+0.9x0.8)	62.9 W.m^{-2}
Net radiation	R_N	3.5	(1-0.06)284.4-62.9	204.4 W.m^{-2}
Aerodynamic resistance	r_a	3.13	245/(0.54x2.1+0.5)	149.9 s.m^{-1}
Open water evaporation	E_o	3.10	86400/(2.45x10^6){0.256x204.4+1004 .6x1.025x(4.49-1.72)/149.9}/ (0.256+0.059)	7.8 mm/d

Table 3.7 Example computation of Penman Open water evaporation

Neglecting the storage of heat below the evaporating surface, the evaporation from the reservoir at Marib in June may thus be estimated at 7.8 mm/d.

Penman-Monteith potential evapotranspiration of grass
All parameters computed above may be used for estimating the potential evapotranspiration of grass, except for R_N, because of the difference in albedo, and for r_a, because of a different wind function. The computation is carried out for the standard grass crop, defined by FAO with $r_c = 70$ s.m^{-1}, $r = 0.23$ and the crop a height $h_c = 0.12$ m.

Parameter	Symbol	Equation	Computation	Result
Aerodynamic resistance	r_a	3.15	208/2.1	99.0 s.m^{-1}
Net radiation	R_N	3.5	(1-0.23)284.4-62.9	156.1 W.m^{-2}
Potential evapotrans-piration of grass	ET	3.14	86400/(2.45x10^6){0.256x156.1+ 1004.6x1.025x(4.49-1.72)/99.0}/ {0.256+0.059x(1+70/99.0)}	6.8 mm/d

Table 3.8 Example computation Penman-Monteith potential evapotranspiration of grass

The potential evapotranspiration of grass or the FAO reference evapotranspiration may thus be estimated at 6.8 mm/d for Marib in the month of June.

3.9 Evaporation measurement

Direct measurement of evaporation or evapotranspiration from extensive water or land surfaces has not as yet been realized. There are several indirect methods, which are discussed below.

Atmometers

These devices consist of a porous surface connected to a water supply. The evaporation from the porous surface is found as the change in the amount of water stored in the water supply. Well-known atmometers are the Piche evaporimeter using absorbent blotting paper, the Livingstone atmometer using a porous porcelain sphere and the Bellani atmometer of which the porous surface consists of a thin ceramic disc. The devices are designed to represent the transpiration of leaves, but it is obvious that the presence of stomata and its biological control cannot be simulated. Moreover, it is found that atmometers are very responsive to wind, and less to net radiation, which is the dominant factor governing evaporation. Nevertheless, there are examples of satisfactory relations that have been established between the evaporation from an atmometer and the potential evapotranspiration of a crop.

Evaporation pans

The FAO methods on crop water requirements use data on evaporation pans to estimate reference evapotranspiration. The technique is discussed in the section 3.7.

Hydrologic budget method

For a lake, reservoir or river basin that do not show any significant leakage, evaporation may be obtained from the water balance equation:

$$\mathbf{E = P - Q - \Delta S / \Delta t} \tag{3.29}$$

The method is less simple than if appears. Many reservoirs show leakage, which is difficult to quantify. Errors in the measurements of the net outflow from the reservoir are reflected upon the accuracy of the obtained evaporation values. Determination of the change in storage is very difficult for a river basin. Annual values may be obtained after careful selection of the water year, so that the change in storage can be neglected (see section 1.3). To obtain the change in storage for a reservoir an accurate relation between water level and storage in the reservoir must be known.

Soil water budget method

The water balance of the root zone may be written as

$$\mathbf{I + P_s + G = E + D + Q_s + \Delta S / \Delta t} \tag{3.30}$$

where
I	irrigation
P_s	precipitation minus interception
G	groundwater contribution through capillary rise

E   evapotranspiration
D   percolation from the root zone to the groundwater system
Q_s surface runoff
$\Delta S/\Delta t$ rate of change in storage

All terms in the water balance are in the unit of mm per time. Application of the method is difficult in particular in the presence of a shallow water table and in sloping areas, because the values of *G, D* and Q_s are difficult to evaluate.

The boundary conditions for applying the water balance equation are much better defined with the use of a lysimeter, a closed container in the soil from which the outflow (drainage) can be measured. In some lysimeters the water table may be controlled (see figure 3.7).

The change in storage is obtained from measurements of the moisture content (e.g. a neutron probe using one or two permanent access tubes) or by weighing the lysimeter. The container is preferable placed in the

Fig. 3.7   Lysimeter with controlled water table

middle of a field, filled with the same type of soil (monolith) and covered with the same crop.

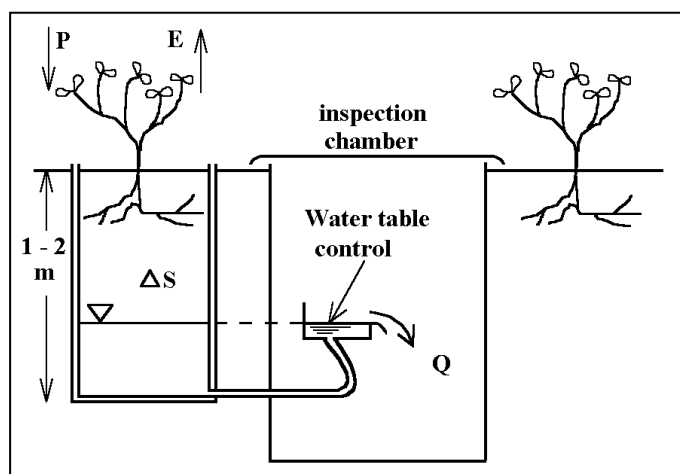A different type of lysimeter was constructed in 1940 in the dunes near Castricum, The Netherlands. The lysimeters are provided with a drainage system at the bottom, the outflow of which can be monitored. Since the change in storage is not measured, the device is only suitable to obtain evaporation rates for large account periods (water years).

Remote sensing
Another indirect method to measure (actual) evapotranspiration from large areas is through remote sensing using satellites or airplanes. The images in the visible part of the spectrum, the reflection images, give information on the type of crop and with the thermal infra-red images the surface temperatures of the crop may be detected. The method is to be used in combination with a soil moisture simulation model (Nieuwenhuis et al., 1985). For situations of drought, the soil moisture deficit causes the stomata of the leaves to close, reducing the transpiration of the plant. Consequently, the surface temperatures of the vegetation suffering from drought will be higher than for other plants in the same growth stage, not short of water. Simulation results from water balance models are required to calibrate the relative differences in the actual evapotranspiration rate.

In desert areas the surface reflectivity and thermal behaviour have been used in combination with ground measurements to determine the areal actual evaporation (Menenti, 1983).

3.10 Is evaporation a loss?

In most water balances, evaporation is considered a loss. Hydrological engineers, who are asked to determine surface runoff, consider evaporation a loss. Water resources engineers, who design reservoirs, consider evaporation from the reservoir a loss. For agricultural engineers, however, it depends on where evaporation occurs, whether it is considered a loss or not. If it refers to the water evaporated by the crop (transpiration), then evaporation is not a loss, it is the use of the water for the intended purpose. If it refers to the evaporation from canals or from spill, then evaporation is considered a loss, which reduces the irrigation efficiency.

However, there is a situation where evaporation, whether intentional or non-intentional, is not a loss. This is in the case of large continents where water vapour is transported inland by a prevailing wind. Such a situation occurs, for instance, in West Africa. Moist air is transported inland by the monsoon. Most of the air moisture precipitates on the tropical rainforests near the coast. Further inland it becomes dryer. Further inland, beyond the rainforest belt, lies the Savanna woodland, followed by the Sahel and the desert.

It has been shown by Savenije and Hall (1993) that the rainfall that falls in the Sahel, for a very large portion (more than 50%), consists of water that has evaporated from the areas nearer to the coast. Recycling of moisture through evaporation is responsible for the relatively small amounts of rain that fall in the Sahel. Evaporation in the rainforest and the savanna woodlands, hence, is essential for the climate in the Sahel. In this case, evaporation is not a loss, it is the most important source of rainfall further inland.

In the Sahel, evaporation is not a loss. What is a loss to the system is surface runoff. Not only does it extract water from the system, it also carries nutrients and soil particles. Reduction of runoff and, hence, increase of local evaporation is an important element of water harvesting. Measures that can be used to decrease runoff are reforestation, erosion control, watershed management, restoration of infiltration capacity, forest-fire prevention and prevention of over-grazing.

4 GROUNDWATER RESOURCES

4.1 Occurrence

Two zones can be distinguished in which water occurs in the ground:

- the saturated zone
- the unsaturated zone.

For the hydrologist both zones are important links and storage devices in the hydrological cycle. For the engineer the importance of each zone depends on his field of interest. An agricultural engineer is principally interested in the unsaturated zone, where the necessary combination of soil, air and water occurs for a plant to live. The water resources engineer is mainly interested in the groundwater which occurs and flows in the saturated zone.

The process of water entering into the ground is called infiltration. Downward transport of water in the unsaturated zone is called percolation, whereas the upward transport in the unsaturated zone is called capillary rise. The most important flow components above the phreatic surface (watertable) are depicted in figure 4.1. The flow of water through

Fig. 4.1 Flow components above the watertable

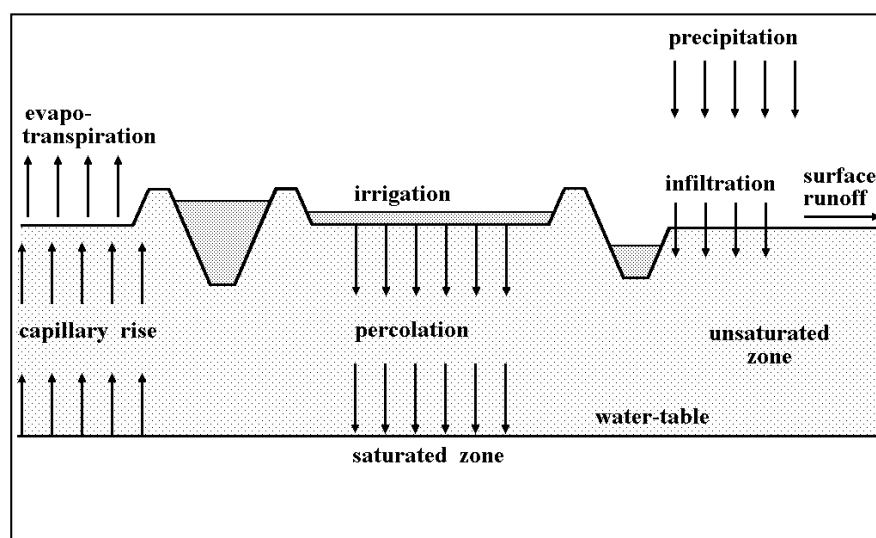saturated porous media is called groundwater flow. The outflow from groundwater to surface water is called seepage.

The type of openings (voids or pores) in which groundwater occurs is an important property of the subsurface formation. Three types are generally distinguished:
1. *Pores*, openings between individual particles as in sand and gravel. Pores are generally interconnected and allow capillary flow for which Darcy's law (see below) can be applied.
2. *Fractures, crevices or joints in hard rock* which have developed from breaking of the rock. The pores may vary from super capillary size to capillary size. Only for the latter situation application of Darcy's law is possible. Water in these fractures is known as fissure or fault water.
3. *Solution channels and caverns in limestone* (karst water), and openings resulting from gas bubbles in lava. These large openings result in a turbulent flow of groundwater which cannot be described with Darcy's law.

The porosity n of the subsurface formation is that part of its volume which consists of openings and pores:

$$\mathbf{n} = \frac{\mathbf{V_p}}{\mathbf{V}}$$

(4.1)

where V_p is the pore volume and V is the total volume of the soil.

When water is drained by gravity from saturated material, only a part of the total volume is released. This portion is known as specific yield. The water not drained is called specific retention and the sum of specific yield and specific retention is equal to the porosity. In fine-grained material the forces that retain water against the force of gravity are high due to the small pore size. Hence, the specific retention of fine-grained material (silt or clay) is larger than of coarse material (sand or gravel).

4.2 Unsaturated zone

Infiltration

Infiltration is the transition of water from the soil surface into the soil. The maximum rate at which a given soil in a given condition can absorb water is known as the infiltration capacity. Infiltration of water in the soil is an important component of the hydrological cycle as it determines the part of the precipitation that runs off overland into the river contributing to the peak discharge. A reduction of the flood hazard may be obtained through an increase of the infiltration capacity. Unfortunately most of man's activities decrease the infiltration capacity. E.g. urbanization creates large impervious areas and deforestation eliminates the retention mechanism which allows time for precipitation to infiltrate into the soil. Overgrazing affects infiltration in two ways: it reduces the vegetation (vegetation enhances infiltration) and cattle hoofs can destroy the surface layer in a way that infiltration is reduced. In sloping areas low infiltration rates contribute to the erosion of the land surface.

The infiltration capacity of the soil is not only important in relation to flooding and erosion. Water that infiltrates into the soil replenishes the soil moisture deficit in the unsaturated zone and when the situation of field capacity is reached, it percolates down to the watertable to recharge the groundwater reservoir. A large infiltration capacity is, therefore, important for the water supply to the crop and the groundwater recharge. An improvement of the availability of moisture for crop and vegetation increases the evapotranspiration and reduces the total runoff from the catchment. In areas where groundwater is used for e.g. irrigation, or drinking water supply, the recharge of the groundwater system is of primary importance. Moreover, groundwater recharge determines the base flow component of the river discharge and the minimum flow during periods of drought when the discharge is fully sustained by the groundwater outflow into the river.

The following factors affect the infiltration capacity:
- *The type of soil*, e.g. gravel is more permeable than loam.
- *Presence and type of vegetation*. Vegetation improves the structure of the soil, increases the porosity and biological activity, causing root- and worm channels which facilitate the transport of water. Moreover, vegetation delays the runoff process, allowing more time for the precipitation to infiltrate.

- *Agricultural tillage*. In view of the erosion hazard various tillage practices have been developed (e.g. contour ploughing), which aim to restrict the surface runoff.
- *The moisture content of the soil*. A dry soil absorbs water more readily than a wet soil. Moreover, in case of swelling and shrinking clay, the cracks that are formed during the dry period largely increase the infiltration capacity.

Infiltration is governed by the under-pressure of water in the soil (the matric pressure) and the force due to gravity. In a dry soil the under-pressure exerted by the soil matrix is extremely high and it is the dominant driving force for water infiltration. With time, as the soil becomes wetter, the matric force and thus the infiltration rate reduces and gravity becomes the most important driving force. Other reasons why the infiltration capacity reduces over time are:
- the closing of the surface by the falling raindrops;
- swelling of clay and humus particles;
- enclosure of air bubbles in the pores.

Several empirical formulae have been suggested to describe the change of the infiltration capacity with time. The most commonly used expression is probably the formula proposed by Horton (1940), which may be written as:

$$\mathbf{f_p = f_c + (f_0 - f_c)\ e^{-k\,t}} \tag{4.2}$$

where:

f_p : infiltration capacity (mm/h)
f_0 : initial infiltration capacity at t = 0 (mm/h)
f_c : infiltration capacity at large value of t (mm/h)
 t : time from beginning of infiltration period (min)
 k : constant for a particular soil and surface cover (min^{-1})

The parameters f_c and k are dependent on soil type and vegetation, and have to be determined with field experiments. Due to the large under-pressure of the soil water in a dry soil, initial infiltration rates into a dry soil are larger than for a wet soil. Hence, f_0 depends on the initial 'dryness' of the soil . Examples of infiltration capacity rates with time for wet and dry soil are given in figure 4.2. The curves have been computed with $k = 0.2$ hr^{-1}, $f_c = 5$ mm/hr, $f_o = 15$ mm/hr for wet and $f_o = 25$ mm/hr for dry soil. The formula applies for the situation of *ponded infiltration*, i.e. there is water standing on the surface, for instance when using infiltrometer rings (see below). Measurements with the latter instrument yield the cumulative infiltration with time, $F(t)$. The equation for cumulative infiltration is found by integrating equation 4.2 from time t_o to t which gives:

$$\mathbf{F(t) = f_c(t - t_0) + \frac{f_0 - f_c}{k} * \left(e^{-k\,t_0} - e^{-k\,t}\right)} \tag{4.3}$$

Application of this equation to the infiltration capacity curve for dry soil in figure 4.2 yields the cumulative infiltration curve in figure 4.3.

The actual infiltration rate f is, of course, the minimum of rainfall intensity i and infiltration capacity f_p, or $f = min(i, f_p)$. Knowledge of the infiltration parameters is of importance in surface irrigation, erosion control and several specific studies in the field of hydrology. The infiltration characteristics show a large spacial variability. It is, therefore, difficult to determine
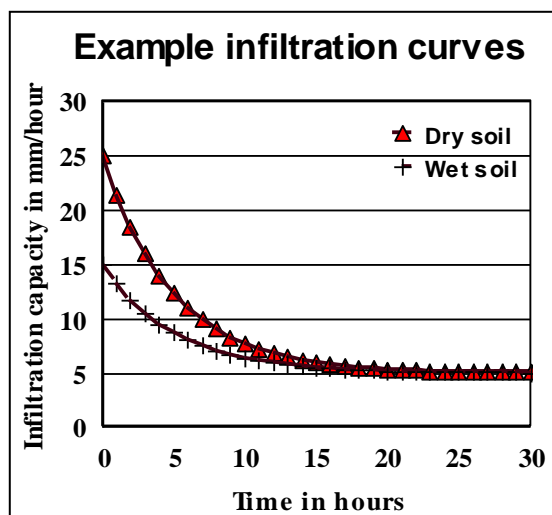
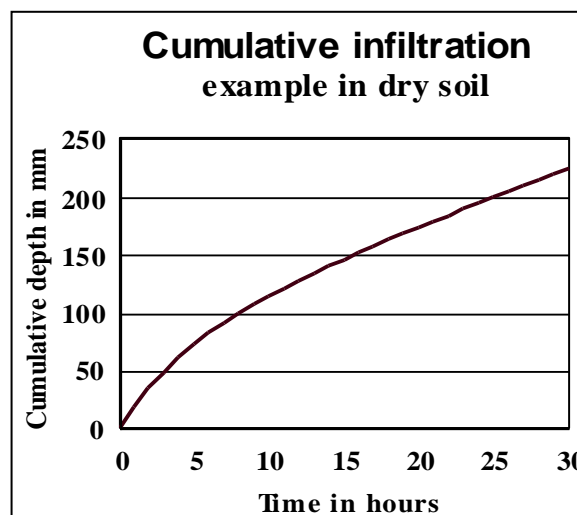**Fig. 4.2 Examples of infiltration curves for a wet and dry soil**

Fig. 4.3 Example cumulative infiltration curve for dry soil

average values for an entire catchment. Infiltration formulae are sometimes used to determine - what hydrologists often call - "losses", which are defined as the difference between precipitation and direct runoff. However, losses also include interception and surface detention, which may not always be neglected.

Infiltration measurement

Measurements of infiltration capacity should be carried out under field conditions, because the process is affected by the natural situation of soil structure, moisture content and plant cover. Two methods of infiltration measurement are in common use: (a) infiltrometer and (b) sprinkling test.

a) *Infiltrometers* (see figure 4.4) usually consist of a single or double ring which are driven into the ground to a depth of a few centimetres. Water is applied from a graduated burette and maintained at a constant head over the soil surface. Readings of the water level in the burette are taken at successive time intervals. The water level in the concentric or double ring infiltrometer is maintained in both rings at the same level, but measurements are only taken on the inner ring. The outer ring serves to reduce the disturbing boundary effects of lateral flow. The side effect does not exist for tubes which are driven into the ground to depths of 40-50 cm. Placing the tube without disturbing the natural structure of the soil and the possible unsatisfactory contact between soil and side of the tube may, however, create a problem.

b) *Sprinkling tests* are carried out on a well-defined plot of a few tens of square meters in size. Sprinklers are used simulating a known intensity of rainfall i which is greater than the infiltration capacity ($i > f_p$). The plot is slightly sloping and the water that runs off over the surface ($i - f_p$) is collected in a gutter and continuously measured. After a long time the surface runoff becomes approximately constant, indicating that f_p approaches a constant value f_c. The sprinkling is then terminated and the runoff monitored until it has ceased. Several methods described in various textbooks are available to analyze the results of sprinkling tests.

The sprinkling tests normally yield values of infiltration about half those obtained from the flooding-type infiltrometers. This is because of the dynamic action of falling water drops. The results should, therefore, be applied to similar field conditions.
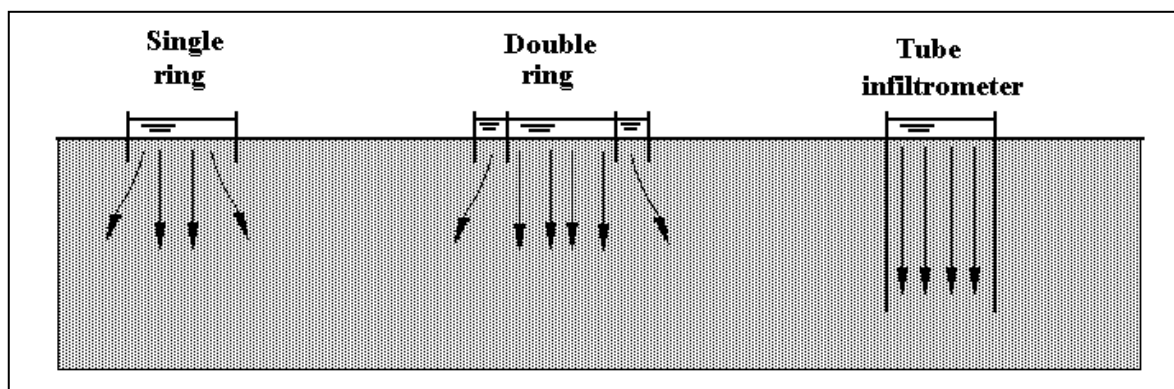
Fig. 4.4 Infiltrometers

Soil moisture

The moisture content (volume of water per volume of soil) in the unsaturated zone is not constant but varies with the depth and with time. The maximum moisture content is found at the watertable, where all the pores are filled with water. At the soil surface the moisture content may be lowest, except after rainfall or irrigation. Figure 4.5 gives an example of the distribution of water, air and solids with the depth. The porosity of the soil is usually not constant with the depth. In agricultural land the top layer has often a high porosity due to tillage, although at plough depth a dense layer may have formed. Figure 4.5 shows the schematisation of the porosity in two constant values, one for the root zone and one for the subsoil.

The pressure of water in the soil is expressed with respect to atmospheric pressure. Since the watertable is defined as the level in the soil where the pressure is atmospheric, the water pressure at this level is zero, positive below and negative above the phreatic surface. The negative pressure in the unsaturated zone results from the attraction of water by the soil matrix, and is,
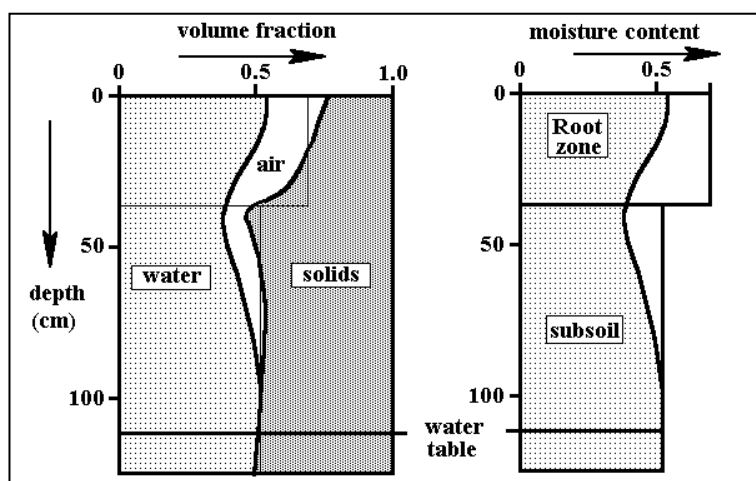

Fig. 4.5 An example of the distribution of water, air and solids with the depth and the schematisation into a root zone and subsoil with a constant porosity

therefore, also referred to as *matric pressure*. Its value varies from 0 at the watertable to -10^7 mbar in air-dry soil. Nowadays the pressure is preferably expressed in SI units ($N.m^{-2}$ = Pascal), where the pressure of 1 cm water column $= 1$ mbar $= 100$ Pa $= 1$ hPa. In view of the large range of the water pressures in the soil the logarithm of the absolute value of the pressure in hPa, known as pF, is often used.

The relation between the moisture content and the water pressure is known as the *soil moisture characteristic* or *pF-curve*. Examples of pF-curves for different types of soil are presented in figure 4.6.

Important conditions in the unsaturated zone are the *wilting point* and the *field capacity*. Field capacity refers to the soil moisture situation a few days after irrigation or heavy rainfall, when excess water in the unsaturated zone has percolated. Field capacity is often defined to correspond to a pressure of -100 hPa (pF 2), but also larger pF values are used (pF 2.3 or even pF 2.7).

Wilting point corresponds to a minimum soil moisture content for which the plant is no longer capable of taking up the soil moisture and dies. The corresponding water pressure is about -16 bar = -16,000 hPa! (pF 4.2).

At the phreatic surface, where the soil is completely saturated, the pressure is zero (pF $\approx$ 0) and the moisture content equals the porosity.

The soil moisture characteristic may be used to determine the amount of water that is available to the crop in the root zone. Consider as an example the pF-curve for loam, given in figure 4.6. The moisture content that is retained after irrigation (field capacity) equals 27.5%, corresponding to pF 2. In the absence of rainfall or irrigation the crop will take up water from the root zone until the wilting point situation is reached (at which stage the plant dies due to lack of water). Figure 4.6 shows that the moisture content for loam has then reduced to 6.5%, corresponding to pF = 4.2. The amount of water that is available for the crop in a root zone with a thickness of for example 60 cm is then computed as 60 x (0.275 - 0.065) = 12.6 cm or 126 mm. The amount is known as the *Available Moisture* (AM). Long before the soil moisture situation in the root zone reaches wilting point the plant suffers from drought. Some crops are very sensitive (in particular vegetables), others (most cereals) do not show a reduction in yield until the pF reaches a value of 3. The amount of water that may be extracted from the root zone before the crop shows a significant reduction in yield is known as the *Readily Available Moisture* (RAM). Irrigation engineers often estimate the Readily Available Moisture as half the Available Moisture (RAM = ½ AM). Hence, for the example discussed above RAM = 63 mm. Given an evapotranspiration rate of, e.g. 6 mm/d, the irrigation interval should, in the absence of rainfall, not be longer than 10 days in order to avoid yield reduction due to water stress in the root zone.
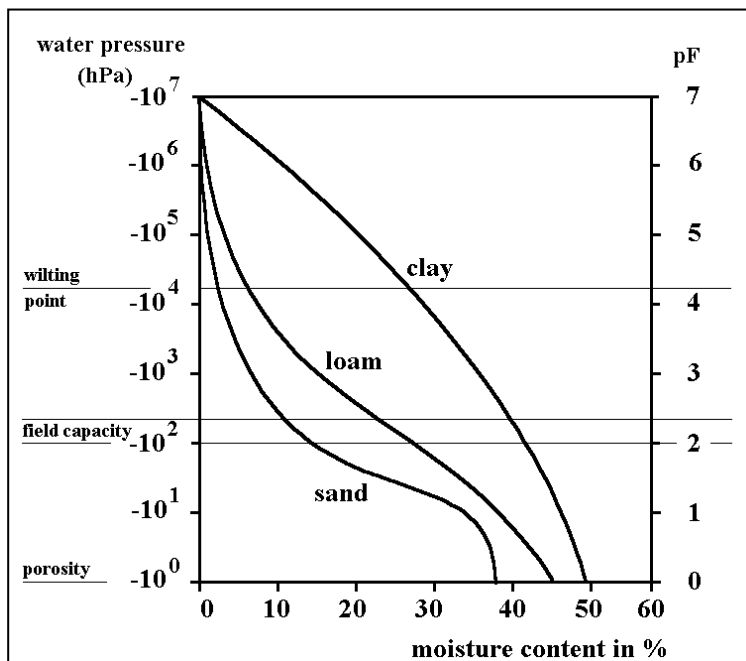

Fig. 4.6 Soil moisture characteristics (pF curves)

4.3   Saturated zone

Groundwater is the water which occurs in the saturated zone. The study of the occurrence and movement of groundwater is called groundwater hydrology or geohydrology. The hydraulic properties of a water-bearing formation are not only determined by the porosity but also by the interconnection of the pores and the pore size. In this respect the subsurface formations are classified as follows:

1. *Aquifer*, which is a water-bearing layer for which the porosity and pore size are sufficiently large to allow transport of water in appreciable quantities (e.g. sand deposits).
2. *Aquiclude* is an impermeable layer, which may contain water but is incapable of transmitting significant quantities.
3. *Aquitard* is a less permeable layer, not capable of transmitting water in a horizontal direction, but allowing considerable vertical flow (e.g. clay layer).
4. *Aquifuge* is impermeable rock neither containing nor transmitting water (e.g. granite layers).

Classification of rocks

The water transmitting properties are dominated by the type of geological formation. Rocks can be divided in three main groups:

1. *Igneous rocks*, which are formed at the solidification of cooling magma (e.g. granite) or volcanic material (e.g. basalt). Igneous rocks have a crystalline structure and a very low porosity (often less than 1 %). The water-bearing properties are generally very low unless an extensive jointing, fracturing and faulting is present.
2. *Sedimentary rocks* are formed by deposits of weathered material of pre-existing rocks. Depending on the type of transport mechanism the following sedimentary rocks may be distinguished:
   a. *Fluvial or alluvial (river) deposits*, which include gravel, sand, silt and clay. These formations are characterized by stratification. The porosity varies between 20 and 60 %, but only gravel and sand show macro-pores. Due to cementing, pressure and/or temperature sand may have changed in sandstone and lime deposits into limestone. These consolidated rocks have a much lower ability to transmit water unless fractures or karst phenomena (limestone) are present.
   b. *Aeolian (wind) deposits* include sand and silt (loess). Often large areas are covered with relatively homogeneous material.
   c. *Glacial (ice) deposits*. During the Pleistocene glaciers deposited glacial till which usually is a mixture of silt, sand and clay in which pebbles and huge boulders may be present. These deposits are in general poor water producers. Other sedimentary rocks are named in relation to their origin, location and environmental conditions, e.g. marine (sea) deposits, organogenic deposits (from organic life), terrestrial deposits, etc.
3. *Metamorphic rocks* are formed from igneous or sedimentary rocks by chemical and physical processes (heat and pressure). Examples are slate, gneiss, quartzite and marble. These rocks are the poorest water producers.

Aquifers

For a description or mathematical treatment of groundwater flow the geological formation can be schematized into an aquifer system, consisting of various layers with distinct different hydraulic properties. The aquifers are classified into three types (see figures 4.7 and 4.8):

1. *Unconfined aquifer* (also phreatic or watertable aquifer) which consists of a pervious layer underlain by a (semi-) impervious layer. The aquifer is not completely saturated with water. The upper boundary is formed by a free watertable (phreatic surface).
2. *Confined aquifer*, consisting of a completely saturated pervious layer bounded by impervious layers. The water level in wells tapping those aquifers rises above the top of the pervious layer and sometimes even above soil surface (artesian wells).
3. *Semi-confined or leaky aquifers* consist of a completely saturated pervious layer, but the upper and/or under boundaries are semi-pervious.

The pressure of the water in an aquifer is measured with a piezometer, which is an open-ended pipe with a diameter of 3 - 10 cm. The height to which the water rises with respect to a certain reference level (e.g. the impervious base, mean sea level, etc.) is called the hydraulic head. Strictly speaking the hydraulic head measured with a piezometer applies for the location at the lower side of the pipe, but since aquifers are very pervious, this value is approximately constant over the depth of the aquifer. For unconfined aquifers the hydraulic head may be taken equal to the height of the watertable, which is known as the Dupuit-Forchheimer assumption.

Fig. 4.7 Classification of aquifers

Water moves from locations where the hydraulic head is high to places where the hydraulic head is low. For example, figure 4.8 shows that the hydraulic head in the semi-confined aquifer is below the hydraulic head (or phreatic surface) in the unconfined aquifer. Hence, water flows through the semi-pervious layer from the unconfined aquifer into the semi-confined aquifer. A perched watertable may develop during a certain time of the year when percolating soil moisture accumulates above a less pervious layer.

Fig. 4.8 Aquifer types

Groundwater flow

The theory on groundwater movement originates from a study by the Frenchman Darcy, first published in 1856. From many experiments (figure 4.9) he concluded that the groundwater discharge Q is proportional to the difference in hydraulic head ΔH and cross-sectional area A and inversely proportional to the length Δs, thus
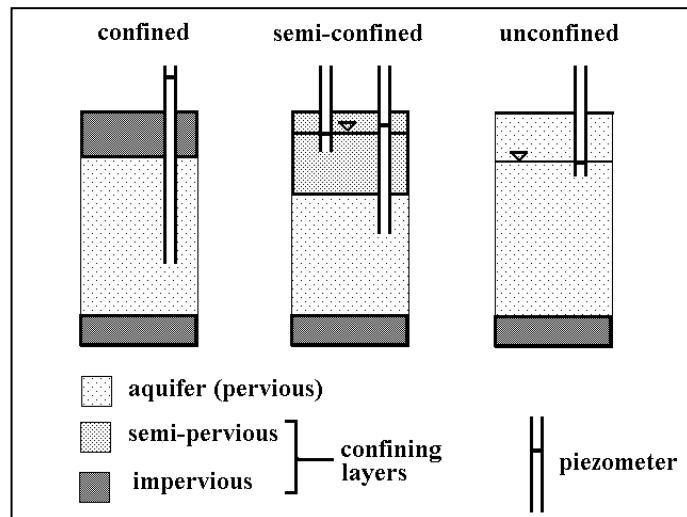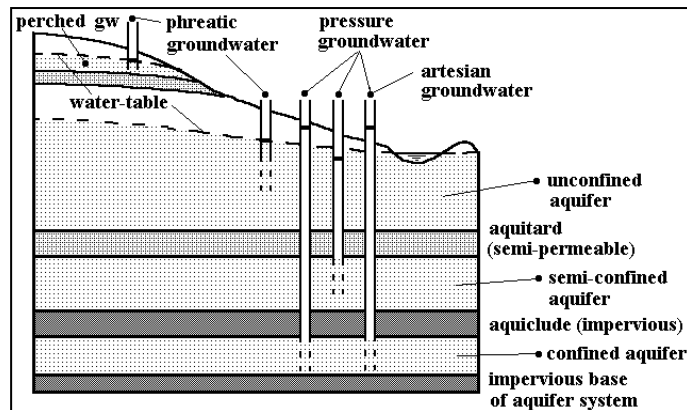
$$Q = A v = - A k \frac{\Delta H}{\Delta s} \tag{4.4}$$

where k, the proportionality constant, is called the hydraulic conductivity, expressed in m/d; and v is the specific discharge, also called the filter velocity ($m^3.m^{-2}.d^{-1}$).

Since the hydraulic head decreases in the direction of flow, the filter velocity has a negative sign. The actual velocity v_{act} of a fluid particle is much larger because only the effective pore space n_e is available for transport, thus

$$v_{act} = \frac{v}{n_e} \tag{4.5}$$

The effective porosity n_e is smaller than the porosity n, as the pores that do not contribute to the transport are excluded (dead end pores). The actual velocity is important in water quality problems, to determine the transport of contaminants.

For a detailed description of groundwater flow and groundwater recovery, reference is made to the respective lectures.
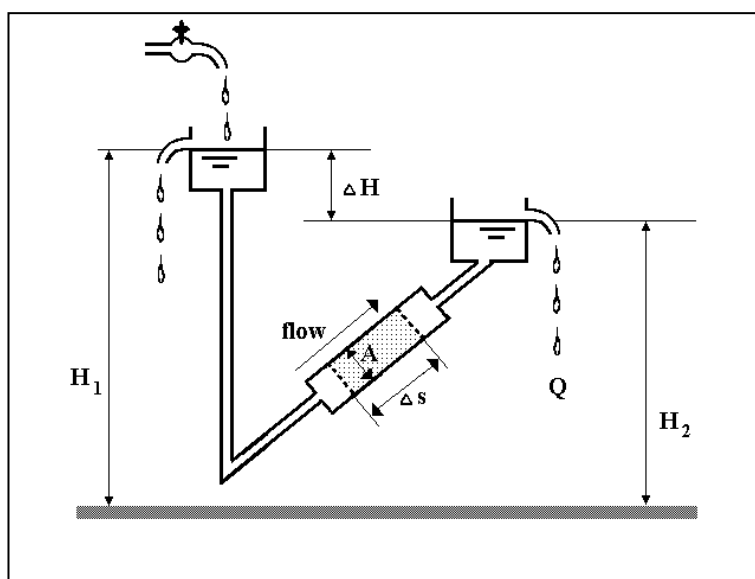
Fig. 4.9 Experiment of Darcy

4.4 Groundwater as a storage medium

For the water resources engineer groundwater is a very important water resource for the following reasons:

- it is a reliable resource, especially in climates with a pronounced dry season
- it is a bacteriologically safe resource, provided pollution is controlled
- it is often available in situ
- it may supply water at a time that surface water resources are limited
- it is not affected by evaporation loss, if deep enough

It also has a number of disadvantages:

- it is a strongly limited resource, extractable quantities are often low as compared to surface water resources
- groundwater recovery is generally expensive as a result of pumping costs
- groundwater, if phreatic, is very sensitive to pollution

- groundwater recovery may have serious impact on land subsidence or salinization

Especially in dry climates the existence of underground storage of water is of extreme importance. The water stored in the subsoil becomes available in two ways. One way is by artificial withdrawal (pumping) the other is by natural seepage to the surface water.

The latter is an important link in the hydrological cycle. Whereas in the wet season the runoff is dominated by surface runoff, in the dry season the runoff is almost entirely fed by seepage from groundwater (base flow). Thus the groundwater component acts as a reservoir which retards the runoff from the wet season rainfall and smooths out the shape of the hydrograph.

The way this outflow behaves is generally described as a linear reservoir, where outflow is considered proportional to the amount of storage:

$$S = KQ \tag{4.6}$$

where K is a conveyance factor with the dimension time. Equation 4.6 is an empirical formula which has some similarity with the Darcy equation (4.4). The water balance equation (1.5) for the aquifer without recharge ($I(t) = 0$) and seepage to the surface water $O(t) = Q$ may be written as

$$Q = - \frac{dS}{dt} \tag{4.7}$$

Combining (4.6) and (4.7) yields

$$\frac{dS}{S} = - \frac{dt}{K} \tag{4.8}$$

Integration for $S_0 = S$ at t_0 gives

$$\int_{S_0}^{S_t} \frac{1}{S} \, dS = - \int_{t_0}^{t} \frac{1}{K} \, dt \tag{4.9}$$

which results in

$$S_t = S_0 \, e^{-\frac{t-t_0}{K}} \tag{4.10}$$

and hence, using (4.6) with $Q_0 = Q$ at t_0

$$Q_t = Q_0 \, e^{-\frac{t-t_0}{K}} \tag{4.11}$$

A more general routing equation may be derived as follows. For $t = 1$ it follows from equation (4.11)

$$Q_1 = Q_0 \, e^{-\frac{1}{K}} \tag{4.12}$$

and for t = 2 we may write

$$Q_2 = Q_0 \, e^{-\frac{2}{K}} = Q_1 \, e^{-\frac{1}{K}} \tag{4.13}$$

or more general

$$Q_t = Q_{t-1} \, e^{-\frac{1}{K}} \tag{4.14}$$

Equations 4.11 and 4.14 are useful for the evaluation of surface water resources in the dry season.

5   SURFACE WATER RESOURCES

5.1   Discharge measurement

Discharge formulae

For the calculation of open channel flow empirical equations (formulae of De Chézy and Manning) are often used. These equations apply to steady, uniform flow. The flow is steady and uniform when in the reach of the channel under consideration, the velocity *v,* the cross-sectional area of flow *A* and the hydraulic gradient *S* are everywhere the same and do not change with time. The hydraulic gradient is the change in water level per unit length. With the assumptions of steady, uniform flow, the hydraulic gradient equals the bed slope of the channel.
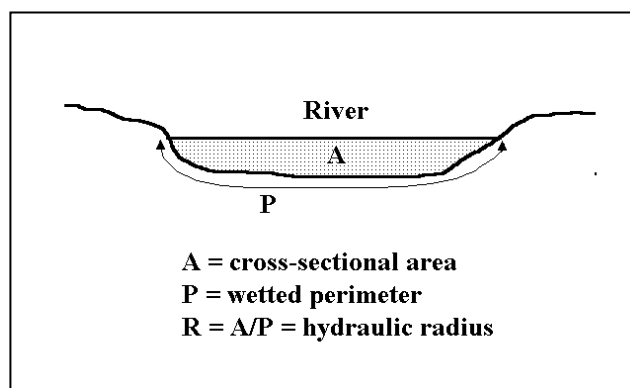
Fig. 5.1 Cross-section of river

The formula of De Chézy may be written as

$$v = C\sqrt{R\,S} \tag{5.1}$$

where

v	average velocity of flow (m.s^{-1})
C	Chézy coefficient (m$^{1/2}$.s^{-1})
R	hydraulic radius (m)
S	channel bed slope (-)

The hydraulic radius is the cross-sectional area divided by the wetted perimeter as explained in figure 5.1.

The equation of Manning may be expressed as

$$v = \frac{1}{n} R^{\frac{2}{3}} S^{\frac{1}{2}} \tag{5.2}$$

where *n* is the Manning coefficient which is related to channel roughness. Examples of the Manning coefficient are given in table 5.1.

From (5.1) and (5.2) it follows that the Chézy coefficient in (5.1) may be approximated as

$$C = \frac{R^{\frac{1}{6}}}{n} \tag{5.3}$$

Since *n* changes less than *C* as *R* varies, the Manning equation is usually preferred above the formula of De Chézy. Application of the flow formulae requires considerable experience. This applies to the estimation of the parameters as well as the assessment of the validity of the formula, which depends on the nature of the flow.

The formulae may be used to estimate flood discharges. After the flood has passed the cross-sectional area *A* and the wetted perimeter can be surveyed. The flood water level is determined from flood mark survey (see Section 5.3). The discharge *Q* is then found from

Concrete lined channel	0.013
Unlined earth channel	0.020
Straight, stable deep natural channel	0.030
Winding natural streams	0.035
Variable rivers, vegetated banks	0.040
Mountainous streams, rocky beds	0.050

Table 5.1 Manning coefficients (After Shaw, 1983)

$$Q = \bar{v} \, A$$

(5.4)

where $\bar{v}$ is the average velocity according to (5.1) or (5.2) and *A* is the cross-sectional area.

The use of empirical formulae to estimate the discharge is not as accurate as the methods discussed below. However, floods come usually unexpected or weather conditions may be such that direct measurements are not possible. In order to extend the relation between water level and discharge (the *rating curve*) to include extreme flow situations, the data thus obtained may prove to be very valuable.

Stage measurement
The following instruments are most commonly used for measuring the stage:

1. *Manual gauges*. Most common is the graduated staff gauge, installed vertically in the stream. The gauge is read once or several times a day, depending on the regime of the river. For small rivers with flashy floods a continuous measurement may be necessary in order not to miss some of the peaks.

2. *Recording gauges*. A float-actuated gauge, using a stilling well to exclude wave action, is the traditional way of continuous registration of the water level. The level may be recorded by a pen on a chart fixed on a rotating drum (figure 5.2). Other recording gauges register the level every 15 min and store the data electronically or transmits the data to the office. Some of these gauges are part of a flood warning system, initiating an alarm when the stage exceeds a prescribed level.
Instead of a float one can make use of a pressure transducer (pressure sensor). The instrument consist of a small steel cylinder that measures water levels at
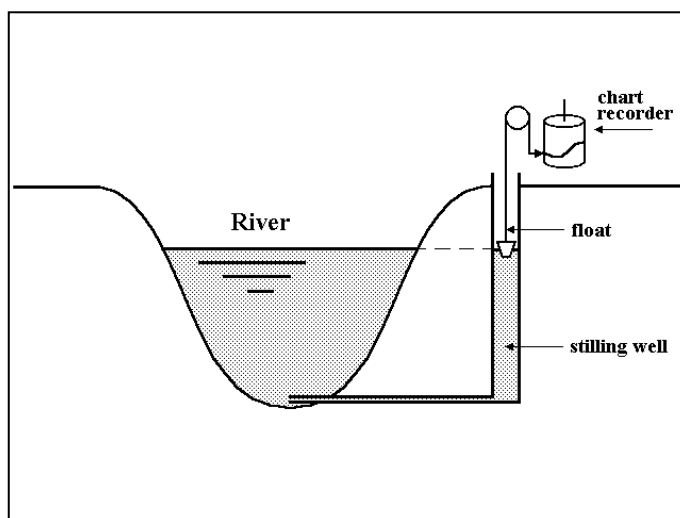

Fig. 5.2 Float-actuated recording gauge of river stage

pre-programmed intervals. The pressure transducers have a data logger that may store more than 10,000 values. Depending on the time interval of measurement, the instruments may collect data during periods of months before reading out the data. The batteries have a lifetime of 8 −10 years.

Another type of recording gauge is known as *bubble gauge*, which is a pressure-actuated system that measures the pressure by pressing small quantities of air through a pipe that is fixed on the river bed. The water level in the river is directly proportional to the pressure. This method does not require a stilling well.

Discharge measurement
The measurement of the discharge is much more laborious than reading the stage; it may take a few minutes to a few hours, depending on the size of the river and the method used. During the measurement of the discharge the water level in the river may change. It is, therefore, essential that at the start as well as at the end of the measurement the water level in the river is recorded, so that the measured discharge can be related to the average observed stage. Fluctuating water levels are especially to be expected during floods, sometimes urging the use of fast, less accurate methods for discharge measurement.

The various methods to measure the river discharge may be classified into the following three categories:

A. Velocity-area method
The method is based on equation (5.4). A survey of the cross-section of the channel is generally easy, but to obtain the average velocity is much more difficult. A typical distribution of the velocity over the cross-section of a river is shown by lines of equal velocity in figure 5.3a. The maximum velocity (here about 1 m.s^{-1}) is found just below the water surface and zero velocity occurs at the river banks. Figure 5.3b shows a velocity profile, a plot of the velocities in vertical direction.

The velocity at a point in the river is usually obtained with current meters. Two types are distinguished:
- *cup type*, having a number of conical cups revolving around a vertical axis. It registers the velocity whatever its direction.
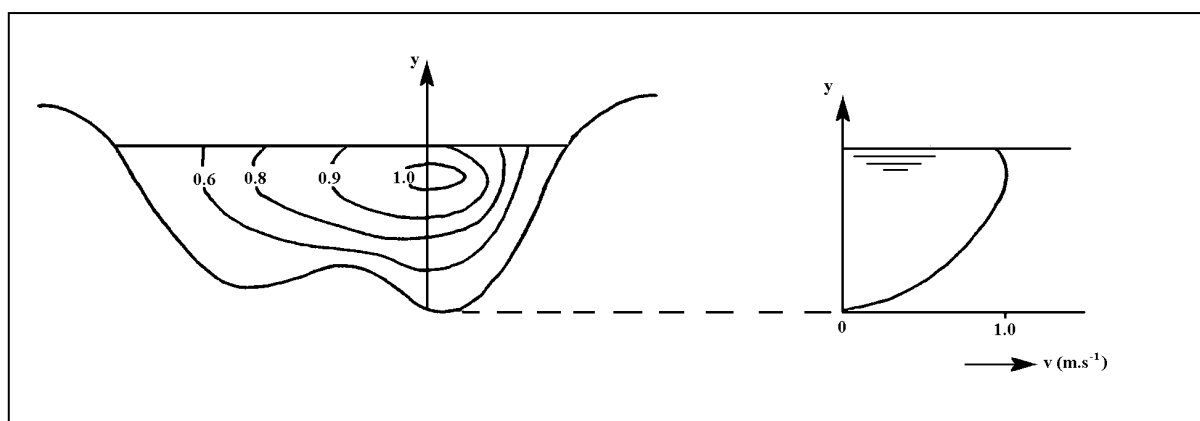- *propeller type*, having a single propeller on a horizontal axis.

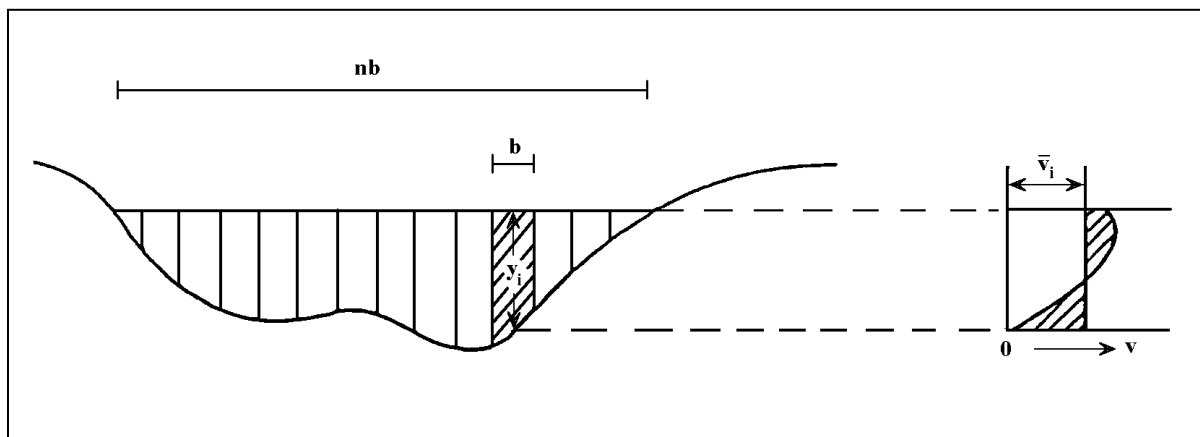**Fig. 5.3 a) Velocity contours (left) and b) velocity profile (right)**

Fig. 5.4 Gauging procedure

A make-and-break contact gives an electric pulse at each revolution, which pulses are counted during a short period using a stopwatch. The current meters are regularly calibrated to obtain (or check) the relationship between the number of revolutions and the water velocity.

A velocity meter without moving parts is the Electro Magnetic flow velocity Sensor (EMS). The method is based on the magnetic induction principle (Faraday's law). The instrument is used as a rod in shallow water.

The gauging procedure may be summarized as follows:
- Divide the width of the river into *n* subsections (figure 5.4), with a size of *b* meter. The value of *n* usually varies between 10 and 20.
- Measure in each vertical situated in the centre of the subsection the water depth y.
- The average velocity *v* in each vertical may be found in various ways:
  - *One point method*. At a depth 0.6y below the water surface the velocity is measured. The one point method is the least accurate.
  - *Two point method*, which takes $= 0.5(v_{0.2} + v_{0.8})$ where $v_{0.2}$ and $v_{0.8}$ are velocities measured at *0.2y* and *0.8y*.
  - *Multiple point method*. At various depths the velocity is measured. The velocity profile is constructed (figure 5.4) and used to obtain $\bar{v}$.
- The discharge *Q* is then computed as

$$\mathbf{Q} = \sum_{\mathbf{1}}^{\mathbf{n}} \mathbf{\bar{v}_i \, A_i} \tag{5.6}$$

where the area of the subsection $A_i = by_i$.

B. Tracer methods
The procedure involves the adding of a chemical solution or tracer of known concentration to the flow and then measuring the dilution at a point downstream where the tracer is completely mixed with the river water. Tracer methods are applicable to small streams which cannot be gauged with current meters due to shallow depths and/or high velocities and turbulence. The method is not suitable for larger streams due to the large quantities of tracer required for an accurate measurement.

The tracer may be a chemical (e.g. sodium dichromat, sodium chloride, etc.), a radio isotope (e.g. tritium) or a biological tracer (e.g. a Serratia culture). The requirements for all types of tracers are:
- harmless to the environment
- (almost) absent in the natural stream
- not absorbed by sediments, flora or fauna
- to be detected by simple methods
- high solubility
- inexpensive

The tracer with a known concentration C_1 is injected with a constant rate q. At a point downstream where complete mixing has occurred the concentration of the tracer in the river water reaches after some time a constant value C_2. If the background concentration, already present in the water is indicated by C_0, then the river discharge Q follows from the balance equation

$$Q\,C_0 + q\,C_1 = (Q + q)C_2 \tag{5.6}$$

which may be rewritten as

$$Q = \frac{C_1 - C_2}{C_2 - C_0}\,q \tag{5.7}$$

C. Hydraulic structures
Hydraulic structures such as weirs and flumes may greatly improve the reliability of the stage-discharge relationship. The structures are based on the hydraulic principle that an increase in the water velocity (from sub-critical via critical, when passing the structure, to super-critical flow) results in a unique and stable relationship between depth of flow and discharge.

Weirs are structures which create the necessary critical flow conditions by a sudden jump in the bed profile. There are many different types of weirs, varying from a thin plate across a small stream (often calibrated in the laboratory) to concrete structures in larger rivers.

The general formula for a rectangular weir takes the form

$$Q = k\,b\,H^{\frac{3}{2}} \tag{5.8}$$

where b is the width of the weir, H is the measured water level upstream above the crest of the weir and k is a coefficient depending on the structure. For trapezoidal and triangular (V-notch) weirs different formulae have to be used.

Flumes are structures that narrow the channel width in order to increase the water velocity. They are particularly suitable for small streams carrying a considerable sediment load. The water level discharge relation given by (5.8) is also applicable for flumes.

5.2 Rating curves

The water level (stage) in the river is much more easily to measure than the discharge. Runoff is therefore generally determined on the basis of water level recordings in combination with a stage-discharge relation curve, called a rating curve. A unique relationship between water level and river discharge is usually obtained in a stretch of the river where the river bed is stable and the flow is slow and uniform, i.e. the velocity pattern does not change in the direction of flow. Another suitable place is at a tranquil pool, just upstream of some rapids. Such a situation may also be created artificially in a stretch of the river (e.g. with non-uniform flow) by building a control structure (threshold) across the river bed. The rating curve established at the gauging station has to be updated regularly, because scour and sedimentation of the river bed and river banks may change the stage discharge relation, particularly after a flood.

The rating curve can often be represented adequately by an equation of the form:

$$Q = a\left(H - H_0\right)^b \tag{5.9}$$

where Q is the discharge in m³/s, H is the water level in the river in m, H_0 is the water level at zero flow, and a and b are constants. The value of H_0 is determined by trial and error. The values of a and b are found by a least square fit using the measured data, or by a plot on logarithmic paper and the fit of a straight line (see figure 5.5, double log-scale !)
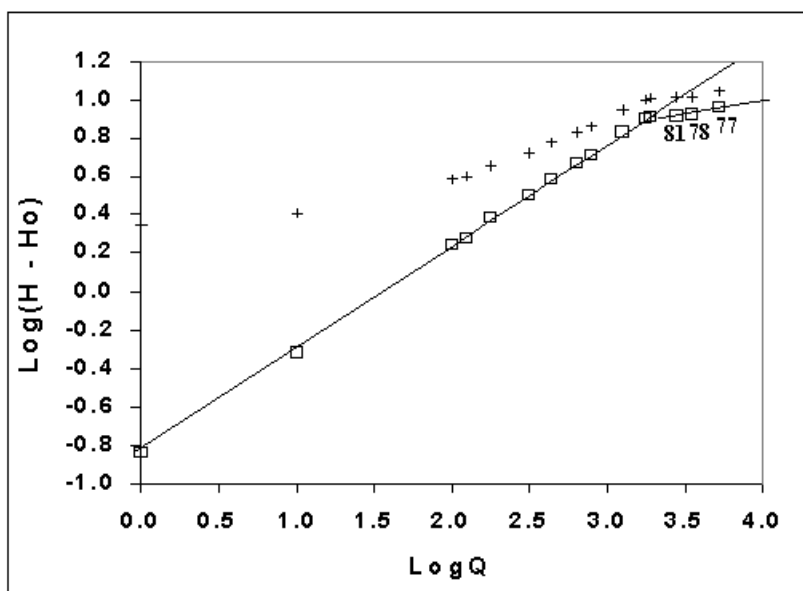
Fig. 5.5 Rating curve in Limpopo river at Sicacate

Equation (5.9) is compatible with the Manning formula (5.10) where the cross-sectional area A and the hydraulic radius R (see figure 5.1) are functions of ($H - H_0$).

$$Q = \frac{A}{n} R^{\frac{2}{3}} S^{\frac{1}{2}} \tag{5.10}$$

Consequently, it can be shown that the coefficient b in equation (5.9) should have a value of 1.67 in a rectangular channel, a value of 1.69 in a trapezoidal channel with 1:1 sideslopes, a value of 2.16 in a parabolic channel, and a value of 2.67 in a triangular channel (Water Resources Board, 1965).

Figure 5.5 shows the rating curve of the Limpopo river at Sicacate; the value of b equals 1.90. The Limpopo is an intermittent river which falls dry in the dry season and can have very high

flash floods during the flood season. The station of Sicacate has a value of H_0 equal to 2.1 m. In figure 5.1 a clear flood branch can be distinguished which is based on peak flows recorded during the floods of 1981, 1977 and 1978 in the Limpopo river. The gradient of a flood branch becomes flat as the river enters the flood plain; a small increase in water level then results in a large increase in discharge.

To illustrate the trial and error procedure in determining the value of H_0, a plot of data with H_0 = 0 has been added. It can be seen that the value of H_0 particularly affects the determination of low flow.

5.3   Flood surveys

To the engineer, extreme floods are often the critical situation for design. Consequently, monitoring of the processes involved in the occurrence of an extreme flood (rainfall, water levels, flows) is important. However, extreme floods only occur once in a lifetime, and one is seldom adequately prepared to monitor the event effectively.

Applying Murphy's law to the occurrence of extreme floods, one could state that extreme floods occur:

- at night, when everybody is sound asleep;
- on public holidays when all offices are closed;
- after torrential rains when telephone lines are broken and radios do not work as a result of static;
- when roads are blocked by flooding and culverts have been washed out;
- when the car is being repaired, or without petrol;
- when the Director of Water Affairs is on holiday.

This implies that although an observation network may work perfectly under normal flow condition, the critical observations of extreme rainfall, peak water levels and peak discharges are generally not recorded. Here follows a short list of problems which, unfortunately, are the rule rather than the exception during a critical flood:

- the reservoir of the raingauge overtopped; it was raining so hard that the observer was reluctant to go and empty the reservoir;
- the raingauge was washed away by the flood;
- the pen of the recorder had no ink;
- the clockwork of the recorder had stopped;
- the housing of the water level recorder was submerged by the flood; the instrument was lost;
- the rating weir was completely destroyed by the flood;
- the bridge on which the recorder was installed was blocked by debris, overtopped and the instrument destroyed;
- while trying to measure the velocity, the current meter was caught by debris and lost.

One can therefore conclude that the routine observation network generally fails during extreme floods. Therefore attention should be paid to special flood surveys.

 A number of flood survey methods are presented to deal with extreme flood situations. In particular:

- discharge measurement using floats
- flood mark survey
- slope area method
- simplified slope area method

The first method is used during the flood, the latter three methods are "morning after" methods.
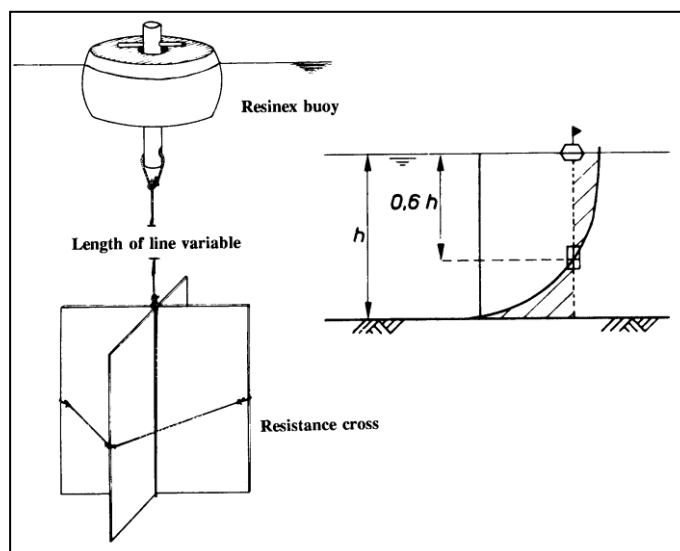

Fig. 5.6 Float with resistance body and location of the resistance body in the vertical

Floats

Contrary to what most hydrologists and hydrometrists wish to believe, floats are the most reliable and scientifically most appropriate instruments for measuring discharges during peak flows. The hydrometrist often considers floats below his professional standard and thinks incorrectly that his current meter is the most accurate instrument for determining peak discharges. Floats, well positioned, and with a resistance body at the right depth (see figure 5.6) are best for the following reasons:

- floats move at the same velocity as the surrounding water (provided they are made as in figure 5.6) and integrate the velocity in the longitudinal direction; they thus provide an accurate sample of the real mean velocity; current meters that integrate the velocity over time at a fixed position may be affected by local accelerations (e.g. due to bedforms); moreover, current meters do not always measure the point velocity accurately;
- floats are stagnant in relation to the moving water, thus the vertical position of the resistance body in the flow is correct; the vertical position of a current meter in the stream, on the other hand, is not certain; often velocities are so high that the instrument just "takes off" after touching the water surface;
- a float measurement can be carried out in a shorter period of time than a current meter measurement, which is an advantage under rapidly changing conditions;
- floats are cheap compared to current meters; it is not a disaster if one gets lost;
- at the peak of the flood, the river is full of debris; use of a current meter then is completely impossible;
- if no professional floats are available, it is easy to improvise.

If one arrives at the site unprepared, it is always possible to clock the velocity of floating debris. The larger the debris, for example trees, the better they describe the mean velocity in the vertical.

In the following intermezzo, a float measurement is briefly described.

A straight stretch is selected of 100m length (see figure 5.7). The width is divided into approximately eleven equal distances in which ten measuring points are established. If there are constraints in time or resources, try as many points as possible. At each measuring point a float is used with a resistance body at 60% of the average depth at that point.

Two measuring sections at the upstream and downstream end of the measuring reach should be marked by beacons placed on both banks in a line perpendicular to the flow. On each bank of a measuring section the two beacons should stand with sufficient distance between them to allow the observer to determine his position from a boat (if a boat is used). At night, the floats and the stacks should carry lights.

A float measurement is carried out by launching a float at a particular point in the cross-section. The positioning may be done from a cable mounted across the river, or from markings on a bridge (if present) or if necessary by sextant. The float should be launched (from a bridge or from a boat) at least 10 m upstream from the cross-section where the measurement starts, so as to allow the float to adjust itself to the flow velocity. When a boat is used, the observer should stay with the float, keeping next to it. When the
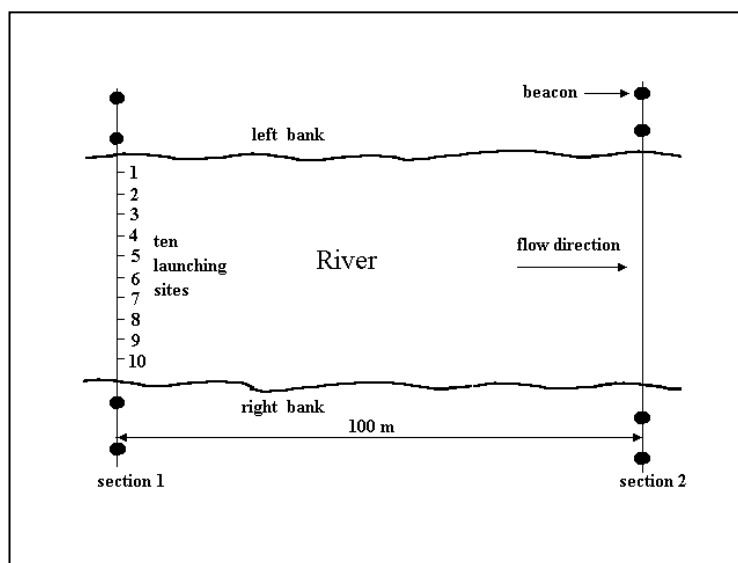

Fig. 5.7 Layout of float measurement

float enters the measuring section, the observer starts the stopwatch; he then follows the float until the measuring cross-section 100 m downstream where he stops the stopwatch, notes down the time and (if using a boat) recovers the float to return and repeat the measurement at the next observation point.

The advantage of a boat moving with the float is that only one observer is needed per float and no communication problems occur. The disadvantage is that the determination of the moment in which the float passes the section is less accurate.

If no boat is available, floats should be launched from a bridge, and followed along the bank. More observers could work at the same time, and one observer could clock more than one float. The advantage of this method is a greater degree of accuracy when starting and stopping the stopwatch; the disadvantage, however, is the more complicated communication system required and that the floats are lost.

A very elegant alternative is to use a float attached to a string with two knots 50 m apart (the distance can be less than in the above method since the accuracy is greater). The time which elapses between the passage of the knots can be measured. The float can only be recuperated if the amount and size of debris is small.

A float measurement over a distance of 100 m, has a relative error in the measurement of the velocity of 1%. A current meter does not have that degree of accuracy. Moreover, by following the flow trajectory, the velocity is correctly averaged in the longitudinal direction. The only

problem remains the averaging over the cross-section. The variation over the cross-section may be substantial. The variation over the width appears to be the largest source of errors. Therefore, one should select at least ten measuring positions in the cross-section.

This still leaves the problem of determining the cross-sectional area. Unless one has an echosounder at one's disposal (and the river is navigable), this has, unfortunately, to be left to the "morning after" programme.

Flood mark survey

Immediately after the flood peak has passed one should go to the field and search for flood marks. Flood marks can be found in the colour of mud on bridges, pillars, or - in case of extreme flooding - on the walls of buildings. Also the presence of small floating debris in trees and bushes are good indications of the flood level. One should take into account, however, that bushes bend under the force of the flow and that considerable waves may occur. Both actions indicate higher flood levels than actually occurred. Flood marks on the banks, where wave action and run-up from surge are at a minimum, are generally preferable to those in bushes and trees. However, they disappear fast.

The first action to be taken is to paint the observed flood marks on walls and trees, where possible accompanied by the date of occurrence of the flood. A record of flood marks on the wall of a solid structure is an important future source of information. Try to get as many reliable flood marks as possible along the river. Also in areas which at the time are not yet developed. A good survey of flood marks of an extreme flood is an invaluable asset for the planning of future projects.

Sometimes flood marks are difficult to find, principally because one is too late and rains have cleared the colouring, or winds have cleared the debris from the trees. A good method then is to install a levelling instrument at the suspected flood level and to look through the instrument towards different objects. If the instrument is indeed at the approximate flood mark position, then the accumulation of sometimes insignificant marks may help to verify the flood level.

If one is really too late to find back any traces of the flood, one should gather information from people living in the area. Needless to say that such information is much less reliable. Finally, where possible, take photographs of flood marks, or of people indicating a flood mark.

Slope area method

For a good slope area computation one should look for a fairly straight stable clean channel, without pools, rapids, islands or sharp curves. No bridges or other obstructions should be downstream of the reach.

The reach to determine the cross-sectional area should be about ten times the width of the river; one should survey approximately five to ten cross-sections. The flood mark survey should be over a long enough distance to determine the water level slope accurately, taking into account the error of reading. This will often amount to a distance of several kilometres. The hydraulic calculations are based on Chezy's formula:

$$\mathbf{Q = C\,A\,\sqrt{R}\,\sqrt{S} = C\,K\,\sqrt{S}} \tag{5.11}$$

where

  Q is the discharge in $m^3.s^{-1}$

    C is Chezy's coefficient of smoothness in $m^2.s^{-1}$
    A is the cross-sectional area in m^2
    R is the hydraulic radius in m
    S is the longitudinal slope
    K is the geometric conveyance in $m^{2.5}$

In (5.11) the discharge *Q*, the Chezy coefficient *C* and the slope *S* are considered constant over the reach. However, there are sometimes strong variations in the geometry of the channel along the reach. To eliminate these variations the average value of *K* is determined of the surveyed cross-sections:

$$\mathbf{K} = \frac{\sum\left(\mathbf{A_i}\sqrt{\mathbf{R_i}}\right)}{\mathbf{N}} \qquad (5.12)$$

where *N* is the number of sections surveyed and the index *i* indicates a certain cross-section.

In the above method the greatest difficulty lies in the determination of channel roughness. It is very difficult for even an experienced surveyor to arrive at an objective value. As long as people carry out the survey, the result obtained will always be subjective.

Simplified slope area method
A remarkable method developed by H.C. Riggs (1976) may be used to overcome the difficulty of subjectivity. Riggs postulates that in alluvial streams, slope and roughness are related. In more popular terms this means that the river adjusts its roughness (through bedforms) to the slope, or that the river adjusts its slope (through meandering) to the roughness. Experiments have shown that there indeed is a relation between roughness and slope, although the relation shows considerable scatter.

However, Riggs showed that the error in the relation between slope and roughness is less than the error made by experienced surveyors in estimating the roughness.

The equation of the simplified method reads:

$$\mathbf{\log Q = 0.188 + 1.33 \log A + 0.05 \log S - 0.056 \left(\log S\right)^2} \qquad (5.13)$$

In this equation the value of *A* should be representative for the reach under study. The cross-sectional area *A* should be determined on the basis of five to ten cross-sections:

$$\mathbf{A = \frac{\sum \mathbf{A_i}}{\mathbf{N}}} \qquad (5.14)$$

where *N* is the number of sections surveyed. The equation was tested in 64 rivers in the USA with discharges ranging from 2 m^3/s to 2500 m^3/s, and with Chezy coefficients ranging from 14 to 65 $m^{0.5}$/s . The method is extremely useful, also as a check on the previously mentioned slope area method.

5.4 Hydrograph analysis

A hydrograph is a plot of the stage or discharge against time at a location along the river (see figure 5.8). It includes the integrated contributions from surface runoff, groundwater seepage, drainage and channel precipitation. The shape of a hydrograph of a single storm occurring over the drainage area follows a general pattern. This pattern shows a period of rise that culminates in a peak, followed by a period of decreasing discharge (called recession) which may, or may not, decrease to zero discharge, depending on the amount of groundwater flow.

The hydrograph has two main components, a broad band near the time axis representing baseflow contributed from groundwater, and the remaining area above the baseflow, the surface runoff (or direct runoff), which is produced by the storm. In the beginning of the rainfall, the river discharge is low and a period of time elapses before the river begins to rise. During this period the rainfall is intercepted by vegetation or soaks into the ground to make up the soil moisture deficit. The length of the delay before the river rises depends on the wetness of the catchment before the storm and on the intensity of the rainfall itself.

When the rainfall has made up the catchment deficits and when surfaces and soils are saturated, the rain begins to contribute to the stream flow. The proportion of rainfall that finds its way to the river is known as *effective rainfall*, the rest being "lost" in evaporation, detention on the surface or retention in the soil. As the storm proceeds, the proportion of effective rainfall increases and that of lost rainfall decreases, resulting in a strongly rising limb.

The peak of the hydrograph usually occurs after the effective rainfall has reached its maximum. The time from the beginning of the rainfall to the peak of the hydrograph is generally called the 'time to peak'. There are many definitions for the *lag or lag time* between rainfall and runoff, which is a measure for the catchment response time. A definition frequently used for the lag is the time between the centre of gravity of the effective precipitation and the centre
of gravity of the direct runoff.

There is time required for the surface runoff to reach the station where the hydrograph is observed. First the area closest to the station contributes to the surface runoff, followed by the areas further upstream. This means that in a small catchment, for a given uniformly distributed rainfall, the time to peak, and also the lag time, will be shorter than in a large catchment.

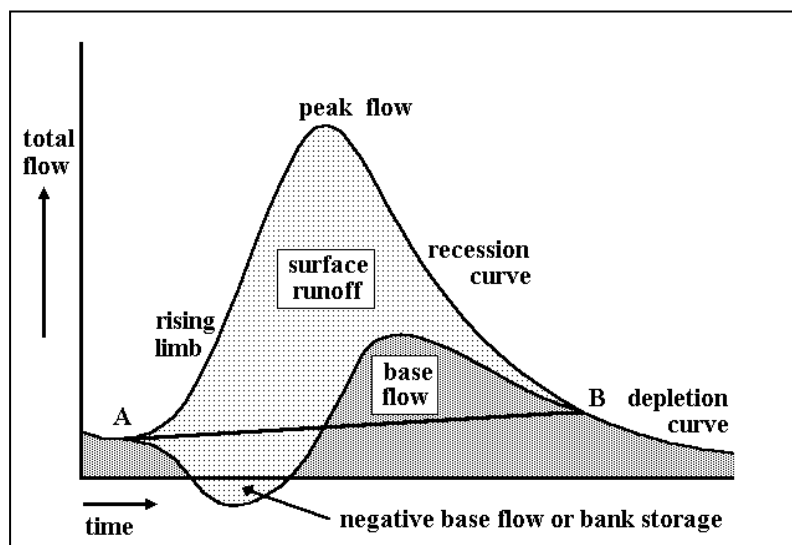The shape of the hydrograph changes when it travels along the river from

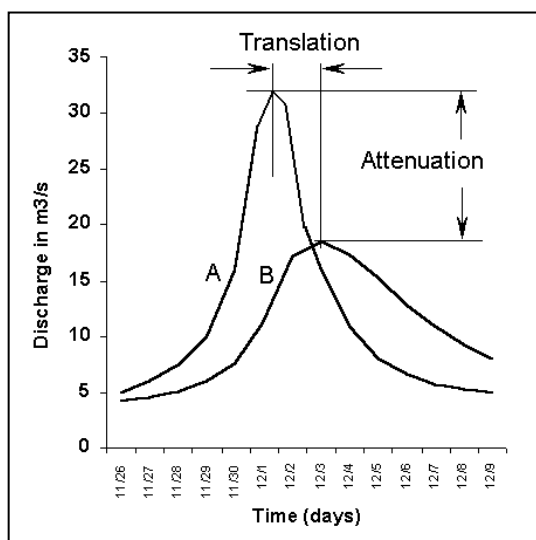**Fig. 5.8 Components of hydrograph and separation**

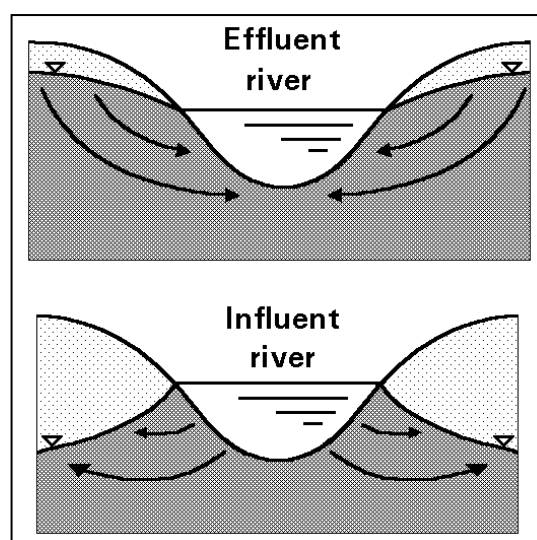**Fig. 5.9 Hydrograph translation and attenuation**

Fig. 5.10 Influent and effluent streams

point A to point B (see figure 5.9). If lateral in- and outflows between A and B are negligible, the peak of the hydrograph arriving in B will be lower (attenuation) and the time of arrival later (translation). In the (hypothetical) case that the flood wave travels from A to B without changing shape, there is only translation, which phenomenon is known as a *linear channel*. The storage effects are most important when a flood wave is routed through a reservoir, causing predominantly attenuation and little translation.

The boundary between surface runoff and baseflow (figure 5.8) is difficult to define and depends strongly on the geological structure and composition of the catchment. Permeable aquifers, such as limestone and sandstone strata, react much faster than impervious clays. During the course of an individual rainfall event, the baseflow component continues to fall even after river levels have begun to rise, and only when the storm rainfall has had the time to percolate down to the water table does the baseflow component begin to increase. The baseflow component usually finishes at a higher level at the end of the storm than at the rise of the hydrograph, and thus there is an increase in the river runoff from groundwater seepage. Groundwater provides the total flow of the general recession curve until the next period of rainfall.

Since baseflow represents the discharge of aquifers, changes occur slowly and there is a lag between cause and effect that can easily extend to periods of days or weeks. This will depend on the transmissivity of the aquifers bordering the stream and the climate.

In this context it is important to distinguish between *influent* and *effluent* streams (see figure 5.10). During periods when the groundwater level is higher than the water level in the river, water will flow from the groundwater into the stream channel, and the river is considered effluent, draining the surrounding area. For the situation that the water level in the stream is higher than the groundwater level, water will flow from the river into the soil and the stream is considered influent. A stream that is influent over considerable length may dry up during rainless periods (e.g. the wadi's in desert areas). Such a stream is called ephemeral. More common are intermittent rivers, which dry up during only a short period of the year during which (part of) the river becomes influent. Rivers that carry water all year round are often fed by rain as well as snow melt and known as perennial rivers. Characteristic hydrographs for the
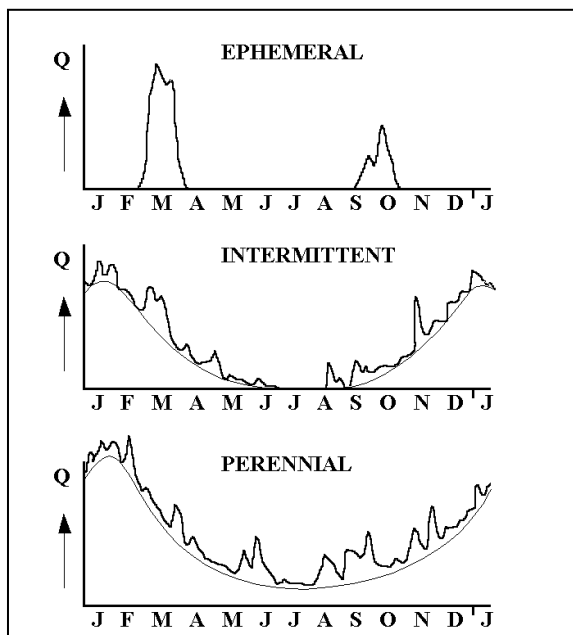
Fig. 5.11 Classification of rivers
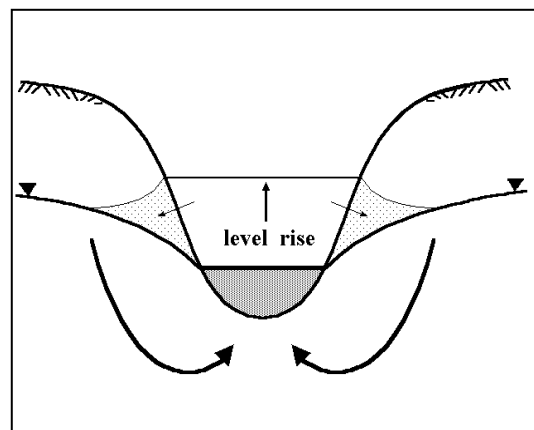
Fig. 5.12 Temporary change of river from effluent to influent due to a sudden rise of water level

various types of rivers are given in figure 5.11.

The fact that water may flow from the river into the groundwater affects the separation line between surface water and groundwater. Figure 5.12 shows that a sudden rise in the water level may change the river temporary from an effluent to an influent type. Consequently, the seepage from the groundwater into the surface water is, during a relatively short period reversed, which may sometimes even result in a negative base flow as indicated in figure 5.8.

If the recession curve is sustained by ground seepage only, it is called depletion curve and may be described by (4.11), derived previously as:

$$Q_t = Q_0 \, e^{-\frac{t-t_0}{K}} \tag{5.15}$$

The equation produces a straight line when plotted on semi-logarithmic paper, which allows the determination of K. Once the value of K has been determined, (5.15) may be used to forecast low discharges. For a continued dry period the available flow may well be predicted by this equation.

In practise it is impossible to determine the separation line between the surface runoff and the base flow. Figure 5.8
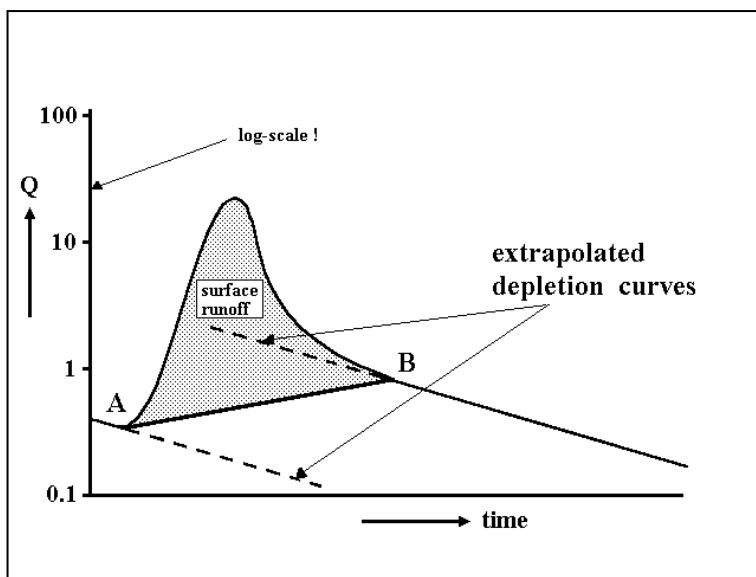
Fig. 5.13 Hydrograph separation

shows an approximate method using a straight line, connecting the points A and B, which points are found from a plot of the hydrograph on semi-logarithmic paper as shown in figure 5.13. The points A and B are located where the extrapolated depletion curves, just before the start of the storm and immediately after the cessation of the surface runoff, depart from the observed hydrograph.

5.5   Factors affecting hydrograph shape

The time distribution of runoff (the shape of the hydrograph) is influenced by climatic, topographic and geological factors. The climatic and topographic factors mainly affect the rising limb whereas the geological factors determine the recession limb.

Climatic factors
The climatic factors that influence the hydrograph shape and the volume of runoff are:
- 1   rainfall intensity
- 2   rainfall duration;
- 3   distribution of rainfall on the basin;
- 4   direction of storm movement;
- 5   type of storm.

1. *Rainfall intensity* affects the amount of runoff and the peak flow rate. For a given rainfall duration, an increase in intensity will increase the peak discharge and the runoff volume, provided the infiltration rate of the soil is exceeded.
2. *Rainfall duration* affects the amount of runoff, the peak flow rate and the duration of surface runoff. For a rain of given intensity, the rainfall duration determines, in part, the peak flow. If a storm lasts long enough, eventually a fixed fraction C of the precipitation will become runoff (the time after which this occurs is called the time of concentration); consequently the peak flow will approach a rate equal to the product $C*i*A$, where C is the runoff coefficient i is the rainfall intensity and A is the area of the basin. This situation is never reached in large basins, but may occur in small watersheds and is frequently used as the criterion for design of storm sewers, airport drainage or small culverts (see Section 6.1).
3. The *areal distribution* of rainfall can cause variations in hydrograph shape. If an area of high rainfall is near to the basin outlet, a rapid rise, sharp peak and rapid recession of the hydrograph usually result. If a larger amount of rainfall occurs in the upper reaches of a basin, the hydrograph exhibits a lower and broader peak.
4. The *direction of storm movement* with respect to orientation of the basin affects both the magnitude of the peak flow and the duration of surface runoff. Storm direction has the greatest effect on elongated basins. On these basins, storms that move upstream tend to produce lower peaks of a longer duration than storms that move downstream.
5. The *type of storm* is important in that thunderstorms produce peak flows on small basins, whereas large cyclonic or frontal-type storms are generally determinant in larger basins.

Topographic and geologic factors
The topographic and geologic factors affecting runoff represent the physical characteristics of the basin. The factors involved are numerous, some having a major bearing on the phenomena, whereas others may have a negligible effect, depending on the catchment under consideration. The following are the dominant factors:
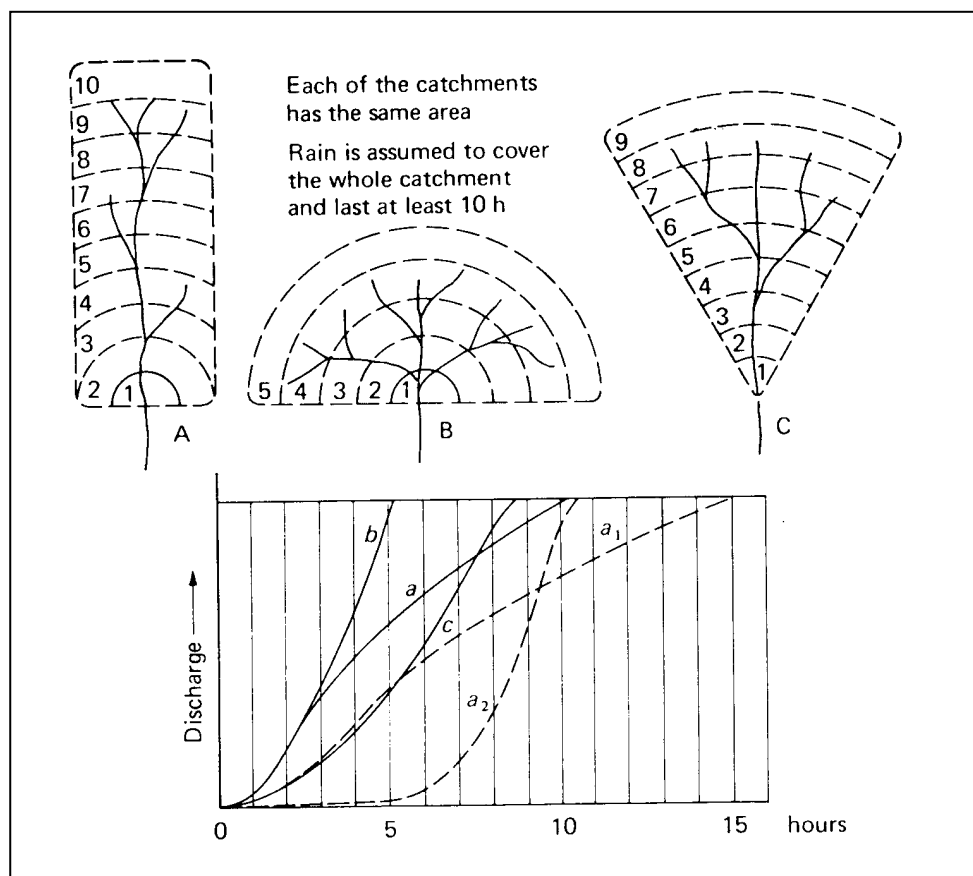
Fig. 5.14   The effect of shape on catchment runoff (after Wilson, 1983)

1   catchment size
2   catchment shape
3   distribution of watercourses
4   slope of the catchment
5   storage in the catchment
6   geology of the catchment
7   landuse

1. The major effect of increasing the *drainage area* on the hydrograph shape is that the time base of the hydrograph is lengthened. The peak flow per unit area thus reduces with catchment size for a given rainfall depth. This is partly due to the rainfall intensity being less for storms of extensive size, and partly due to the longer time required for the total catchment area to contribute to the peak runoff (time of concentration).

2. The effect of *shape* can best be demonstrated by considering the hydrographs of discharges from three differently shaped catchments with the same surface area, subject to rainfall of the same intensity (see figure 5.14). The lines of equal run-time (isochrones) to the outlet show that shape B has the smallest time of concentration (5 hours), and thus reaches the peak after 5 hours. The most elongated catchment needs 10 hours to reach the peak. Also the effect is shown in the hydrographs of a storm that moves upstream (a1) and downstream (a2) in the elongated catchment. It can be seen that the rise is sudden when the storm moves downstream and slow when it moves upstream.

3. The *pattern and arrangement of the natural stream channels* determine the efficiency of

the drainage system. Other factors being constant, the time required for water to flow a given distance is directly proportional to length. Since a well-defined system reduces the distance water must move overland, the corresponding reduction in time involved is reflected by an outflow hydrograph having a short time to peak.

4. The steeper the *slope* of the catchment, the more rapidly surface runoff will travel. The time to peak will be shorter and the peaks will be higher. Infiltration capacities tend to be lower as slopes get steeper, thus accentuating runoff.

5. Since *storage* must first be filled before it empties, it has a delaying and modifying effect on hydrograph shape. Much of the variation caused by the above factors are smoothed out by natural or artifical storage.

6. The *pedology and geology* of the catchment influence primarily the groundwater component and the "losses". High infiltration rates reduce the surface runoff; high permeabilities combined with high transmissivities substantially enhance the baseflow component. The type of stream (influent, effluent or intermittent) can have a substantial impact on hydrograph shape (see figure 5.11).

7. *Landuse*, finally, can strongly influence the runoff coefficient. Urbanized areas may have a runoff coefficient of almost 100%, whereas natural vegetation may have low runoff. Plowing, drainage, cropping intensity, afforestation etc. also have a considerable effect on runoff.

5.6 Flow duration curves

Of primary importance in the study of surface water are river discharges and related questions on the frequency and duration of normal flows (e.g. for hydropower production or for water availability) and extreme flows (floods and droughts). We shall first deal with the normal flows, and in the next section with extreme flows.

The question which a hydraulic engineer would ask a hydrologist concerning normal flows, is the length of time (duration) that a certain river flow is expected to be exceeded. An answer to this question is provided by the flow duration curve, that is the relationship between any given discharge and the percentage of time that the discharge is exceeded. The flow duration curve only applies for the period for which it was derived. If this is a long period, say more than 10 to 20 years, the flow duration curve may be regarded as a probability curve, which may be used to estimate the percentage of time that a specified discharge will be equalled or exceeded in the future.

As a numerical example to elucidate the derivation of the flow duration curve, consider the average daily discharges in m^3/s for a 20-day period as presented in table 5.2. A period of 20 days is used in this example to restrict the number of values, but it should be noted that the derivation of flow duration curves for periods less than one year is generally not very useful.

The range of discharges are normally divided into 20 to 30 class intervals. In this example only 12 intervals are used as shown in table 5.3. In the second column the number of days is given in which the flow belongs to the respective class interval. The cumulative totals of the number of days are presented in the third column. In the last column the cumulative percentages are listed.

A plot of the discharge against the percentage of time that the discharge is exceeded (figure 5.15) shows the typical shape of the flow duration curve. The presentation of the flow duration

discharge in m³/s		
days	k = 1	k = 10
1	402	
2	493	
3	912	
4	1256	
5	1580	
6	1520	
7	1416	
8	1193	
9	1048	
10	966	1079
11	890	1127
12	846	1163
13	792	1151
14	731	1098
15	682	1008
16	602	917
17	580	833
18	512	765
19	473	707
20	442	655

Table 5.2　　Average discharges for daily (k = 1) and 10-day periods (k = 10) observed during the 20 consecutive days

Class interval lower bound	Total in c.i.	Number greater than bottom of c.i.	Percentage greater than bottom of c.i.
1500	2	2	10
1400	1	3	15
1300	0	3	15
1200	1	4	20
1100	1	5	25
1000	1	6	30
900	2	8	40
800	2	10	50
700	2	12	60
600	2	14	70
500	2	16	80
400	4	20	100

Table 5.3　　　Derivation of flow duration curve

curve is much improved by plotting the cumulative discharge frequencies on log-probability paper (figure 5.16). The logarithmic scale applies well to flows because the argument of the logarithmic function, just like real river flow, has a lower boundary of zero, which is reached asymptotically. The probability scale on the horizontal axis of figure 5.16, is the Normal (or Gaussian) distribution. For normal flows, the Normal distribution generally leads to good results in combination with the logarithms of the flow. This is also called the Log-Normal distribution.

The same procedure can also be followed for periods of longer duration, e.g. ten days (k = 10) or one month (k = 30). The average discharges for 10 day periods are presented in table 5.2 and the resulting flow duration curve is shown in figure 5.16. The slope of this curve is flatter since the averaging of discharges removes the extremes. One may read from this curve that in 90 % of the time the average discharge during 10 consecutive days is equal to or greater than 700 m³/s. This type of information is important for instance in sewage works design, because it indicates the time during which the flow in the river may not provide adequate dilution for the effluent; but also for the design or licensing of water withdrawal, power plants, storage reservoirs, etc.
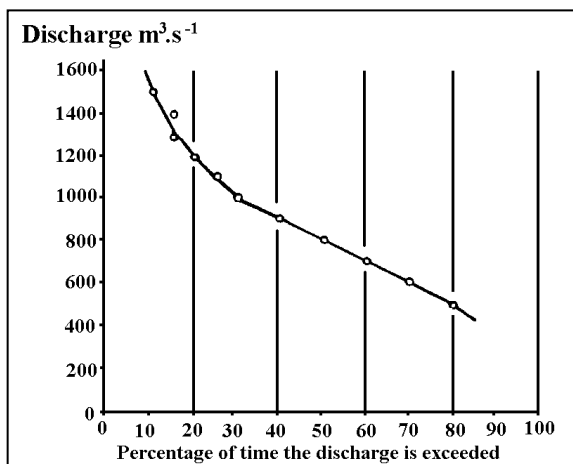

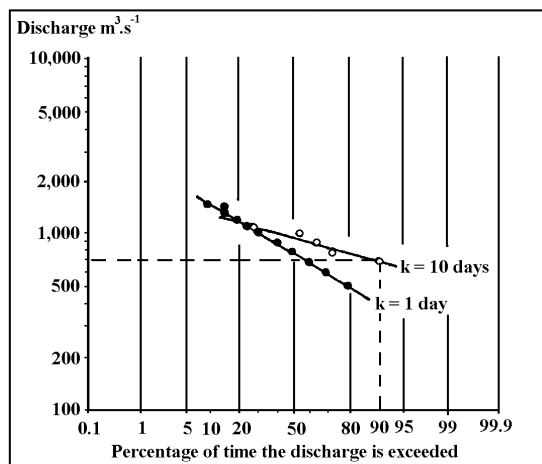**Fig. 5.15 Flow duration curve for the example discussed in the text**

Fig. 5.16 Flow duration curve on log-probability paper for flow duration of k = 1 and k = 10 days

5.7   Flood frequency analysis

Apart from normal flow frequency, hydrologists are also interested in the occurrence of extreme events. For this purpose flow frequency curves may be derived which yield the probability that a certain annual maximum discharge is exceeded. For minimum flows similar curves may be developed giving the probability of occurrence of an annual minimum less than a given discharge. The statistical methods are similar to the methods discussed in Chapter 2 for precipitation data and result in a relation like the one presented in figure 2.20.

Depending on the phenomenon, different probability distributions are recommended. For example for droughts the Log-Gumbel type III distribution may be used, and for flood flows the Gumbel type I, Log-Gumbel, Pearson or Log-Pearson type III distribution. The Gumbel type I distribution applied to flood levels is presented first.

In the case of floods, where possible, extreme analysis should be done on flows. However, if flow records do not exist, or if a rating curve has not yet been established, then we may have no other choice than to analyze water levels. This is, however, dangerous, particularly if we want to design flood protection (a dike).

If a river has a flood plain where we consider building a dike, then the water levels in the original situation (without a dike) will be less high during a flood than in the case where the dike is present. Hence, a dike elevation which is based on the recorded flood levels will underestimate the flood level after the dike has been built. Flows are not affected by the shape of the cross-section, or, at least, to a much lesser extent. Therefore, extreme analysis should be done on discharges whenever possible. If no rating curve exists, then flood level analysis should be done with caution.

In the following, the Gumbel type I, Log-Gumbel type III and Pearson type III distributions are presented for the analysis of flood levels and flows. In addition a method is presented to estimate the flood frequency distribution in the case that no records exist.

Gumbel type I
In 1941, Gumbel developed the Extreme Value Distribution. This distribution has been used with success to describe the populations of many hydrological events. As applied to extreme values, the fundamental theorem can be stated:

> If $X_1, X_2, X_3, ... X_N$ are independent extreme values observed in N samples of equal size n (e.g. years), and if X is an unlimited exponentially-distributed variable, then as n and N approach infinity, the cumulative probability q that any of the extremes will be less than a given value X_i is given by:

$$q = \exp(-\exp(-y)) \qquad (5.16)$$

where q is the probability of non-exceedence, y is the reduced variate. If the probability that X will be exceeded is defined as $p = 1 - q$, then (5.16) yields:

$$y = -\ln(-\ln(1-p)) = -\ln(-\ln(1-1/T)) \qquad (5.17)$$

where T is the return period measured in sample sizes n (e.g. years). Table 5.4 lists a number

of values of the reduced variate y, the probability of non-exceedence q and the return period T. According to Gumbel, there is a linear relation between X and y:

$$y = a(X - b) \tag{5.18}$$

where a is the dispersion factor and b is the mode. Moreover, Gumbel showed that if the sample N goes to infinity:

$$b = \overline{X} - 0.45005\, s_x \tag{5.19}$$

$$a = 1.28255 / s_x \tag{5.20}$$

where $\overline{X}$ is the mean of X and s_x the standard deviation of the sample. If the sample is finite, which they always are - already a series of 30 years ($N = 30$) is large -, the coefficients a and b are adjusted according to the following equations:

$$b = \overline{X} - s_x \frac{y_N}{\sigma_N} \tag{5.21}$$

$$a = \frac{\sigma_N}{s_x} \tag{5.22}$$

values of σ_N (the standard deviation of the reduced variate) and y_N (the mean of the reduced variate) as a function of N are tabulated in table 5.5. Equation 5.18 is thus modified to:

$$X = \overline{X} + s_x \frac{y - y_N}{\sigma_N} \tag{5.23}$$

q %	T years	y
1.0	1.01	-1.53
5.0	1.05	-1.10
10.0	1.11	-0.83
20.0	1.25	-0.48
30.0	1.43	-0.19
50.0	2	0.37
66.6	3	0.90
80.0	5	1.50
90.0	10	2.25
95.0	20	2.97
98.0	50	3.90
99.0	100	4.60
99.5	200	5.30
99.8	500	6.21
99.9	1000	6.91

N	y_N	σ_N	y_N/σ_N
5	0.459	0.793	0.579
10	0.495	0.950	0.521
20	0.524	1.062	0.493
30	0.536	1.112	0.482
40	0.544	1.141	0.477
50	0.549	1.160	0.473
60	0.552	1.175	0.470
70	0.555	1.185	0.468
80	0.557	1.193	0.467
90	0.559	1.200	0.466
100	0.560	1.206	0.464
150	0.565	1.225	0.461
200	0.567	1.236	0.459
∞	0.577	1.283	0.450

Table 5.4   Values of the reduced variate as a function of the probability q and return period T

Table 5.5 Theoretical values for the mean and the standard deviation of the reduced variate

On probability paper, see figure 2.23 where the horizontal axis is linear in *y*, equation 5.23 plots a straight line. To plot the data points on the horizontal axis a, so-called, plotting position, or estimator, of the probability of non-exceedence *q* is required. For the example below the Weibull formula is used (equation 2.9 with $\alpha = 0$):

$$q = 1 - p = 1 - \frac{m}{N+1} \tag{5.24}$$

where *m* is the rank number of the maximum occurrences in decreasing order and *N* is the total number of years of observations. At the bottom of figure 2.23 the linear axis of the reduced variate is accompanied by the frequency scale of *q* and on the top of the figure by the scale of the return period *T*. In figure 5.17 an example is given of the maximum annual flood levels occurred in the Sabie river in Mozambique at Machatuine.
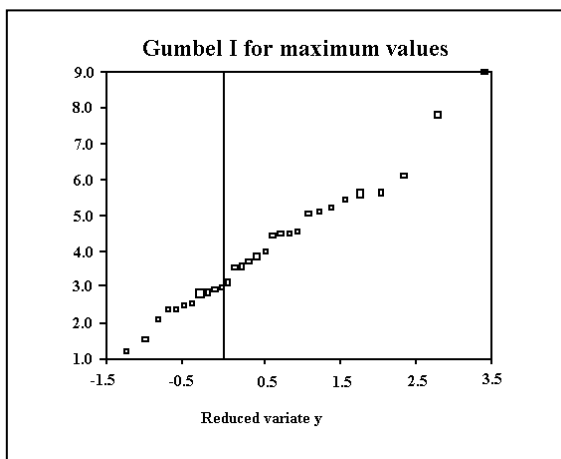
Fig. 5.17 Gumbel probability of annual maximum flood levels in the Sable river at Machatuine

Log-Gumbel type III

The Log-Gumbel III distribution is often quite adequate for droughts, the analysis of extreme low flows. In figure 5.18 it is applied to the Sabie river catchment in Mozambique at Machutuine. The probability of exceedence *p* for the case of minimum flow is computed from equation 2.9 with $\alpha = 0.25$:

$$p = \frac{m - 0.25}{N + 0.5} \tag{5.25}$$

The reduced variate *y* is computed by:

$$y = -\ln(-\ln(p)) \tag{5.26}$$

For maximum flow the Log-Gumbel distribution can be used. Figure 5.19 presents the case of the Incomati river in Mozambique at Ressano Garcia. In this case the probability of non-exceedence *q* is determined by equation 5.24 and the reduced variate by equation 5.17.

It is not advisable to use partial duration series (see Section 2.7) for runoff, as the observations within one year are generally correlated. The chance of independent data is greatly enhanced if an annual series is used on the basis of a properly selected hydrological year (see Section 1.3). Application of statistical methods to flow data is, in general, more difficult as compared to precipitation data, because a time series of runoff observations is often not homogeneous (activity of man) and the record is seldom long enough.
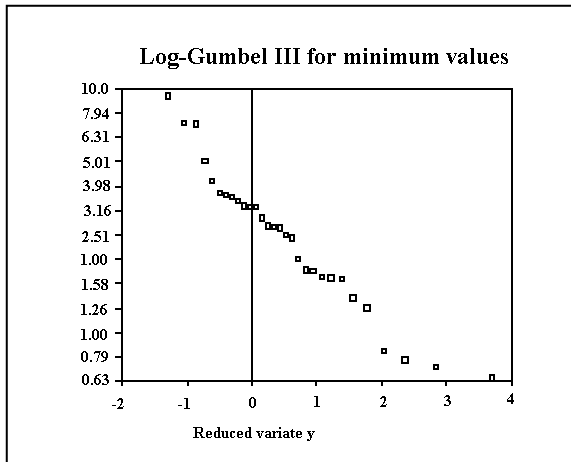
Fig. 5.18 **Log-Gumbel III analysis for minimum flow in the Sabie river at Machatuine**
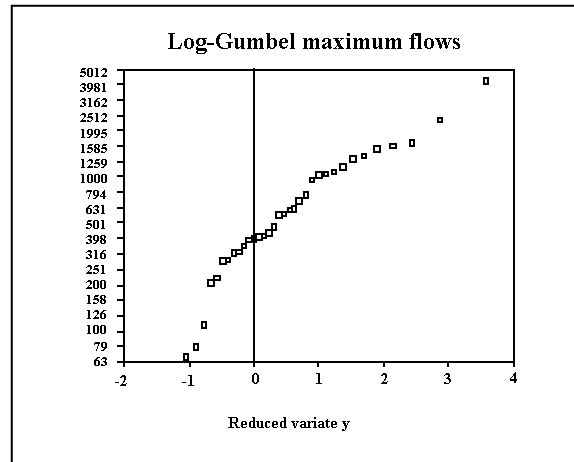
Fig. 5.19 Log-Gumbel distribution for maximum flows in the Incomati river at Ressano Garcia

Pearson type III

The Pearson type III equation does not necessarily plot a straight line on Gumbel paper. It assumes that the water levels are distributed as a three-parameter gamma distribution. For more details about the computation of the distribution, reference should be made to text books. In figure 5.20, the frequency distributions obtained with both Gumbel and Pearson III are
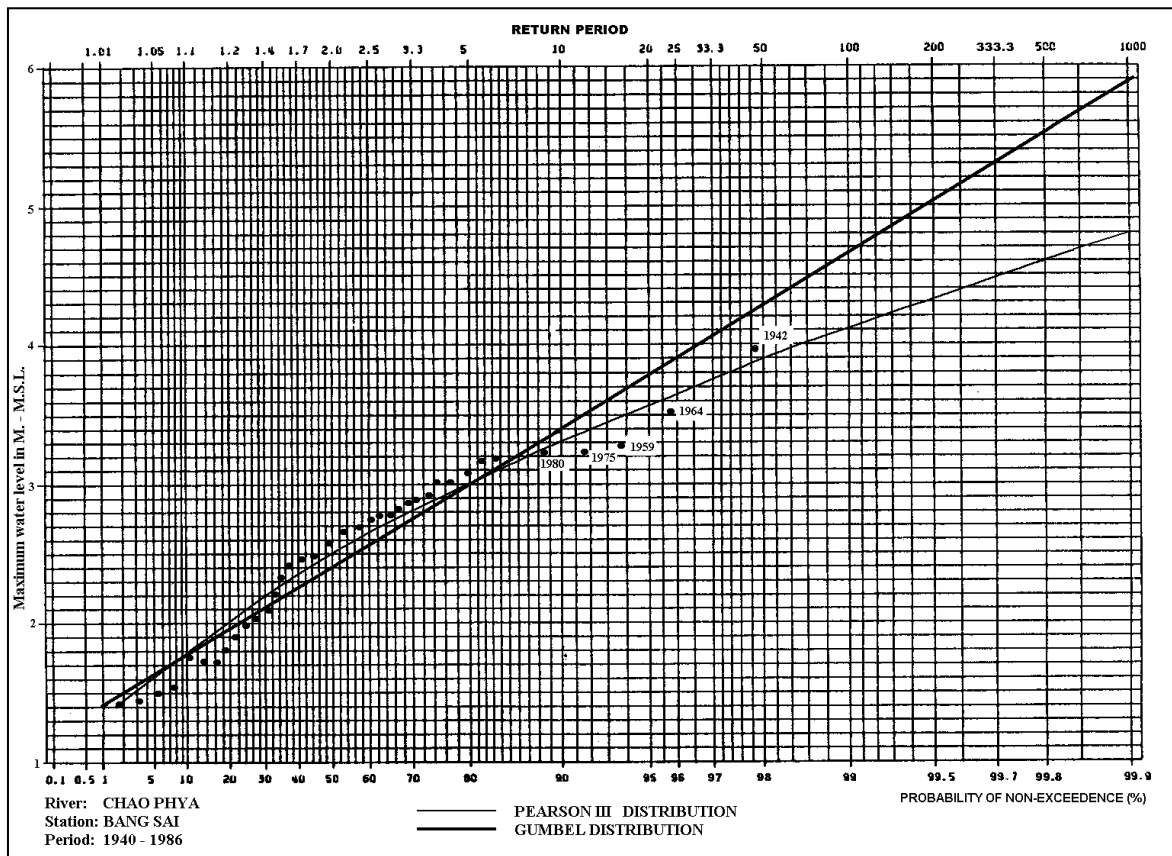
Fig. 5.20 **Gumbel and Pearson III distribution of annual flood levels in Bang Sai, Chao Phya river, Thailand (from Euroconsult, 1987)**

presented for the hydrometric station of Bang Sai in the Chao Phya river in Thailand (after Euroconsult, 1987). It can be clearly seen that the Pearson type III distribution performs better. However, this does not mean that the Pearson type III distribution reflects the real physical situation, and may be extrapolated indiscriminately.

It has been stated before that frequency analysis is a useful, but very limited method of determining design discharges or design water levels. The statistical methods used for frequency analysis have no physical basis; they are merely tools to help extrapolation.

Therefore one has to check in the field if a discharge or a water level indicated by frequency analysis has indeed some physical meaning. The above methods for slope area calculations can be used to determine the discharge corresponding to a design water level, or to determine the water level corresponding to a design discharge. The effect of floodplains, natural levees, dikes etc. should then be taken into account.

5.8 Lack of data

The statistical analysis of extremes requires a homogeneous time series of data of at least some 20 to 30 years. If such a time series is not available, which is often the case, one may distinguish between the situation that absolutely no data are available or that a short series has been observed.

No records available

If no records of any substantial length are available the following rule of thumb may prove valuable. The mode of the Gumbel annual flood frequency distribution (return period $T \approx 1.5$ years) generally lies at bankfull level, the elevation of the natural levee, or the natural bank height (see figure 5.21). The consideration behind this is that the natural bank elevation is maintained at a level where it is regularly replenished with new alluvial material. This knowledge allows tofix one point of the frequency distribution on Gumbel probability paper. The second point should be derived from interviews in the field. Detailed questioning of as many inhabitants of the area as possible may give you an indication of the largest flood in say 20 years. Interviews should contain questions like:

- In which year do you remember the biggest flood?
- What age were you then?
- What age are you now?
- Where were you at the time of the flood?
- Can you indicate the level of the flood (on a tree, a house, a wall)?
- When did the second biggest flood that you can remember occur? (followed by the same detailing questions as above)

Always ask some questions that may confirm or contradict earlier statements like:

- Did you stay in the area or did you flee?
- If you fled, how do you know?
- Could you walk through the water or did you use a boat?
- Was there loss of life?
- Did cattle drown? If not, why?
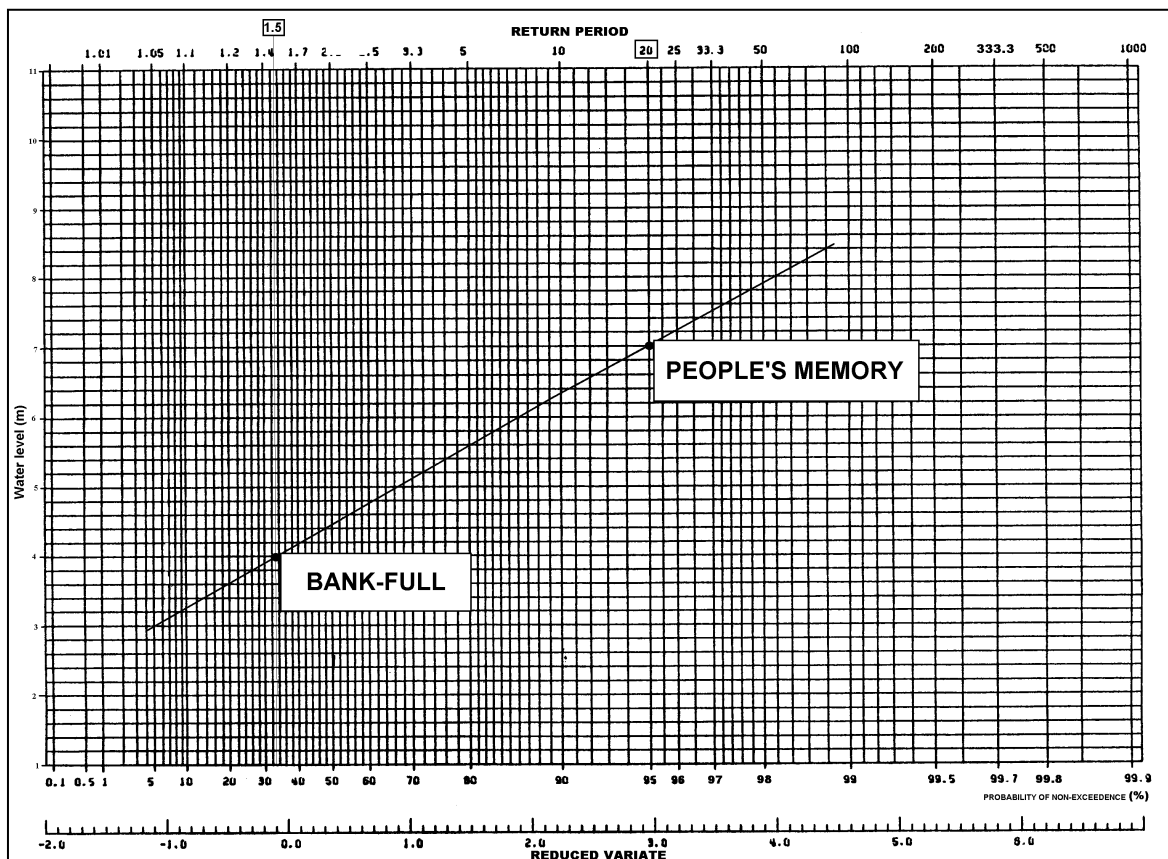
Fig. 5.21 **Gumbel distribution based on merely field observation and interviews**

Care should be taken to interview the right people. The more influential people who often present themselves as resource people, are not always the people who were on the spot during the event. Also, do not solely interview men, in many countries, the women do the work on the land and know the land best. Men are often away from home and hear the story afterwards.

In figure 5.21 the second point that determines the Gumbel line has been indicated, as an example. In this case it followed from interviews that the flood with a return period of 20 years had a level of 7 m.

Short series available
In the event of a short homogeneous record one may proceed along two different lines. One approach is known as stochastic hydrology. The short time series is analyzed with respect to a trend component (a gradual change), a cyclic variation (periodic component) and a stochastic component. The first two components are deterministic in nature, while the stochastic component contains random elements. Each component is reproduced by mathematical simulation. The stochastic model is used to generate synthetic runoff data in sufficient large quantities to allow a statistical analysis.

This method is very risky when used as a frequency analysis tool. It has no physical foundation and the statistical material used to arrive at a long duration series is purely based on the short series of observations. Therefore, no justification exists to extrapolate the probability function beyond the duration of the observation period. Data generation, however, may be useful to

determine time series for system simulation, for example to calculate the size of a reservoir. Thus it is an appropriate tool to generate normal flows but not to facilitate the analysis of extreme flows.

A completely different approach is called deterministic hydrology. It involves the development of a mathematical model to simulate the rainfall-runoff process. The deterministic approach requires a relatively short period of simultaneously observed rainfall and runoff to calibrate and verify the deterministic model. A deterministic model is a mathematical analogon that describes the link between cause (rainfall) and event (runoff). This does not necessarily mean that a deterministic model is physically based.

Some deterministic models are more physically based than others. So-called black box models do not really try to describe the physics; they are merely a one-to-one relation between input and output. This means that black box models have to be recalibrated after changes have occurred in a catchment, and that they may not be used far beyond the range of calibration.

By making use of a deterministic model, the problem of finding a sufficiently long flow sequence is reduced to finding a sufficiently long rainfall series, which are generally more easily obtainable than runoff series.

From the rainfall series a design rainfall with a frequency of occurrence of for example once in 100 years may be derived. The deterministic model is then used to simulate the runoff from this event, implicitly assuming that the simulated runoff has the same return period of 100 years. Another approach is the simulation of runoff for the complete time series of rainfall observations, followed by a statistical analysis of the simulated runoff data. Especially in the case of complicated water resource systems, for example downstream of a confluence of different catchments, or in a system with a number of reservoirs, the latter method may yield different flow return periods from the rainfall return periods assumed.

Deterministic models are also used in real time to forecast flows on the basis of an existing situation. This subject is further dealt with in Section 6.3.

6   RAINFALL RUNOFF RELATIONS

A distinction is made between short and long duration rainfall-runoff relations. Short duration rainfall-runoff relations describe the process of how extreme rainfall becomes direct storm runoff. It yields peak flows and hydrographs that are used for the design of drainage systems (such as culverts, bridges sewers, retention ponds, etc.), spillways, or flood control storage. Long duration rainfall-runoff relations aim at establishing catchment yield for the purpose of water resources assessment.
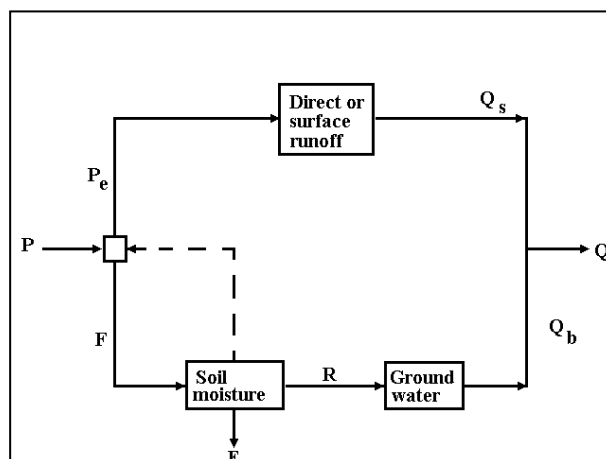
Fig. 6.1 Simplified catchment model (Dooge, 1973)

6.1   Short duration peak runoff

For the determination of direct storm runoff use can be made of the simplified catchment model of Dooge (see figure 6.1). Part of the net rainfall P runs off over land (effective precipitation P_e) and the remaining part infiltrates F. The surface runoff, also termed direct runoff, contributing to the total river discharge Q, is indicated by Q_s. The infiltrated water F replenishes the soil moisture deficit or, if there is no deficit, it recharges the groundwater system R. The wetness of the soil affects the infiltration, so there is a feedback of the soil moisture situation on the division of precipitation into effective precipitation and infiltration. The soil moisture may evapotranspirate E or flow into the saturated groundwater system R. Outflow from the aquifer into the river is called base flow, Q_b. To determine the direct runoff, the effective precipitation P_e is required as input data. The effective precipitation P_e may be written as:

$$\mathbf{P_e = P - F}$$

(6.1)

where P is the observed precipitation and F is the infiltration. It should be noted that in a more detailed approach to rainfall-runoff modelling, interception and surface detention should be added to this equation.

When discussing rainfall-runoff processes, infiltration, interception and surface detention are generally considered "losses". Although it is not right to speak of losses (see Section 3.10), in the following, the term losses will in some places be used to indicate reduction of runoff, since this is considered common terminology in this regard.

The infiltration changes with time and depends on antecedent conditions (wet or dry soil) as shown previously in figure 4.3. A plot of two exactly equal rainstorms and the corresponding runoff hydrograph under different antecedent conditions is given in figure 6.2. Note that the discharge Q is usually measured in m^3/s. For convenience the values have been divided by the area of the catchment (m^2) to yield m/s. This unit is converted to mm/h, so that it is compatible with the unit of observed precipitation P.

At the start of the first storm the basin is dry and the infiltration rate, which is initially high, decreases with time. After the end of the rainstorm some recovery of the infiltration capacity takes place.

At the start of the second storm the basin is relatively wet and the infiltration is less than for the first storm. Subtraction of the infiltration from the observed rainfall P yields the effective rainfall P_e which is indicated by the shaded area. Since the direct storm runoff Q_s (in mm/h) equals the effective precipitation the second storm causes a larger peak, neglecting a change in the base flow contribution to the total runoff.
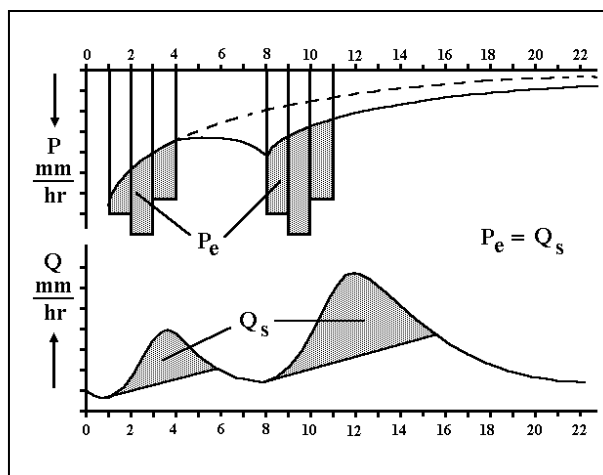
Fig. 6.2 The effect of infiltration losses on the effective precipitation and direct runoff

Figure 6.2 shows the variation in infiltration with time. In general, the available data do not justify such a detailed approach. An alternative is the separation of the base flow from the total runoff, which yields the surface runoff Q_s. Since $Q_s = P_e$ (if expressed in mm) the losses are found by subtracting Q_s from the observed rainfall. This may be done for each individual rainstorm and expressed as a fixed loss rate, which is known as the Φ-index. Consider for example a rainstorm producing 30 mm of rain (see figure 6.3). Assume that the direct runoff, found from hydrograph separation equals 17 mm. The Φ-index line is drawn such that the shaded area above this line equals 17 mm. For this example the Φ-index is 2 mm/h. Though a constant loss rate is not very realistic, the method has the advantage that it includes interception and detention losses.
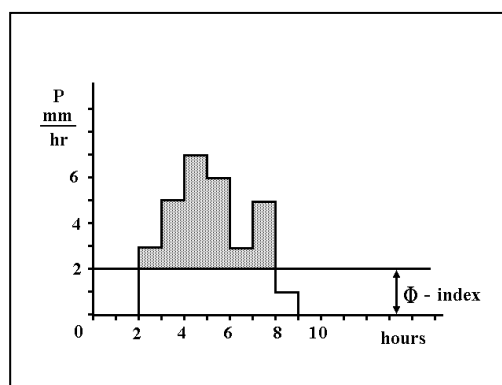
Fig. 6.3 The Φ-index to indicate losses

There are various other methods to estimate the losses or its complement, the runoff coefficient (the fraction of rainfall that comes to runoff). Well-known empirical methods are the Coaxial Correlation Analysis developed by the US Weather Bureau and the Curve Number Method published by the Soil Conservation Service of US Department of Agriculture. The best results, however, are obtained by simulation of the relevant processes (evapotranspiration, interception, unsaturated flow, etc.)

Rational method

If no records are available to evaluate the relation between rainfall and peak runoff, a number of methods exist to arrive at peak runoff and hydrograph shape. For small catchments the most widely known and applied method is the "Rational Formula".

In the method of the Rational Formula it is assumed that the peak runoff occurs when the
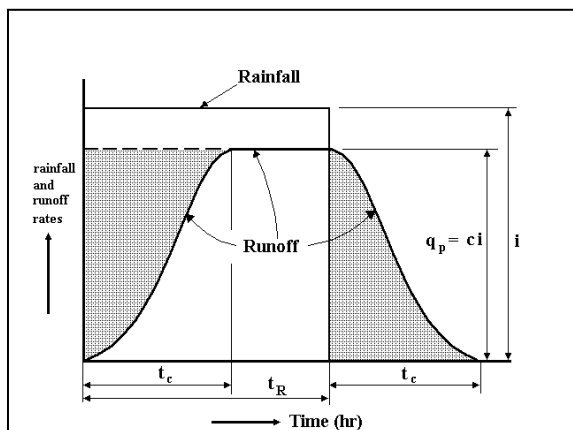
Fig. 6.4   Runoff   from   uniform   rainfall   in   the
            Rational Method

Type of drainage area	Runoff coefficient
Sandy soil	0.05 - 0.20
Heavy soil	0.13 - 0.35
Business	0.50 - 0.95
Residential	0.25 - 0.75
Industrial	0.50 - 0.90
Streets	0.75 - 0.95
Roofs	0.75 - 0.95
Forests	0.10 - 0.60
Pastures	0.10 - 0.60
Arable land	0.30 - 0.80

Table 6.1   **Values of runoff
                         coefficients**

duration of the rainfall equals the *time of concentration*, the time required for the farthest point of the catchment to contribute to runoff. Numerous formulae exist for the time of concentration, each of which is applicable in the catchment for which it has been derived. However, the most widely applied formula is the Kirpich formula:

$$t_c = 0.015 \left(\frac{L}{\sqrt{S}} \right)^{0.8} \tag{6.2}$$

where t_c is the time of concentration in minutes, L is the maximum length of the catchment in metres and S is the slope of the catchment over the distance L . The formula to give the peak flow Q_p is:

$$Q_p = C\ i\ A \tag{6.3}$$

where C is the coefficient of runoff (dependent on catchment characteristics), i is the intensity of rainfall during time t_c and A is the catchment area. The value of i is assumed constant during t_c and the rain uniformly distributed over A. The peak flow Q_p occurs at time t_c. Figure 6.4 illustrates this. In the figure it can be seen that after the time t_c the maximum discharge continues until the end of the rain. The per unit area peak runoff
$q_p = Q_p / A$ then equals $C\ i$. For the determination of a design flow, however, the duration of the rainfall t_R should be taken as equal to t_c. This is required to apply the intensity-duration-frequency curve (figure 2.19): given the return period, the intensity is selected corresponding to the duration t_c.

It can be seen from figure 6.4, that the volume of water accumulated in storage must be equal to the volume enclosed in the recession limb (shaded area). Thus, C represents not only the runoff coefficient for the peak, but also the runoff coefficient for the total volume of runoff. Values of C vary from 0.05 for flat sandy areas to 0.95 for impervious urban surfaces, and considerable knowledge is needed in order to estimate an acceptable value. Some values for the runoff coefficient are given in table 6.1.

Although the Rational Formula is widely used, it is certainly not the best method available.

Considerable uncertainty lies in the determination of the runoff coefficient, and its applicability is limited to small catchments (smaller than 15 km^2).

A more advanced method of arriving at a peak flow and a design hydrograph is the unit hydrograph method, which can be applied on catchments of up to 1000 km^2. Unit hydrographs may be derived from observed rain storms and corresponding hydrographs, but there are also a number of methods for obtaining synthetic unit hydrographs.

Long duration catchment yield

Water resources engineers are primarily concerned with catchment yields and usually study hydrometric records on a monthly basis. For that purpose short duration rainfall should be aggregated. In most countries monthly rainfall values are readily available. To determine catchment runoff characteristics, a comparison should be made between rainfall and runoff. For that purpose, the monthly mean discharges are converted first to volumes per month and then to an equivalent depth per month *R* over the catchment area. Rainfall *P* and runoff *R* being in the same units (e.g. in mm/month) may then be compared.

A typical monthly rainfall pattern is shown in figure 6.5 for the catchment of the Cunapo river in Trinidad. The monthly runoff has been plotted on the same graph. Figure 6.6 shows the difference between *R* and *P*, which partly consists of losses *L* and partly is caused by storage. On a monthly basis one can write:

$$\textbf{R = P - L - } \Delta\textbf{S}/\Delta\textbf{t} \qquad\qquad\qquad (6.4)$$

The presence of the loss and the storage term makes it difficult to establish a straightforward relation between *R* and *P*. The problem is further complicated in those regions of the world that have distinctive rainy and dry seasons. In those regions the different situation of storage and losses in the wet and dry season make it difficult to establish a direct relation.

Figure 6.7 shows the plot of monthly rainfall *P* against monthly runoff *R* for a period of four years in the Cunapo catchment in Trinidad. The plots are indicated by a number which signifies the number of the month. The following conclusions can be drawn from studying the graph.
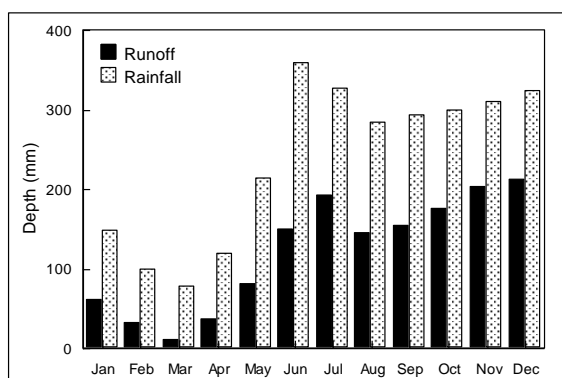
Fig. 6.5 Monthly mean rainfall and runoff in the Cunapo catchment
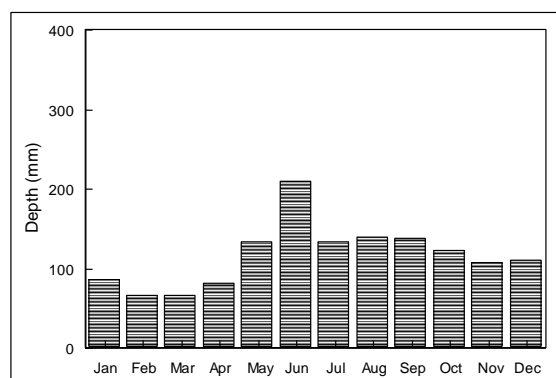
Fig. 6.6 Mean monthly losses and change in storage in the Cunapo catchment

- There appears to be a clear threshold rainfall below which no runoff takes place. The threshold would incorporate such effects as interception, replenishment of soil moisture deficit, evapotranspiration, surface detention, and open water evaporation.
- It can be seen that the same amount of rainfall gives considerably more runoff at the end of the rainy season than at the start of the rainy season. The months with the numbers 10, 11 and 12 are at the end of the rainy season, whereas the rainy season begins (depending on the year) in the months of May to July. At the start of the rainy season the contribution of seepage to runoff is minimal, the groundwater storage is virtually empty and the amount to be replenished is considerable; the value of $\Delta S / \Delta t$ in (6.4) is thus positive, reducing the runoff R. At the end of the rainy season the reverse occurs.

The threshold rainfall is quite in agreement with (6.4) and has more physical meaning than the commonly used proportional losses. Proportional losses are rather a result of averaging. They can be derived from the fact that a high amount of monthly rainfall is liable to have occurred during a large number of rainy days, so that threshold losses like interception and open water evaporation have occurred a corresponding number of times.

By taking into account the threshold loss T and the groundwater storage S, a relation can be obtained between R and P. The following model, which can easily be made in a spreadsheet, has been developed for that purpose.
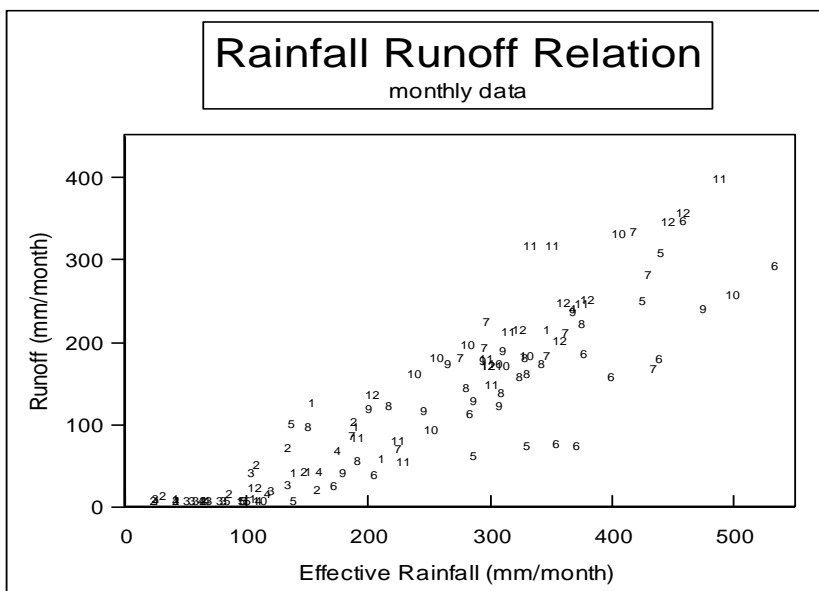
Fig. 6.7 Rainfall plotted versus runoff in the Cunapo river basin

Multiple linear regression model for monthly runoff using threshold losses
As the amount of storage available during a particular month depends on the amount of rainfall in the previous months, a relation is sought that relates the runoff in a particular month to the rainfall in the month itself and the previous months. A simple linear backward relation is used:

$$\mathbf{R_t = a + b_0(P_t - T) + b_1(P_{t-1} - T) + b_2(P_{t-2} - T) + ...} \tag{6.5}$$

under the condition that if $(P_{t-i} - T) < 0$, then $(P_t - T) = 0$. T is the threshold loss on a monthly basis, b_i is the coefficient that determines the contribution of the effective rainfall in month $t - i$ to the runoff in month t (proportional loss); and a is a coefficient which should be zero if the full set of rainfall contributions and losses were taken into account.

In matrix notation (6.5) reads:

$$\mathbf{R_t = B(P - T) + a} \tag{6.6}$$

where R_t is a scalar, the runoff in month t, **B** is an n by 1 matrix containing the coefficients b_i and $(\mathbf{P} - \mathbf{T})$ is a state vector of 1 by n containing the effective monthly precipitation values of the present and previous months. The value $n - 1$ determines the memory of the system. Obviously n should never be more than 12, to avoid spurious correlation, but in practice n is seldom more than 6 to 7.

The effective runoff coefficient C, on a water year basis, is defined as:

$$\mathbf{C = \frac{R}{P - T}} \tag{6.7}$$

where P and R are the annual rainfall and runoff on a water year basis. It can be seen from comparison of equations (6.6) and (6.7) that (if the coefficient a equals zero) the sum of the coefficients in **B** should equal the effective runoff coefficient C:

$$\mathbf{\Sigma(b_i) \approx C} \tag{6.8}$$

meaning that the total amount of runoff that a certain net rainfall generates is the sum of all the components over n months. Obviously C should not be larger than unity.

The coefficients of **B** are determined through multiple linear regression. For the example of figure 6.7 these results are presented in table 6.2. Although the best correlation is obtained with a memory of 5 months, the most significant step is made by including the first month back. Moreover it can be seen that the correlation substantially improves by taking into account the threshold rainfall. Figure 6.8 shows the comparison between computed and measured runoff for a threshold value $T = 120$ mm/month.

Threshold value:						$T = 0$	
Average effective runoff coefficient:						$C = 0.45$	
	t	t-1	t-2	t-3	t-4	t-5	t-6
R^2	0.74	0.75	0.76	0.76	0.77	0.78	0.81
Se	53.5	53.5	52.8	52.9	51.5	51.2	47.5

Threshold value:						$T = 120$	
Average effective runoff coefficient:						$C = 0.85$	
	t	t-1	t-2	t-3	t-4	t-5	t-6
R^2	0.83	0.88	0.88	0.89	0.89	0.90	0.90
Se	43.7	37.0	37.1	36.1	36.1	35.0	35.1

Result best regression:
Memory: $i = 5$ months
constant: $a = -30$

	b_0	b_1	b_2	b_3	b_4	b_5
Coefficients:	0.75	0.21	-0.0	0.05	0.01	0.09

Table 6.2 Summary of correlation Cunapo catchment

6.3 Deterministic catchment models

The previous model is a statistical model on the basis of the water balance equation. In this section deterministic models are presented which try to describe the rainfall runoff process more or less on a physical basis.

Some models attempt to describe each physical process involved in the transfer of rainfall into runoff in detail (*mathematical-physical models*), while others do not try to describe the physics of the system at all (*black box models*). In between the two extremes are the *conceptual models*, which simplify (conceptualize) to a larger or lesser degree the complex rainfall-runoff process.

For the development of a deterministic model the hydrological processes are often drastically simplified. An example of a simplified catchment model has been presented earlier in figure 6.1. The peak flow is dominated by the fast runoff component, the surface runoff Q_s. Many deterministic models, therefore, focus on the development of a relation between P_e and Q_s. The peak flow may then be found by adding the relatively small amount of base flow, which often constitutes less than 10 to 20 % of the peak discharge. Hence, a large error in the estimation of the base flow has only a small effect on the computed peak. The baseflow component can be easily modelled by the linear reservoir method using (4.11).

Fig. 6.8 Measured versus computed runoff in the Cunapo catchment (T = 120)

There is another reason why a separate modelling of the surface runoff system is attractive. It was found that, in particular for small watersheds, the relation between P_e and Q_s could often be considered as a linear system, i.e. twice the amount of P_e results in a doubling of the surface runoff values. It appeared, furthermore, that the relationship is approximately constant in time. The properties of *linearity* and *time-invariance* allow the use of relatively simple techniques for the development of deterministic rainfall-runoff models. Application of these models requires a separation between surface flow and base flow.

The remaining part of the simplified catchment model involves evapotranspiration and groundwater recharge, which constitutes a major problem due to the non-linearity of the processes.

Rainfall-runoff modelling discussed so far treats a whole catchment as if it were homogeneous in character and subject to uniform rainfall. These models are called *lumped models*. Most of the conceptual and black box models are lumped models. The mathematical-physical models usually belong to the category of *distributed models*. These models divide the catchment into small homogeneous subareas which are simulated separately and then combined to obtain the catchment response. Distributed models are generally much more complex than lumped models and often developed to simulate flow in only part of the catchment such as the simulation of flow in a network of open water courses or a regional subsurface flow system.

REFERENCES

Baumgartner, A., 1972. Water and energy balances of different vegetation covers. Proceedings of the Reading symposium. Publ. no. 94. IASH.

Begemann, S.H.A., 1931. Application of the probability theory on hydrological series (in Dutch). De waterstaatsingenieur.

Bell, F.C., 1876. The areal reduction factor in rainfall frequency estimation. Institute of Hydrology. Report No. 35.

Biswas, A.K., 1972. History of hydrology. North-Holland publ. comp.

Blaney, H.F. and W.D. Criddle, 1950. Determining water requirements in irrigated areas from climatological and irrigation data. USDA (SCS) TP-96: 48 p.

Cunnane, C., 1978. Unbiased plotting positions – a review. J.of Hydrol. 37: 205-222

Darcy, H.P.G., 1856. Les fontaine publiques de la ville de Dijon, V. Dalmont, Paris, 647 p.

De Laat, P.J.M., 1995. Design and operation of a subsurface irrigation scheme with MUST. In: Crop-Water-Simulation Models in Practice (Eds. L.S. Pereira et al.), Wageningen Press, pp. 123-140.

Delhomme, J.P., 1978. Kriging in the hydrosciences. Adv. in Water Res. 1(5):251-266.

Dooge, J.C.I., 1973. Linear Theory of Hydrologic Systems. Agriculture Research Service Technical Bulletin No. 1468. US Department of Agriculture.

Doorenbos, J. and W.O. Pruitt, 1977. Guidelines for predicting crop water requirements. Irrigation and Drainage Paper 24, 2nd revised ed., FAO, Rome, 144 p.

Euroconsult et al., 1987. Agricultural development and crop diversification study covering the Chao Phya westbank area, pre-feasibility report, annex B, Hydrology.

Feddes, R.A. et al., 1978. Simulation of field water use and crop yield. Simulation monographs, Pudoc, Wageningen, 189 p.

Feddes, R.A. and K.J. Lenselink, 1994. Evapotranspiration. In: Drainage Principles and Applications (Ed. H.P. Ritzema), ILRI Publication 16, ILRI, Wageningen, pp. 145-173.

Gumbel, E.J., 1958. Statistics of extremes. Colombia University Press, New York.

Harbeck, G.E., 1962. A practical field technique for measuring reservoir evaporation utilizing mass transfer theory. US Geol. Surv. Prof. Paper 272-E, pp 101-105.

Hershfield, D.M., 1961. Estimating the Probable Maximum Precipitation. Proc. ASCE, 87, HY5: 99-116.

Holy, M., 1982. Irrigation systems and their role in the food crises. ICID bulletin, Vol. 31:2.

Horton, R.E., 1940. An approach towards a physical interpretation of infiltration capacity. Proc. Soil Sci. Soc. Am. 5, 399-417.

Jensen, M.E., R.D. Burman and R.G. Allen, 1990. Evapotranspiration and irrigation water requirements. ASCE manuals and rep. on eng. practice 70. ASCE, New York, 332 p.

Kraijenhoff van de Leur, D.A., 1958. A study of non-steady groundwater flow with special reference to a reservoir-coefficient. De Ingenieur 70(19): B87-B94.

Landsberg, H.E., 1981. The urban climate. Academic Press, New York, 275 p.

Makkink, G.F., 1957. Testing the Penman formula by means of lysimeters. Journ. Int. of Water Eng. 11: 277-288.

Menenti, M., 1983. A new geophysical approach using remote sensing techniques to study groundwater table depth and regional evaporation from aquifers in deserts. ICW Report 9, Staring Centre, Wageningen, 15 p.

Monteith, J.L., 1965. Evaporation and environment. Proc. Symp. Soc. Exp. Biol. 19: 205-234.

NEDECO et al., 1983. Masterplan for flood protection and drainage of Thonburi and Samut Prakan West, reconnaissance report, annex B, Hydrology.

Nieuwenhuis, G.J.A., E.H. Smidt and H.A.M. Thunnissen, 1985. Estimation of regional evapotranspiration of arable crops from thermal infrared images. Int.J.Remote Sensing 6(8):1319-1334.

Penman, H.L., 1948. Natural evaporation from open water, bare soil and grass. Proc. Roy. Soc. London A 193: 120-145.

Philip, J.R., 1960. Theory of infiltration. Advances in Hydroscience, Vol. 5, 216-296. Academic Press.

Ponting, C., 1992. A green history of the world. Penguin Books. London.

Riggs, H.C., 1976. A simplified slope-area method for estimating flood discharges in natural channels. Journal Research U.S. Geol. Survey Vol.4, No.3.

Rijtema, P.E., 1965. An analysis of actual evapotranspiration. Agric. Res. Rep. 659, Pudoc, Wageningen, 107 p.

Rodda, J.C. and N.C. Matalas, 1987. Water for the future; Hydrology in perspective. Proceedings of the Rome Symposium. IAHS publ. no. 164.

Savenije, H.H.G. and M.J. Hall, 1993. Climate and Land Use: a Feedback Mechanism? Proceedings of the Delft Conference on Water and the Environment, Key to Africa's Development. June 3-4, 1993, Delft, The Netherlands.

Smith, M., 1991. Report on the expert consultation on procedures for revision of FAO guidelines for prediction of crop water requirements. FAO, Rome. 54 p.

Thornthwaite, C.W., 1948. An approach towards a rational classification of climate. Geog. Rev. 38: 55-94.

Verhoef, A. and R.A. Feddes, 1991. Preliminary review of revised FAO radiation and temperature methods. Dept. of Water Res. Rep. 16. Agricultural University, Wageningen, 116 p.

Water Resources Board, 1965. Logarithmic plotting of stage-discharge observations. Water Resources Board, Reading.

HANDBOOKS

American Society of Civil Engineers, 1996. Hydrology Handbook. NY ASCE.

Anderson, M.G. & T.P. Burt, 1990. Process studies in hill slope hydrology. Wiley.

Black, P.E., 1990. Watershed Hydrology. Prentice Hall, 408 p.

Brooks, K.N., P.F/ Ffolliott, H.M. Gregersen & L.F. DeBano, 1997. Hydrology and the Water Management of Watersheds. Iowa State University Press, 502 p.

Bras, R.L., 1990. Hydrology, an introduction to hydrologic science. Addison-Wesley Publishing Company, Reading Massachusetts.

Burman, R. & L.O. Pochop, 1994. Evaporation, evapotranspiration and climatic data. Elsevier, Amsterdam.

Chow, Ven Te, D.R. Maidment and L.W. Mays, 1988. Applied hydrology. McGraw Hill, New York.

Dingman, S.L., 1994. Physical Hydrology. Prentice Hall, 575 p.

Eagleson, P.S., 1970. Dynamic Hydrology. McGraw-Hill Book Company, New York.

Falkenmark, M. & T. Chapman, 1989. Comparative Hydrology; an ecological approach to land and water resources. Unesco, Paris, 479 p.

Hornberger, G.M., J.P. Raffensperger & P.L. Wiberg, 1998. Elements of Physical Hydrology. John Hopkins University Press, 302 p.

Maidment, D.R., 1993. Handbook of Hydrology. McGraw-Hill, New York.

Raudkivi, A.J., 1979. Hydrology. Pergamon Press.

Ritzema, H.P., 1994. Drainage Principles and Applications. ILRI Publication 16, Second (Revised) Edition, ILRI, Wageningen. 1125 p.

Starosolszky, O., 1987. Applied surface hydrology. Littleton, Col., Water Res. Publ.

Todd, D.K., 1980. Groundwater hydrology. Wiley, New York.

Viessman, W., T.E. Harbaugh and J.W. Knapp, 1977. Introduction to hydrology. Harper and Row, New York.

Ward, A.D. & W.J. Elliot, 1995. Environmental Hydrology. Boca Raton.

Watson, I. & A.D. Burnett, 1995. Hydrology, an environmental approach; theory and applications of groundwater and surface water for engineers and geologists. Boca Raton.

World Meteorological Organization WMO, 1994. Guide to Hydrological Practices: data acquisition and processing, analysis, forecasting and other applications. WMO No. 168.

RECOMMENDED TEXT BOOKS

McCuen, R.H., 1998. Hydrologic analysis and design. Prentice Hall, 814 p.

Shaw, E.M., 1994. Hydrology in practice. Van Nostrand Reinhold, 569 p.

Shaw, E.M., 1989. Engineering hydrology techniques in practice. Ellis Horwood, 350 p.

Ward, R.C. and M. Robinson, 1990. Principles of Hydrology, McGraw-Hill, 365 p.

Wilson, E.M., 1983. Engineering Hydrology. Mc Millan, 309 p.

PROBLEMS

1   The average annual discharge at the outlet of a catchment is 0.5 m³/s. The catchment is situated in a desert area (no vegetation) and the size is 800 km². The average annual precipitation is 200 mm/year.
    a. Compute the average annual evaporation from the catchment in mm/year.

    In the catchment area an irrigation project covering 10 km² is developed. After some years the average discharge at the outlet of the catchment appears to be 0.175 m³/s.
    b. Compute the evapotranspiration from the irrigated area in mm/year, assuming no change in the evaporation from the rest of the catchment.

2   For a watershed with a size of 120 km², the following data on precipitation P, evaporation E and runoff Q are given in mm.

	Jan	Feb	Mar	Apr	May	Jun	Jul	Aug	Sep	Oct	Nov	Dec
P	250	205	165	50	5	0	0	5	10	55	65	190
E	5	25	30	50	80	100	150	70	60	20	10	5
Q	150	110	80	5	0	0	0	0	0	10	15	120

    a. At the end of which month is the amount of water stored in the basin largest and when is the smallest amount of water present in the catchment?
        What is the difference (m³) in the amount of water stored in the basin between these two extremes?
    b. In what climate (arid, humid temperate or humid tropical) do you expect this catchment to be located?

3   A catchment has a size of 100 km². In its original condition, the average annual total runoff from the catchment is 1.1 m³/s. The average annual rainfall is 800 mm/a. In an average year, 50% of the rainfall infiltrates and 12.5% of the rainfall reaches the groundwater . Tests have turned out that the average annual evapotranspiration from the unsaturated zone (being the sum of the transpiration and the bare soil evaporation) amounts to 340 mm/a. In all water balance computations over the year, one may assume that the storage effects are small (dS/dt = ±0).
    a. How much water, in mm/a, reaches the root zone through capillary rise in an average year?
    b. How much water, in mm/a, seeps out from the groundwater to the surface water in an average year?
    c. How much water, in mm/a, evaporates directly from interception in an average year?
    d. How much, in mm/a, is the total evapotranspiration in the catchment in an average year?

    A well field is planned to withdraw 0.16 m³/s from the catchment for drinking water consumption elsewhere . As a result, the groundwater level is expected to go down and capillary rise into the root zone will no longer be possible. The percolation, however is expected to remain the same.

e. What will be the effect of the withdrawal on the different components of the hydrological cycle: the groundwater seepage, the total runoff, the evapotranspiration from the unsaturated zone and the total evapotranspiration? Please quantify in mm/a.

4   A polder in the West of The Netherlands is surrounded by a canal. The water level in the canal is well above the land surface of the polder. The size of the polder is 10 km² and 20% of this area is open water. The average annual open water evaporation is 600 mm/a. The land use in the polder is grass. The open water level in the polder is kept high all year round, consequently the evapotranspiration of the crop equals its potential value. Potential evapotranspiration of grass in The Netherlands may be estimated as 75% of the open water evaporation. The average annual precipitation is 800 mm/a, the average annual amount of water pumped out is $5x10^6$ m³/a while $0.7x10^6$ m³/a is let in to the polder in order to maintain a high water level in the summer period.

a   Compute the average annual groundwater seepage into the polder in mm/a.

b   Do you estimate the error of the computed amount of seepage to be less than 1, between 1 and 10 or greater than 10 mm/a?

c   The Water Board decides to lower the open water level in the polder from the original high level to a much lower level. As a result of this, the annual amount of seepage as well as the evapotranspiration change by 10%. The water intake remains the same (0.7 km³/a).
    Compute for the new situation the average amount that is pumped out in mm/a.

5   A tropical cyclone produces 240 mm of rainfall during a period of 5 days. The figure below gives the percentage mass curve of this rainfall event.
    Plot the hyetograph using daily time intervals.
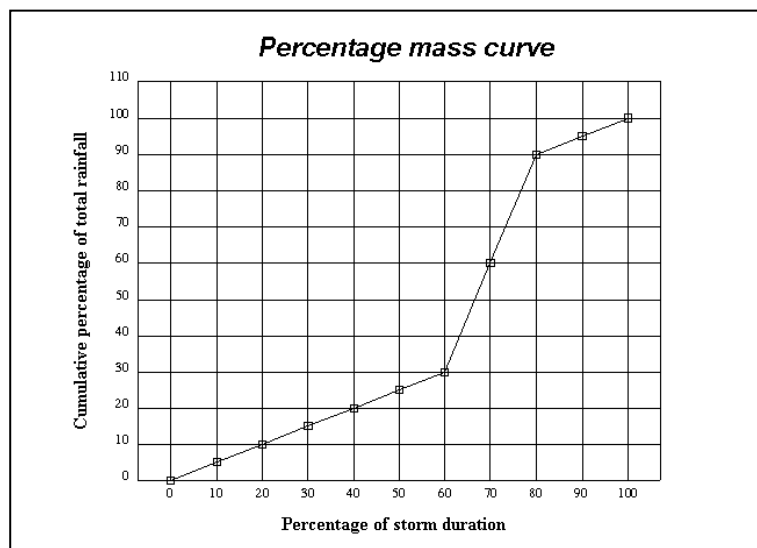
6   For the rainfall gauging stations *A, B* and *C*, which are all situated in the same climatic region, the annual precipitation data (cm) for ten successive years are given below. The data of one station are not reliable. Determine this station with the double-mass curve analysis.

	A	B	C
1971	90	100	100
1972	60	100	80
1973	70	80	70
1974	80	120	100
1975	50	50	50
1976	50	50	50
1977	100	100	100
1978	50	100	80
1979	120	200	170
1980	60	100	100

7   In a rectangular area three raingauges A, B and C are located as shown in the figure below. The recorded rainfall for June is as follows: Station *A*: 75 mm, Station *B*: 40 mm and Station *C*: 30 mm. Use the Thiessen method to compute the areal rainfall of the rectangle for the month of June.
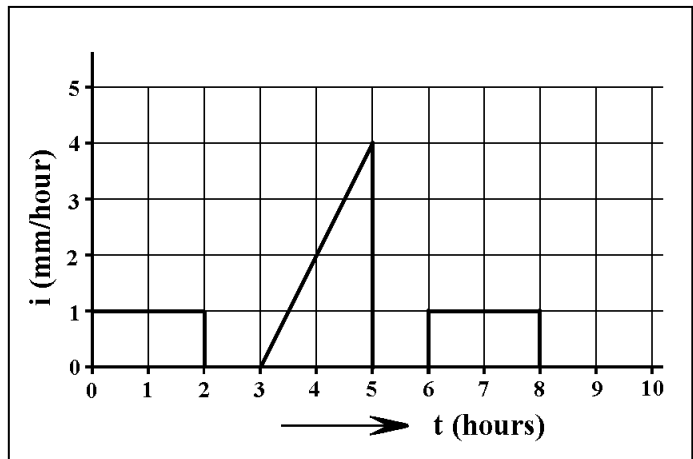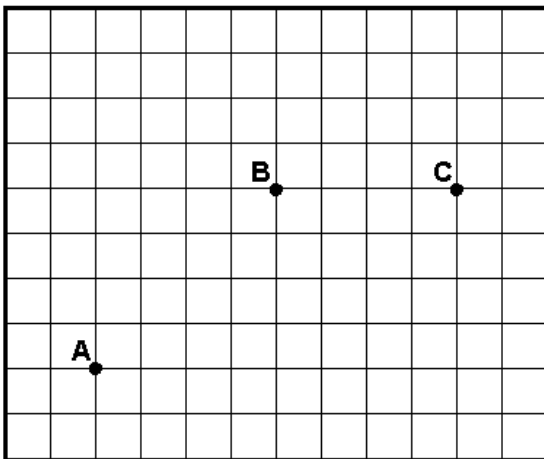
8   The hyetograph in the figure above (right) gives the rainfall intensity in (mm/h) with time (h) which is recorded with a raingauge at a height of 120 cm above soil surface.

    a.   Compute and plot the mass curve (cumulative rainfall depth with time).

    b.   Sketch roughly in the same figure what would have been the mass curve for the situation that the position of the raingauge is changed in such a way that the rim of the collector is at ground level.

9   The following statistical characteristics (frequencies of occurrence) were derived from a
    time series of daily rainfall totals:

Return period (years)	n - day total in mm			
	1 day	3 days	5 days	10 days
1	30	60	80	90
10	40	75	95	110
100	50	?	?	130

a.   Determine the missing figures in the table above.
b.   Derive the intensity duration curve for a return period of 100 years.

10 Consider the following annual maximum daily rainfall data:

Year	1984	1985	1986	1987	1988	1989	1990	1991	1992	1993
Depth (mm)	82	78	110	89	74	80	86	99	93	76

Make a graph of the extreme rainfall depth versus the logarithm of the return period. Do not
use semi-log paper. Estimate the annual maximum daily rainfall with a return period of 20
years.

11 The Gumbel distribution of daily extreme rainfall data (mm) shows that
$$P(X \le 100) = 0.90$$
$$P(X \le 130) = 0.98$$
    a   Compute the daily extreme rainfall for a return period of 100 years. (If you wish you
        can check the answer yourself graphically in figure 2.23).
    b   Mention at least two requirements with regard to the establishment of the Gumbel
        distribution that have to be fulfilled to make the answer of the previous question
        meaningful.

12 For a certain watershed the following monthly data on precipitation P and potential
    evapotranspiration E_{pot} are given in mm.

|	Jan	Feb	Mar	Apr	May	Jun	Jul	Aug	Sep	Oct	Nov	Dec
P	50	50	50	40	40	40	70	70	70	60	60	60
E_{pot}	40	40	40	70	70	70	60	60	60	40	40	40

The annual actual evapotranspiration E_{act} equals 610 mm. Except for one month, the actual
evapotranspiration equals the potential evapotranspiration.
    a.   Indicate the month for which $E_{act} < E_{pot}$.
    b.   Compute the actual evapotranspiration for this month.
    c.   Compute the annual river discharge from the watershed, assuming that the change in
storage can be neglected.

13 For a large catchment the following data on precipitation *P*, free water evaporation E_o, potential evapotranspiration E_{pot} and actual evapotranspiration E_{act} are given in an arbitrarily sequence in mm/year as follows: 40, 100, 2500 and 3000.

   a. Give the values for *P*, E_o, E_{pot} and E_{act}. Explain your answer.

   b. Indicate to which climate these values pertain: humid, semi-arid or arid.

14 The three data sets in the table and chart below refer to monthly evaporation values in mm/d for a shallow lake, a deep lake and a Class A pan in the same region in The Netherlands.

   a   Which data set belongs to the shallow lake, which one to the deep lake and which data set represents the pan evaporation data? Please explain.

   b   Estimate the pan coefficient for the deep lake and for the shallow lake.

Month	A	B	C
1	0.3	0.3	0.1
2	0.5	0.5	0.3
3	0.9	1.0	1.4
4	1.8	2.3	2.5
5	2.7	3.3	3.8
6	3.0	3.7	5.0
7	3.4	3.3	4.8
8	2.4	2.2	3.1
9	1.9	1.6	1.7
10	1.2	0.7	0.5
11	0.4	0.3	0.2
12	0.2	0.1	0.0

15 Measurements in Hodeidah (Yemen, 15 °N, altitude 18 m) of the global radiation results in the following data:

August 15, 1990: $R_S = 20.482$ MJ/d/m^2 August 16, 1990: $R_S = 16.758$ MJ/d/m^2
               $n = 6.3$ hours $n = 4.2$ hours

   a. Compute the parameters *a* and *b* in the radiation equation $R_s = (a + b\, n/N)\, R_A$

   b. Compute the evaporation from a reservoir at Hodeidah for the month of June according to Penman and Makkink, given the following data (24 hour mean values at 2 m height):

                    Sunshine duration   : 10.4 hours
                    Air temperature   : 31.0 °C
                    Relative humidity   : 38.4 %
                    Wind speed   : 2.0 m/s

16 An infiltrometer is used to determine the infiltration capacity of a clay soil. The experiment lasted 120 minutes. During the experiment water was added to maintain a constant water level in the ring. The total volume of water added is tabulated below. The area of the ring is 600 cm^2.

   a. Compute for each time interval the infiltration capacity in cm/hr.

   b. Plot the infiltration capacity (cm/hr) versus time (minutes).

   c. Estimate the ultimate value of the infiltration capacity.

Time (minutes)	0	1	3	5	10	20	40	60	90	120
Volume added since the start (cm^3)	0	60	162	252	427	657	837	957	1122	1272

17 The relation between infiltration capacity in mm/hour and the time (in hours) since the start of the experiment as measured with an infiltrometer is depicted below. The relationship may be described with the empirical formula of Horton (equation 4.2), where f_p, f_c and f_o in mm/h, t in min. and k in min^{-1}.

  a. Derive the parameter values f_o, f_c and k from the measured relationship.
  b. Estimate from the graph below the total amount of water that will infiltrate into the soil during a rainstorm with a duration 20 minutes and a constant intensity of 20 mm/h. Answer the same question for a constant rainfall intensity of 12 mm/h.
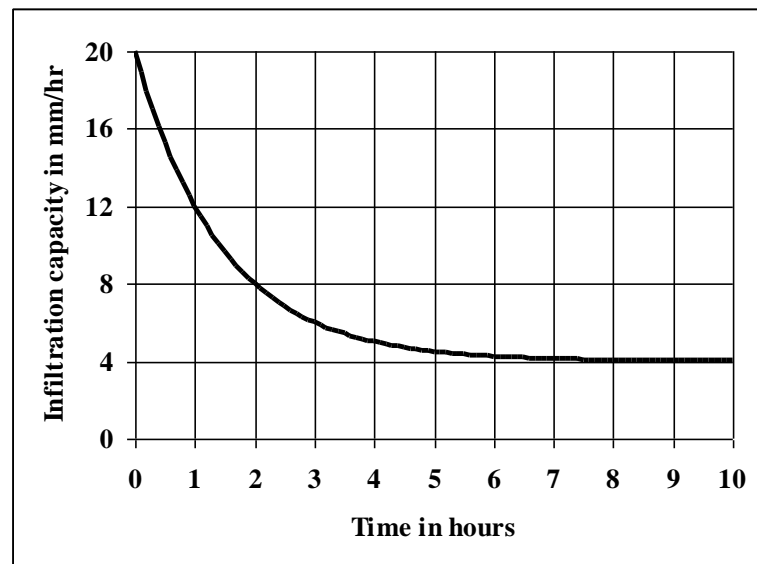
18 The capacity of the interception storage of a forest is 2 mm. After a dry period a rainstorm on this forest with an intensity of 40 mm/hr lasts one half hour. The infiltration capacity during the first 1/4 hour is 40 mm/hr and during the second 1/4 hour is 32 mm/hr. Compute the amount of water that infiltrates into the soil during the rainstorm.

19 A sprinkling test is carried out on a plot of 25 m^2. The simulated rainfall intensity (i) equals 20 mm/h. After 4 hours the surface runoff from the plot becomes constant and equal to 0.05 l/s.

  a. Compute the ultimate infiltration capacity in mm/h.
  b. Sketch in a graph the infiltration capacity with time, given an initial infiltration rate at the start of the sprinkling rest equal to 18 mm/h. Sketch in the same figure the infiltration capacity with time for the situation the experiment is repeated a few hours later.

20 The rooting depth of a crop is 60 cm.
   a. Compute the (maximum) available moisture for the crop from the root zone (the amount between field capacity and wilting point) for sand, loam and clay. Use the soil moisture characteristics in your lecture notes in figure 4.6. Field capacity corresponds to pF2.
   b. If all this water has been used the crop is dead (wilting point condition). In order to prevent reduction in crop yield the farmer will irrigate the crop when half of the available moisture is used. If the evapotranspiration rate of the crop equals 4 mm/d, compute the irrigation interval in the absence of precipitation.

21 In a soil with a deep water-table the root zone has a depth of 50 cm. The moisture content at field capacity for this root zone is 28%. Just before irrigation the moisture content in the root zone is 12%. During irrigation 110 mm of water infiltrates into the soil. How much water percolates from the root zone into the subsoil?

22 Consider the water balance of a reservoir during the last 6 weeks of a long dry season. The reservoir is receiving water from one river only. The river discharge into the reservoir at the start and at the end of the 6 week period is 10 and 1.8 m^3/s, respectively. The surface area of the reservoir is 20 km^2.
   a. Compute for each week the rise of the water level in the reservoir due to the inflow of river water only.

   The following precipitation (P) and evaporation (E) data (mm/week) apply for the 6-week period.

Week	1	2	3	4	5	6
P	0	0	0	0	0	23
E	40	40	40	45	45	45

   At the dam site water is released with a constant rate of 5 m^3/s. There are no other significant flows that should be considered for the water balance of the reservoir.

   b. Compute the water level in the reservoir at the end of each week given a water level of 20 m above mean sea level at the start of the 6 week period.

23 Consider a catchment of 33.3 km^2 situated in an arid region. The outlet of the catchment is a wadi (dry river) that carries water only after heavy rainfall. A rain storm with a depth of 100 mm falls uniformly over the catchment during a period of three hours. The rainfall depth in the first, second and third hour are respectively 45, 35 and 20 mm. The discharge at the outlet due to this rain storm is presented as hydrograph A (solid line) in the chart below.
   a Compute the runoff coefficient for this rainfall event.
   b Compute the constant loss rate (the Φ-index)
   c In the same chart the hydrograph observed at a point B, 20 km down stream in the same river is plotted. The average width of the river section between A and B is 50 m. Estimate the average infiltration rate into the river bed between A and B in mm/hr during the passage of the flood wave.
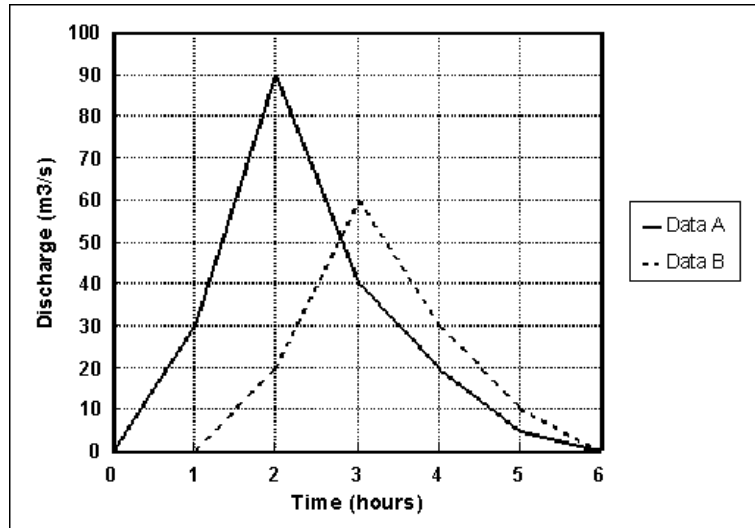
24 For a certain catchment the depletion curve of the hydrograph at the outlet may be described with the equation 4.11. The flood hydrograph Q (mm/d !) at the outlet, as given below, was produced by a rainstorm of 50 mm.

Day	1	2	3	4	5	6	7	8	9	10	11	12	13	14
Q (mm/d)	1.72	1.50	1.31	1.14	1.00	6.00	10.0	6.00	4.00	3.00	2.62	2.29	2.00	1.75

  a   Plot the hydrograph and separate direct runoff from base flow by a straight line. (For the construction of this line semi-log paper may be used, but this is not required).
  b   Estimate the direct runoff in mm.
  c   Estimate the total base flow contribution from this rain storm.

25 Consider a rainstorm with a constant intensity falling uniformly over a catchment of $6\,km^2$. The time of concentration of the catchment is 3 hours. The runoff coefficient is 0.4. The Depth-Duration-Frequency curve for the T = 10 years that applies to this catchment is given below.
Use the Rational Method to compute the maximum peak runoff in $m^3.s^{-1}$ with a return period of 10 years.
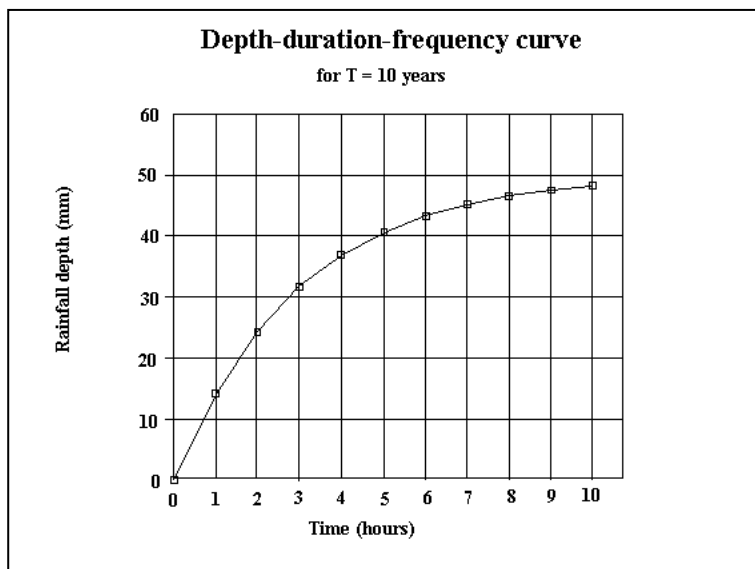
ANSWERS TO PROBLEMS

1a	180.3 mm/a
1b	1200 mm/a
2a	Largest End of March
	Smallest End of September
	Difference $53.4*10^6$ m^3
2b	Humid temperate
3a	40 mm/a
3b	60 mm/a
3c	113 mm/a
3d	453 mm/a
3e	50 mm/a
	337 mm/a
	300 mm/a
	413 mm/a
4a	110 mm/a
4b	> 10 mm/a
4c	547 mm/a
5	1 (24), 2 (24), 3 (24), 4 (144), 5 (24)
6	Station A
7	46.0 mm
9	3 days: 90 mm
	9 days: 110 mm
10	118 mm
11	143 mm
12a	June
12b	50 mm
12c	50 mm

13a	100, 3000, 2500, 40
13b	Arid
14a	A deep, B shallow, C pan
14b	$f_{deep} = 0.8$, $f_{shallow} = 0.825$
15a	a = 0.25, b = 0.60
15b	$E_o = 8.5$ mm/d
	$E_{Makkink} = 7.1$ mm/d
16a	6.0, 5.2, 4.5, 3.5,
	2.3, 0.9, 0.6, 0.55, 0.50
16c	0.5 mm/hr
17a	20, 4, 0.01155
17b	6 mm, 4 mm
18	16 mm
19a	12.8 mm/hr
20a	Sand: 66 mm
	Loam: 126 mm
	Clay: 84 mm
20b	8, 15 and 10 days
21	30 mm
22a	1(264.6 mm), 2(199.0), 3(149.0), 4(112.2), 5(84.1), 6(63.5)
22b	1(20.07m), 2(20.08), 3(20.04), 4(19.96), 5(19.84), 6(19.73)
23a	0.2
23b	30 mm/hr
23c	between 39 and 46.8 mm/hr
24b	18 mm
24c	$\pm$ 25 mm
25	7.3 m^3/s